The innervation of mammalian skeletal muscle by medium and small diameter afferent nerve fibres

Stacey, Michael, J.

Figure 1

Two diagrams illustrating the variation in structure of the lumbo-sacral sympathetic chain of the cat.

a. The connecting nerve tracts between ganglia of succeeding levels are usually bi-lateral in nature, but in this particular animal they are fused at the S1 level, and only a single tract is present between succeeding ganglia caudad of the S1.

b. Fusion of the paired ganglia usually occurs at the S1 or S2 levels, but in this case it occurs as far caudad as the Ca1 level.

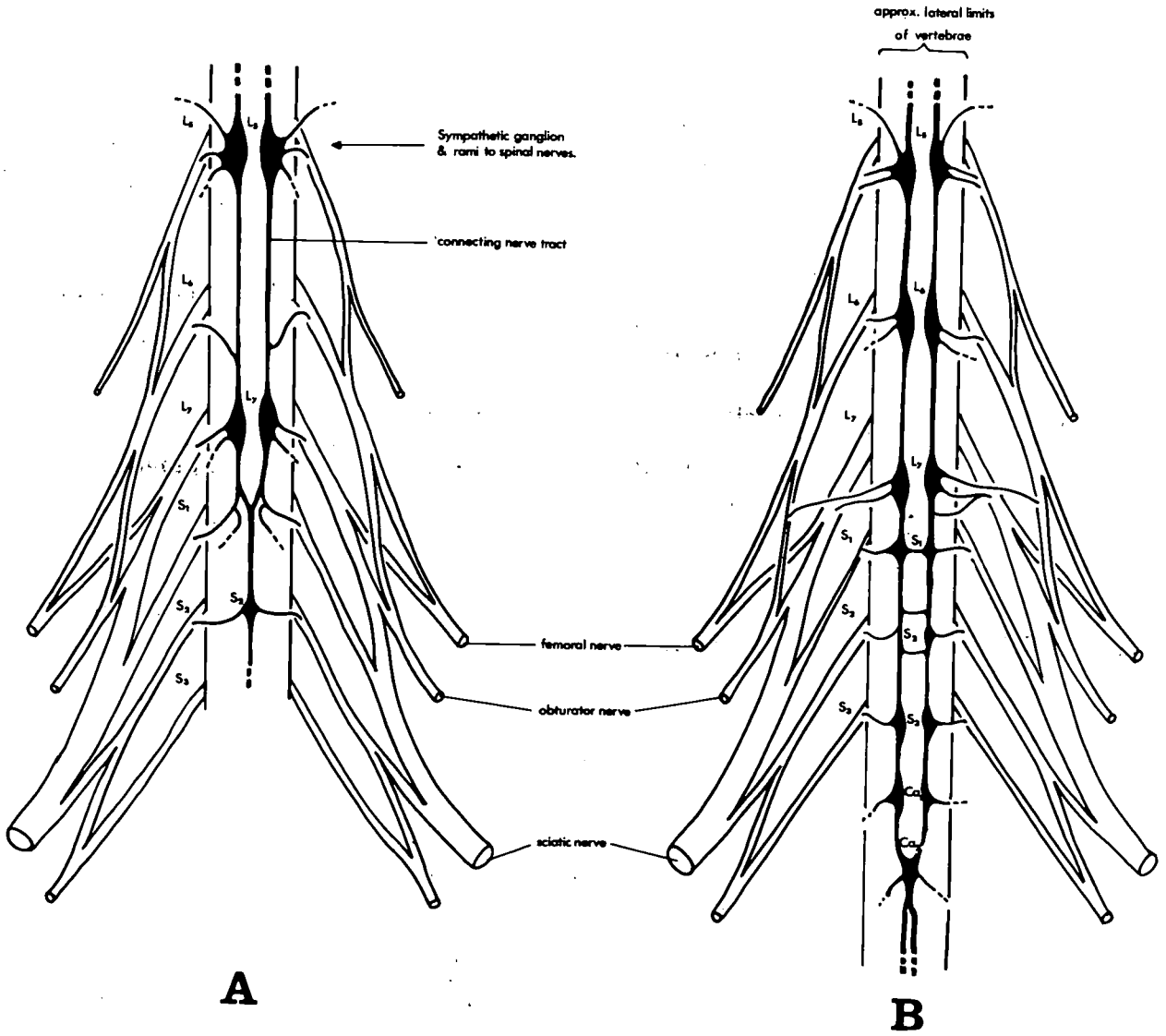

Figure 1 (cont.)

c. Out of twelve animals four had L7 ganglia which produced two rami, one to the L7 spinal nerve and one to the S1 spinal nerve;

d. seven possessed two rami only up to the L6 level and,

e. one animal had two rami from the S2 galglion. In this instance this ganglion was fused, there was no S1 ganglion, the L7 ganglion produced a single ramus to its equivalent spinal nerve. The L6 ganglion produced two rami, one to its equivalent spinal nerve and one to the preceding spinal nerve.

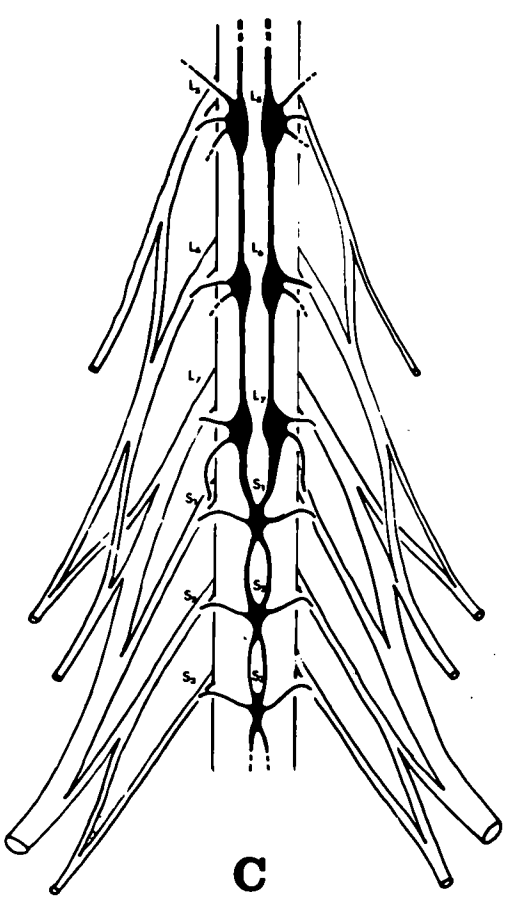

C

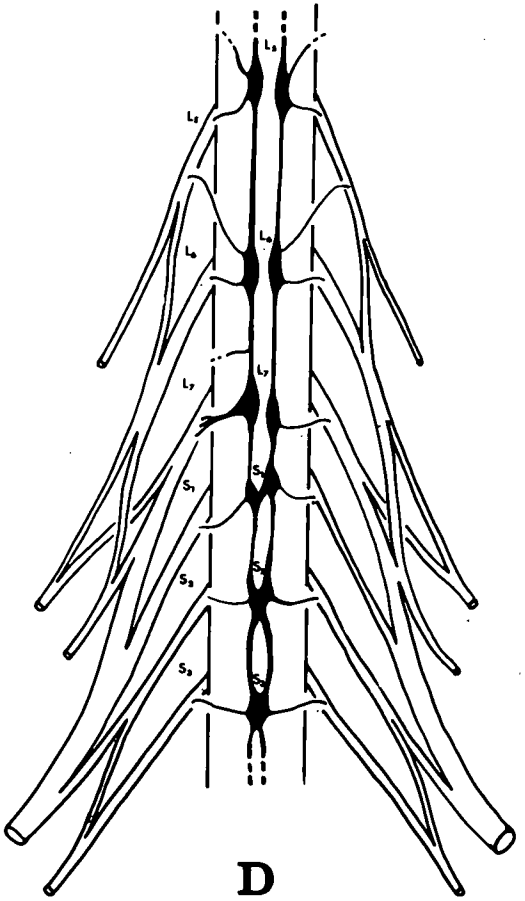

D

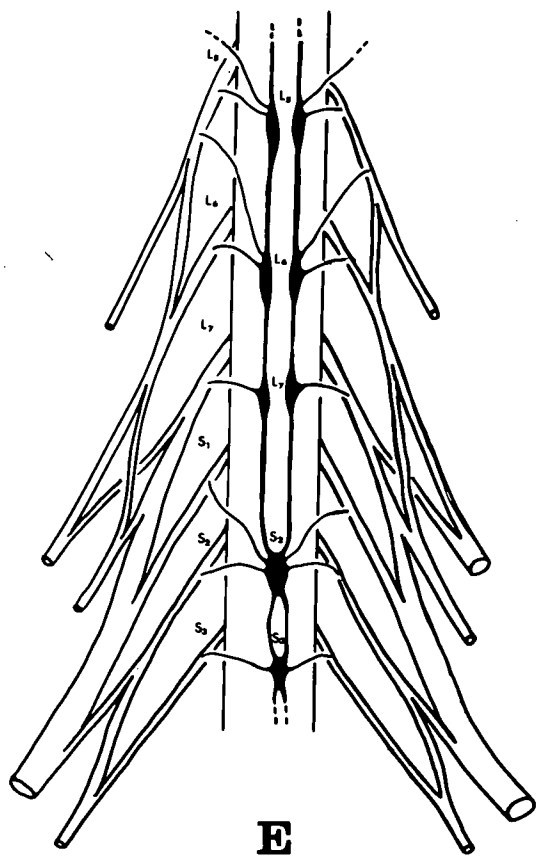

E

Figure 2

A diagrammatic cross-section through the lower-lumbar region of the cat

The dotted line represents the path taken for a retro-peritoneal approach to lumbo-sacral sympathectomy.

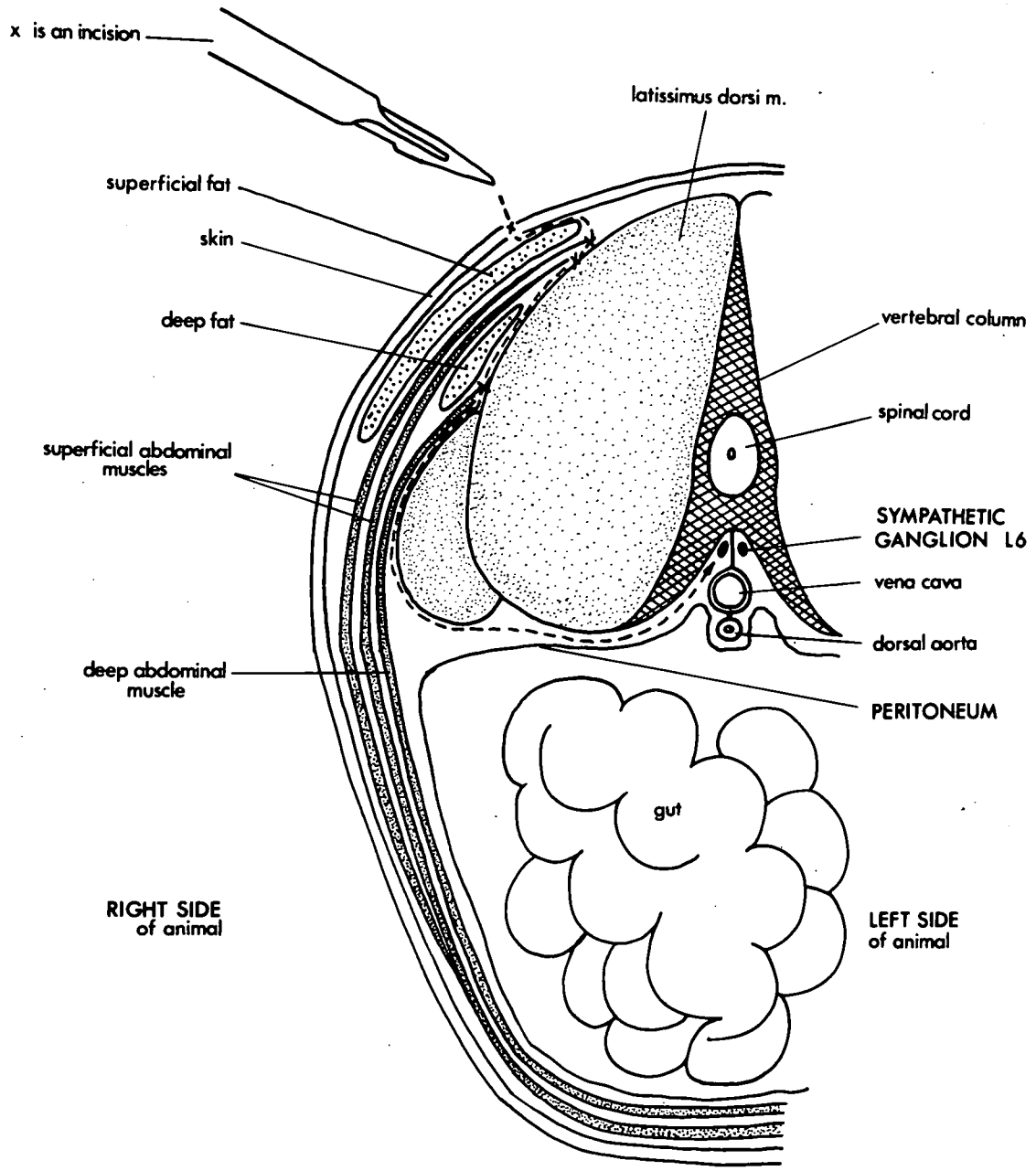
x is an incision
latissimus dorsi m.
superficial fat
skin
deep fat
vertebral column
spinal cord
superficial abdominal muscles
SYMPATHETIC GANGLION L6
vena cava
dorsal aorta
deep abdominal muscle
PERITONEUM
gut
RIGHT SIDE of animal
LEFT SIDE of animal

Figure 3a

Diagrammatic cross-section of a lower-lumbar spinal nerve

The dorsal root ganglion sits in a 'gutter' formed by the ventral root. If root checks are made on longitudinal sections, uncut motor nerve fibres (dotted area) are not recognizable as such unless the roots are sectioned along the plane represented by the line A-B.

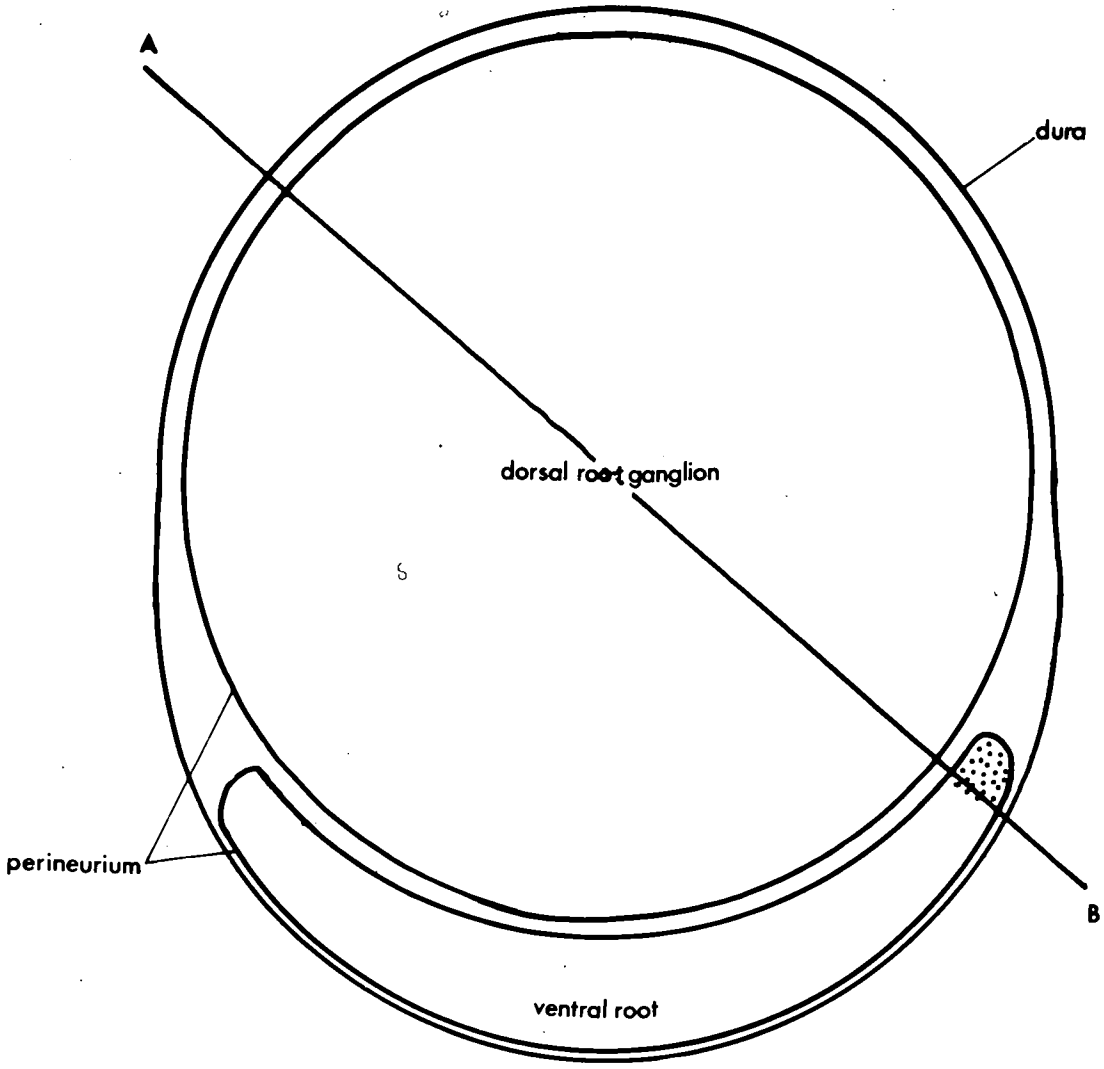
A
dura
dorsal root ganglion
perineurium
B
ventral root

Figure 3b

Transverse section of an L7 spinal nerve of a cat

During laminectomy, a small fascicle of motor nerve fibres was left intact. In transverse section they are clearly seen outside the limits of the dorsal root perineurium (as illustrated in the diagram Fig. 3a). They can be traced throughout the serial sections of the spinal nerve, from the point at which they leave the cord, to the point at which they enter the mixed nerve.

(10 μ section : Holmes silver method)

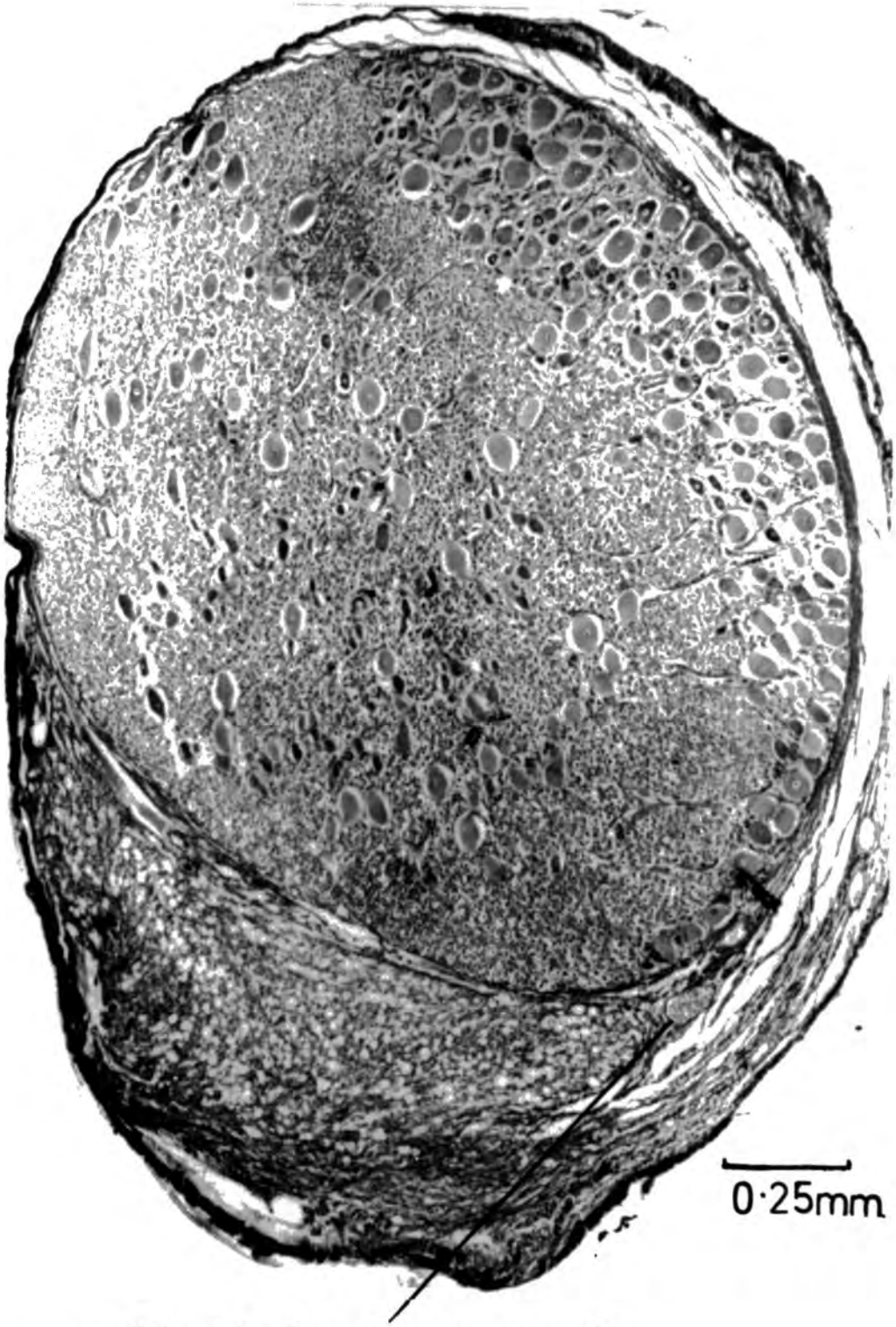

small fascicle of uncut motor nerve fibres.

Figure 4

Three illustrations of dorsal-root ganglia of the cat in transverse section

A. Deliberately damaged L7 dorsal-root ganglion (C 201). The perineurium (peri.) of the dorsal root is broken and an area of scar tissue (sc.t.) has formed. Damaged and degenerating afferent nerve fibres and cell bodies (d. aff.) can be seen within the scar region.

in. aff. - intact afferent nerve fibres and cell bodies.

(10 μ section : Holmes silver method)

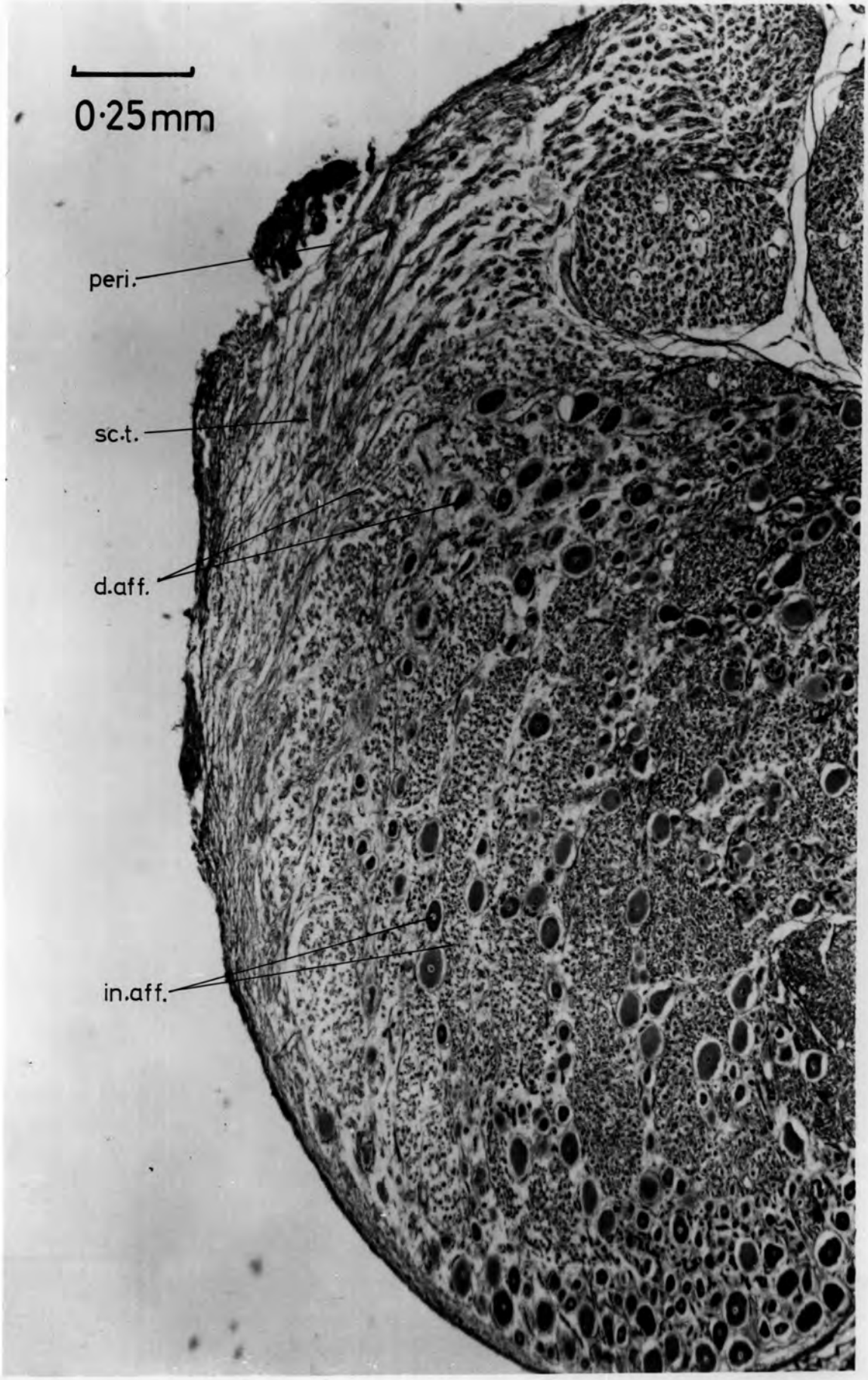
0·25mm
peri.
sc.t.
d.aff.
in.aff.

Figure 4 (cont.)

B. An accidentally damaged S1 dorsal-root ganglion. Scar tissue (sc.t.) and degenerating afferent nerve fibres (d. aff.) are present at the edge of the ganglion.

in. aff. - intact afferent nerve fibres and cell bodies.

(10 μ section : Holmes silver method)


in.aff.
sc.t.
d.aff.
0·25mm

Figure 4 (cont.)

C. Undamaged dorsal root ganglion. All of the degenerating nerve fibres (d.f.) and scar tissue (sc.t.) are outside of the intact dorsal root perineurium (peri.), and are the result of complete motor root section.

(10 μ section : Holmes silver method)


0·25mm
peri.
sc.t.
d.f.

Figure 5

A muscle spindle without any nerve fibre innervation

As a result of damage during ventral root section to afferent nerve fibre cell bodies present in the ventral root, the muscle spindle is totally deprived of any nerve fibre innervation. This was the only example found in this muscle (tibialis posterior C213) of total denervation of a proprioceptor. The tendon organ is supplied by a Ib fibre (C213). De-efferentated and sympathectomized tibialis posterior muscle; modified de Castro impregnation.


tendon organ
Ib fibre
extrafusal muscle fibre
muscle spindle
200µ

Figure 6

Longitudinal section of a normal spinal nerve illustrating afferent nerve-fibre cell bodies in the ventral root

d.r.g. - dorsal root ganglion

v.r. - ventral root

m.n. - mixed nerve

sep. - root separation

aff.c.b. - afferent nerve fibre cell bodies

Although only six afferent nerve-fibre cell bodies are visible in the ventral root of this section, a total of 98 were counted in the complete series of sections of the ventral root and mixed nerve beyond the point of separation.

(C179) S1 spinal nerve, 10 μ section: Holmes silver method

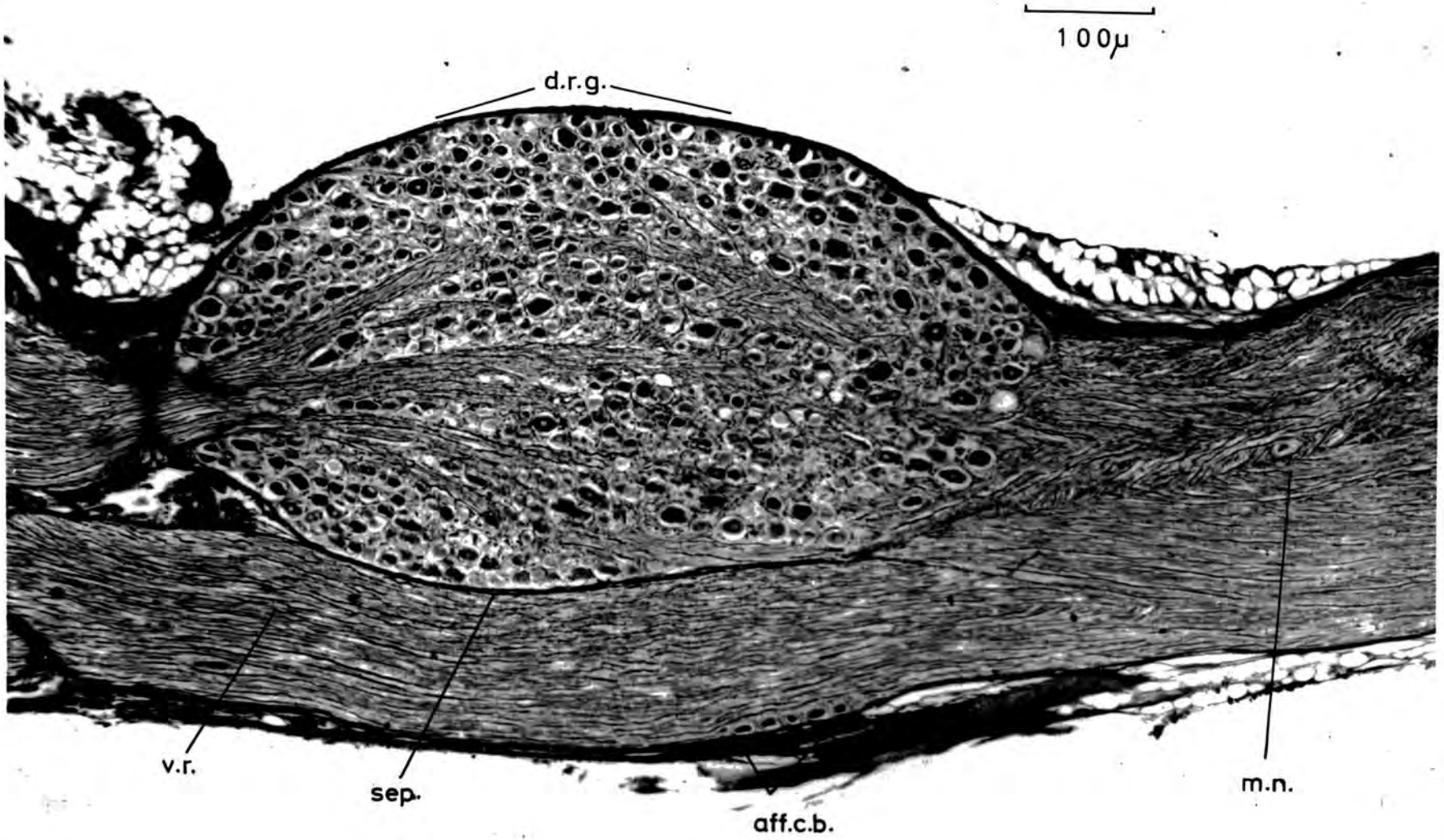
100μ
d.r.g.
v.r.
sep.
aff.c.b.
m.n.

Figure 7

Comparison of nerve-fibre diameter spectra of fusimotor, secondary and primary fibres (a) impregnated with silver (de Castro technique) and (b) stained with osmic acid

The difference between the equivalent spectra peak values varies. It is 2 μ for fusimotor fibres, 4 μ for secondary fibres and 2 μ for primary fibres.

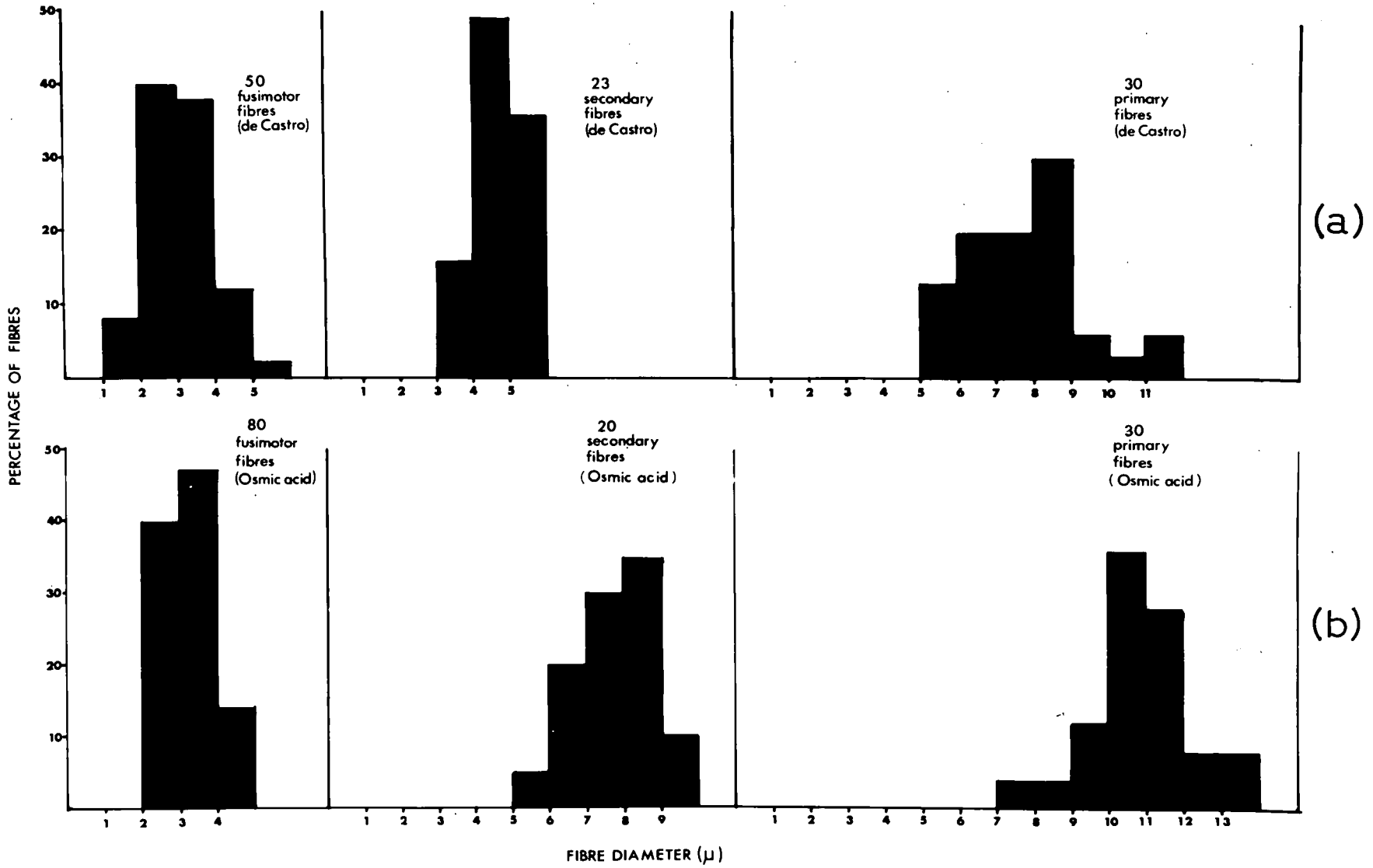
50
fusimotor
fibres
(de Castro)
23
secondary
fibres
(de Castro)
30
primary
fibres
(de Castro)
(a)
80
fusimotor
fibres
(Osmic acid)
20
secondary
fibres
(Osmic acid)
30
primary
fibres
(Osmic acid)
(b)
PERCENTAGE OF FIBRES
FIBRE DIAMETER (μ)

Figure 8

A graphical representation of the conversion of nerve fibre diameters from silver-impregnated material (de Castro technique) to diameters of osmic-acid stained nerves (representative of the fresh-state diameter)

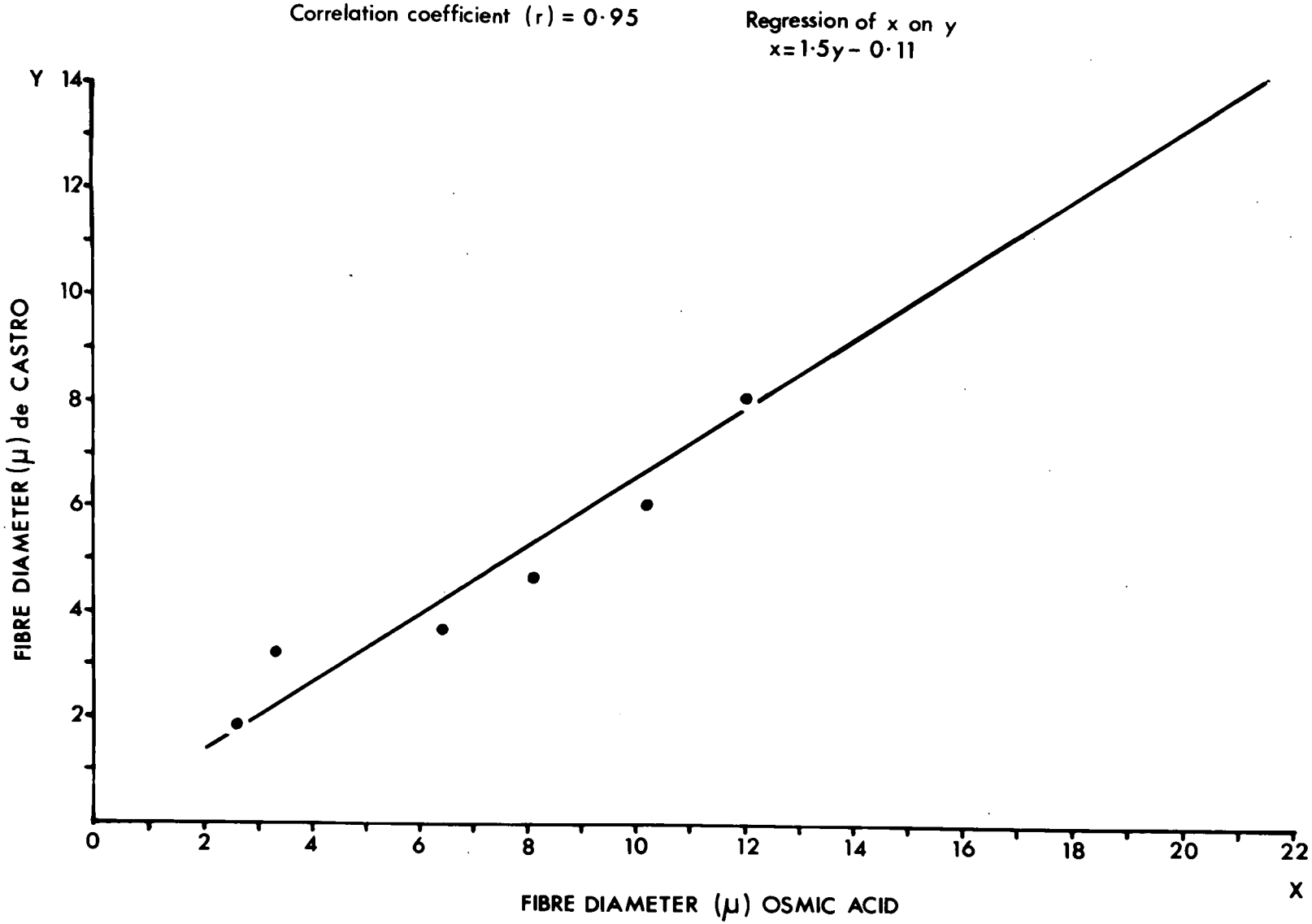
Correlation coefficient (r) = 0·95
Regression of x on y
x = 1·5y – 0·11
Y
14
12
10
8
6
4
2
FIBRE DIAMETER (μ) de CASTRO
0
2
4
6
8
10
12
14
16
18
20
22
X
FIBRE DIAMETER (μ) OSMIC ACID

Figure 9

Nerve-fibre diameter spectrum of soleus muscle-nerve (de Castro impregnation)

Total fibre diameter (axon + myelin) measurements, of myelinated nerve fibres only, were made 1 cm prior to nerve entry in a large fascicle of the de-efferentated and sympathectomized soleus muscle-nerve of C.189.

The peak diameter values of each Group are indicated by large numerals. They are equivalent to osmic diameters of 3 μ (Group III), 7.0 μ - 8.5 μ (Group II) and 15.5 μ (Group I). The following comparisons are drawn with previous data:-

	Extrapolation of peak-diameter values silver to osmic		Lloyd & Chang (1948)	Barker, Ip & Adal (1962)
GR.III	2.0 μ	3.0 μ	3.0 μ	4.0 μ
GR.II	5 u - 6 μ	7 u - 8.5 μ	7 u - 8 μ	7 u - 8 μ
GR.I	11.0 μ	15.5 μ	15.0 μ	16.0 μ

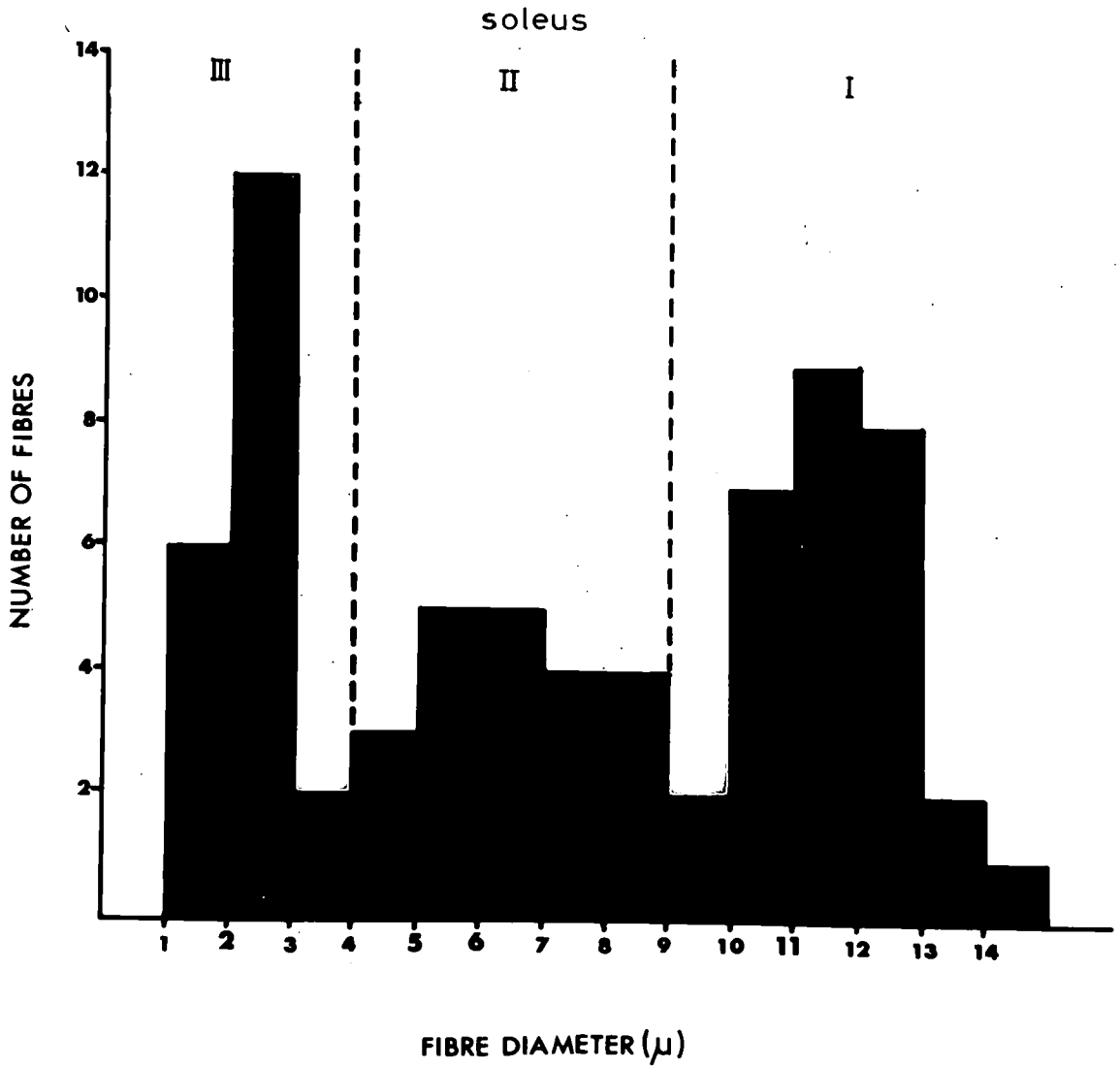
soleus
III
II
I
14
12
10
8
6
4
2
NUMBER OF FIBRES
1
2
3
4
5
6
7
8
9
10
11
12
13
14
FIBRE DIAMETER (μ)

Figure 10

Myelinated nerve-fibre diameter spectra of three muscle nerves

A. tibialis posterior - 4 nerves (cats 223, 228, 234, 235)

B. peroneus I - 3 nerves (cats 223, 228, 234)

C. peroneus III - 1 nerve (cat 234)

Weigert-Pal technique (Williams & Wendell-Smith 1960) :

5 μ sections

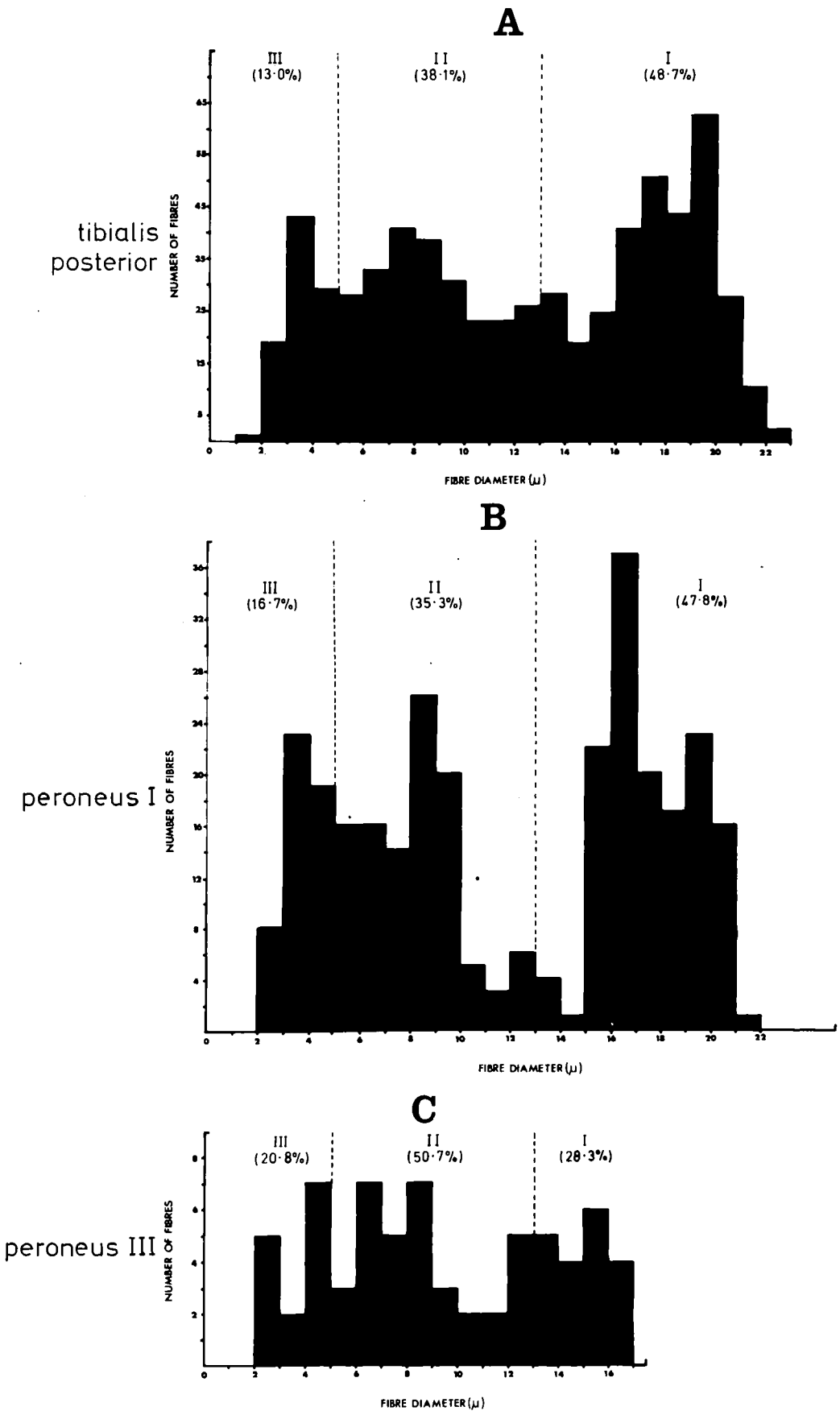
A
III
(13·0%)
II
(38·1%)
I
(48·7%)
tibialis
posterior
NUMBER OF FIBRES
FIBRE DIAMETER (μ)
B
III
(16·7%)
II
(35·3%)
I
(47·8%)
peroneus I
NUMBER OF FIBRES
FIBRE DIAMETER (μ)
C
III
(20·8%)
II
(50·7%)
I
(28·3%)
peroneus III
NUMBER OF FIBRES
FIBRE DIAMETER (μ)

Figure 11

Transverse section of a muscle nerve impregnated with silver (Holmes method)

n.my. - non-myelinated axons in a Schwann-cell bundle

d.d. - degenerated motor and sympathetic nerve-fibre debris

my. - axons of myelinated nerve fibres

my.h. - myelin 'halo'

(C228 tibialis posterior nerve 8 μ transverse section)


my.h.
n.my.
d.d.
my.

Figure 12

Non-myelinated sensory axons in Schwann-cell bundles

a. Transverse section of a muscle nerve
(C213, de-efferentated and sympathectomized tibialis posterior nerve, Holmes silver method, 8 μ section)

b. Teased vascular nerve trunk
(C223, de-efferentated and sympathectomized extensor digitorum longus muscle, de Castro silver impregnation)

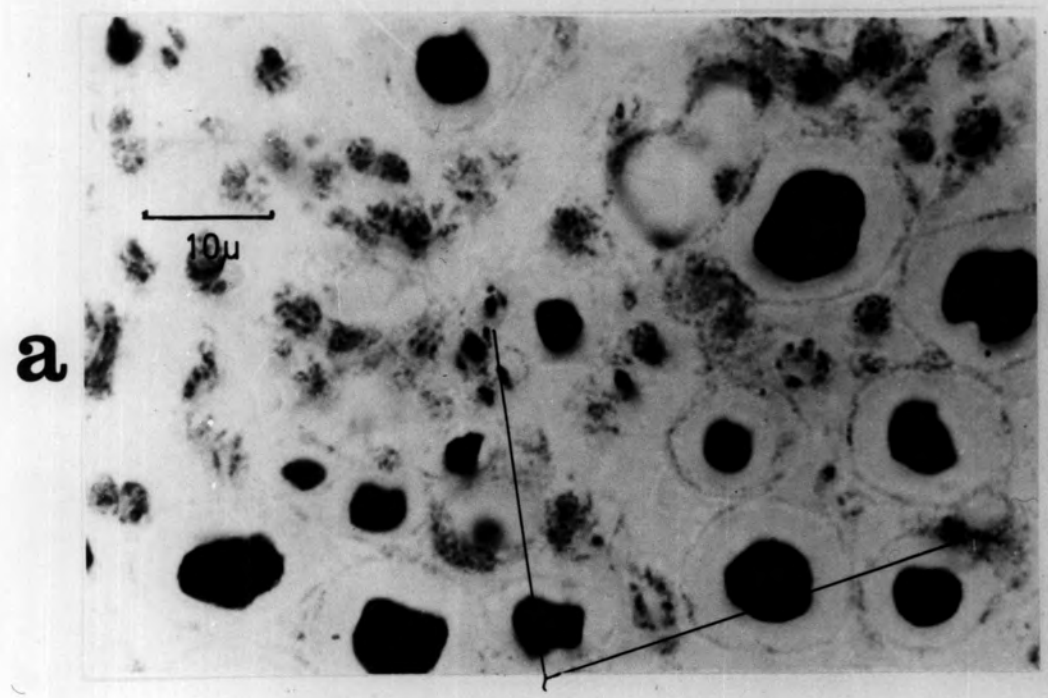
10μ
a
non-myelinated axons in a Schwann-cell bundle

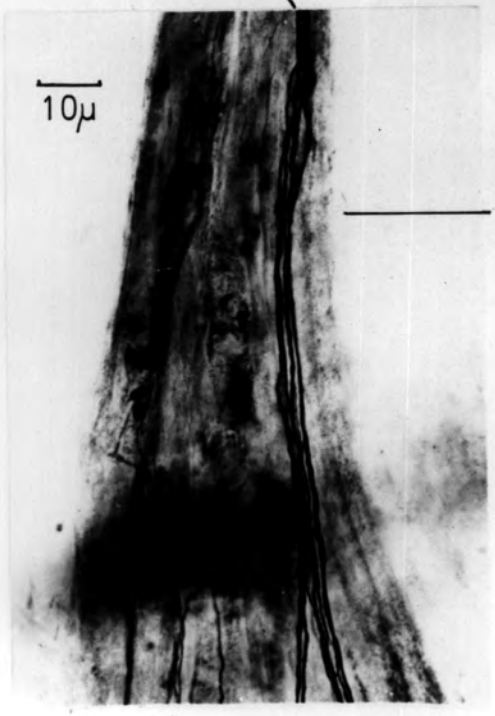
10μ
b
vascular nerve trunk

Figure 13

The fibre-diameter spectrum of the total sensory nerve-fibre component from skeletal muscle as determined by light microscopy

The non-myelinated sensory axons are aggregated within the 0.0 μ to 1.0 μ diameter range and form a large fourth group at the left-hand end of the spectrum

(The histogram is based on data obtained from the tibialis posterior nerves of de-efferentated and sympathectomized C234 and C235; Holmes silver method (Group IV), modified Weigert-Pal method (Groups III, II and I)

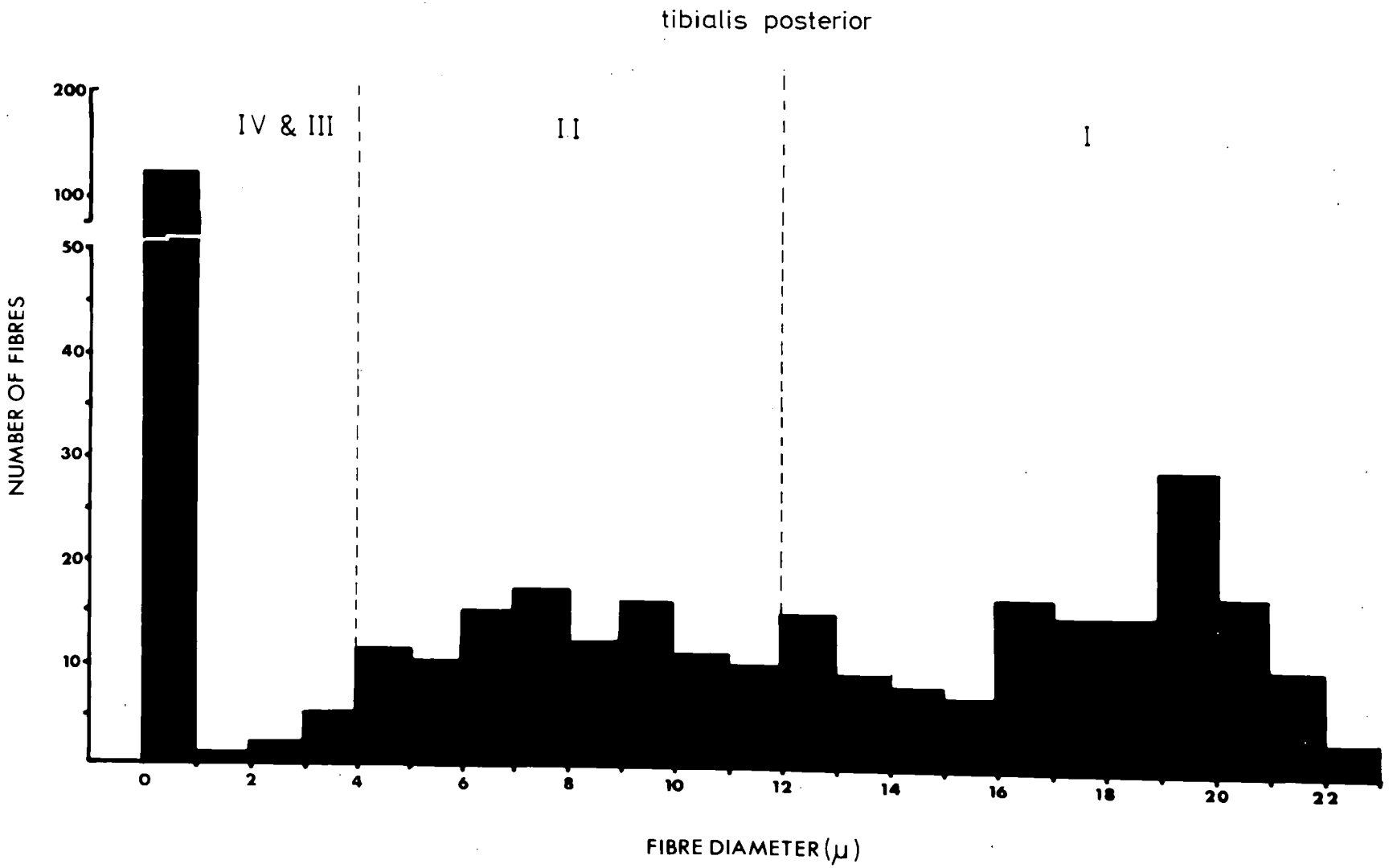
tibialis posterior
IV & III
II
I
200
100
50
40
30
20
10
NUMBER OF FIBRES
0
2
4
6
8
10
12
14
16
18
20
22
FIBRE DIAMETER (μ)

Figure 14

An electron micrograph illustrating a Schwann cell containing non-myelinated sensory axons

ax	-	non-myelinated sensory axon
bm	-	basement membrane
ct	-	cytoplasm of Schwann cell
IN_1	-	inflexions of the basement membrane
IN_2		
my.ax.	-	axon of myelinated sensory nerve fibres
m	-	mesaxon
N	-	Schwann-cell nucleus

(C234, de-efferentated and sympathectomized tibialis posterior nerve, Reynolds (1963) lead-citrate method)

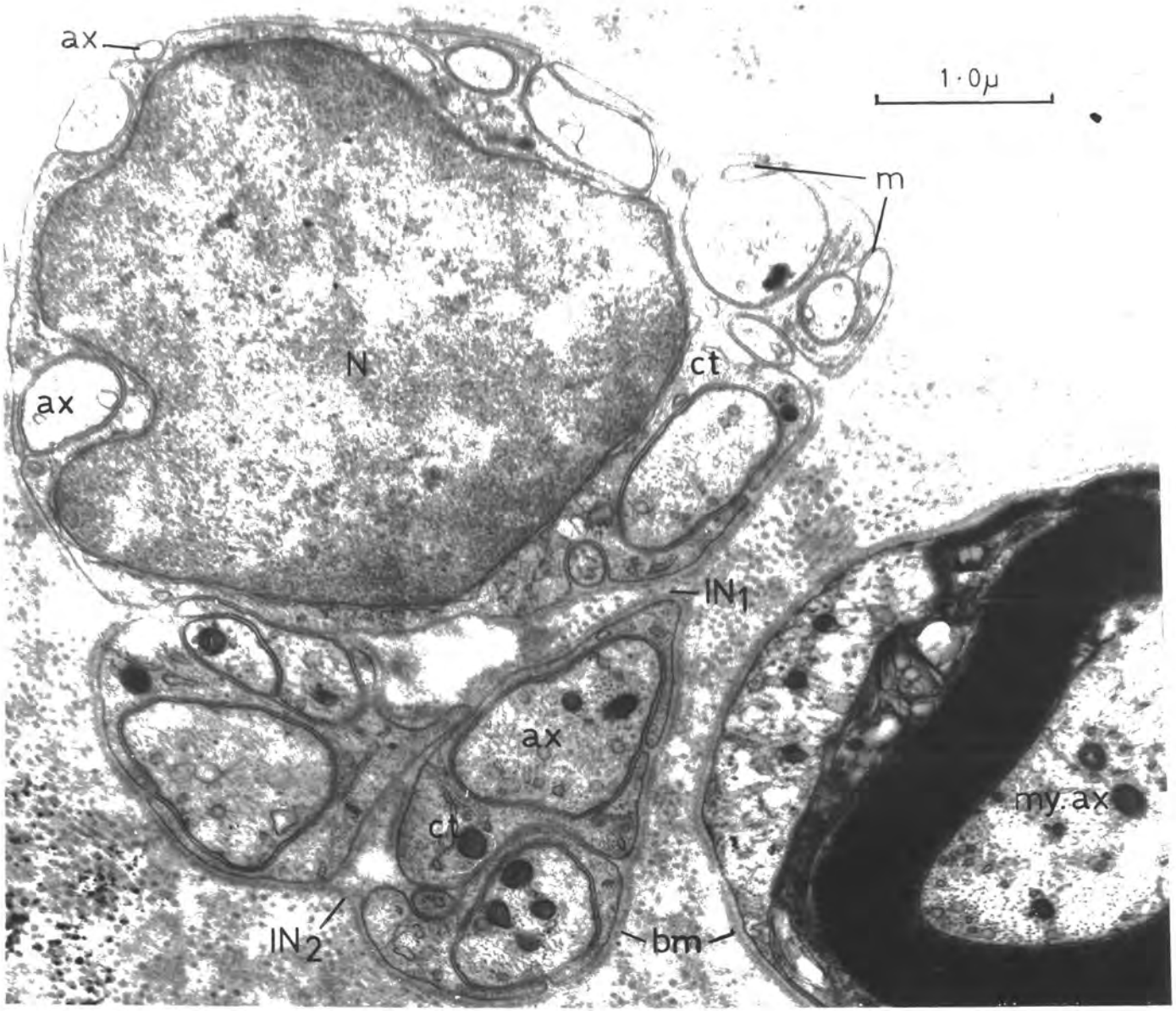
ax
1·0μ
m
N
ct
ax
IN1
ax
my. ax
ct
IN2
bm

Figure 15

Schwann-cell nucleus region of a small-myelinated (Group III) sensory nerve fibre

(C234, de-efferentated and sympathectomized tibialis posterior nerve; Reynolds (1963) lead-citrate method)

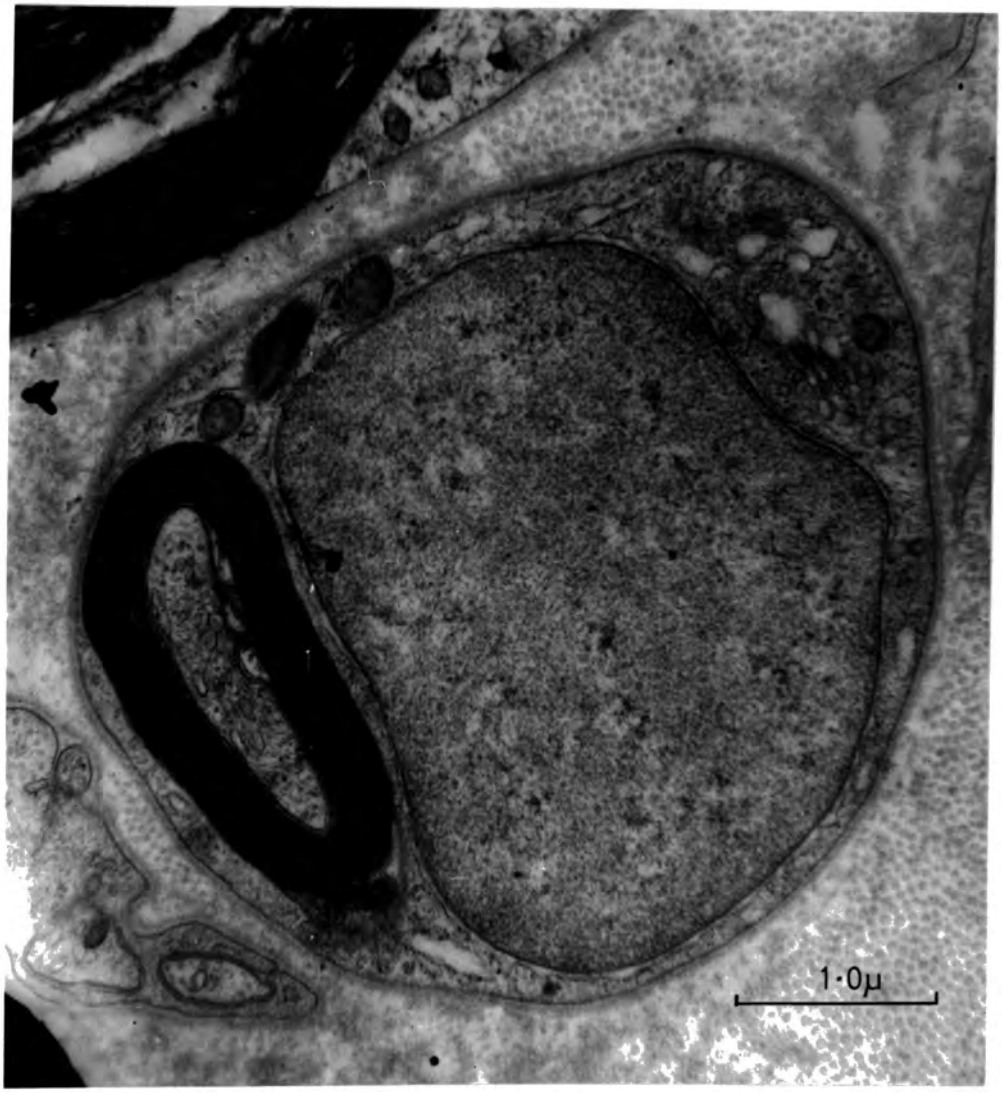
1·0μ

Figure 16

Non-myelinated sensory axons in Schwann-cell cytoplasm

AX - a non-myelinated axon, which is changing course in the cytoplasm, has consequently been cut in oblique section

ax_1 - single axons with a covering of cytoplasm

ax_2

n.ax. - virtually naked axons

ct - Schwann-cell cytoplasm

(C235, de-efferentated and sympathectomized tibialis posterior nerve, Reynolds (1963) lead-citrate method)

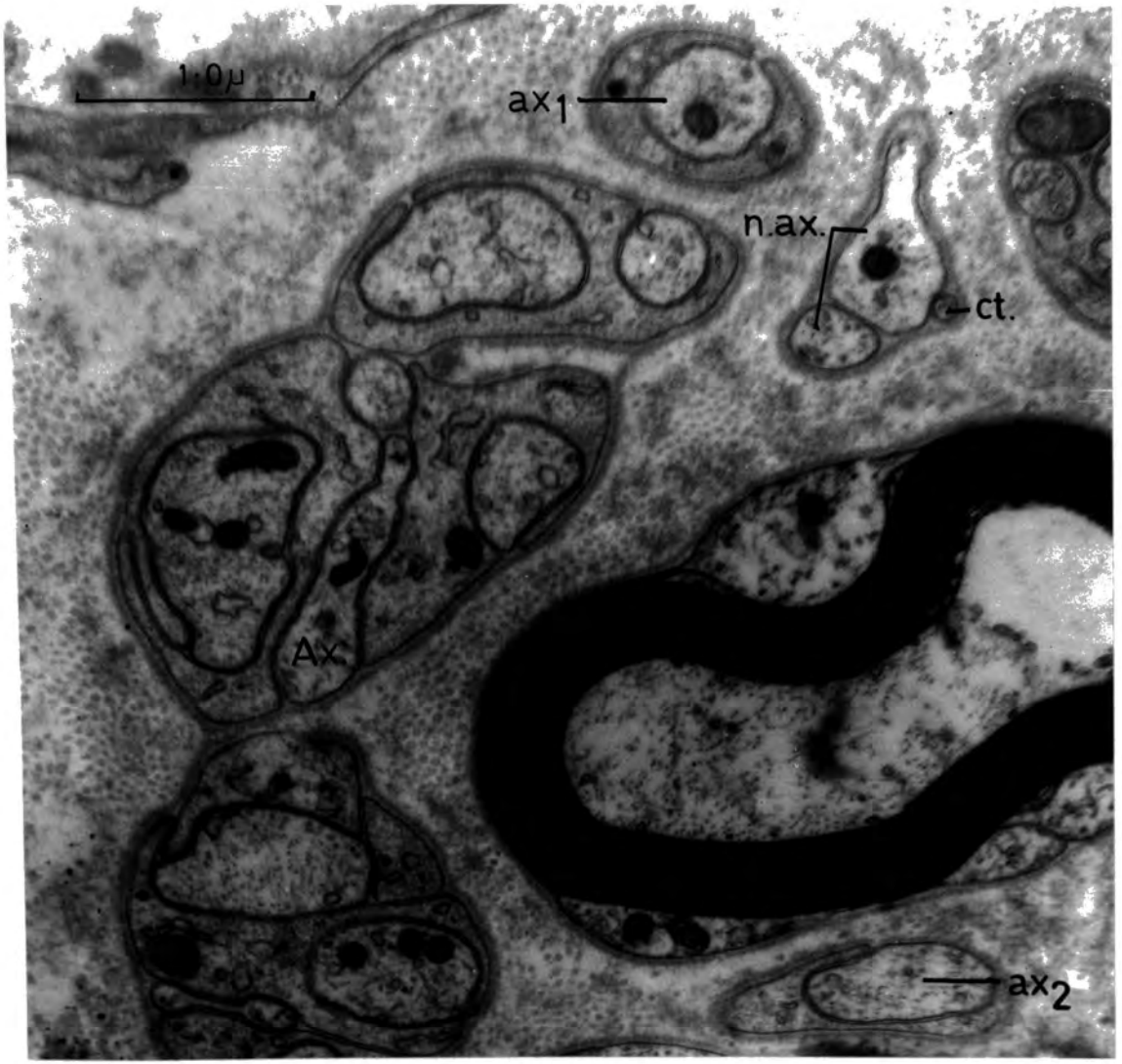
1·0μ
ax1
n.ax.
ct.
Ax
ax2

Figure 17

Illustration of various stages in the envelopment of non-myelinated sensory axons by the cytoplasm of a Schwann cell

See text for description of letters a - f

(C234, de-efferentated and sympathectomized tibialis posterior nerve, Reynolds (1963) lead-citrate method)

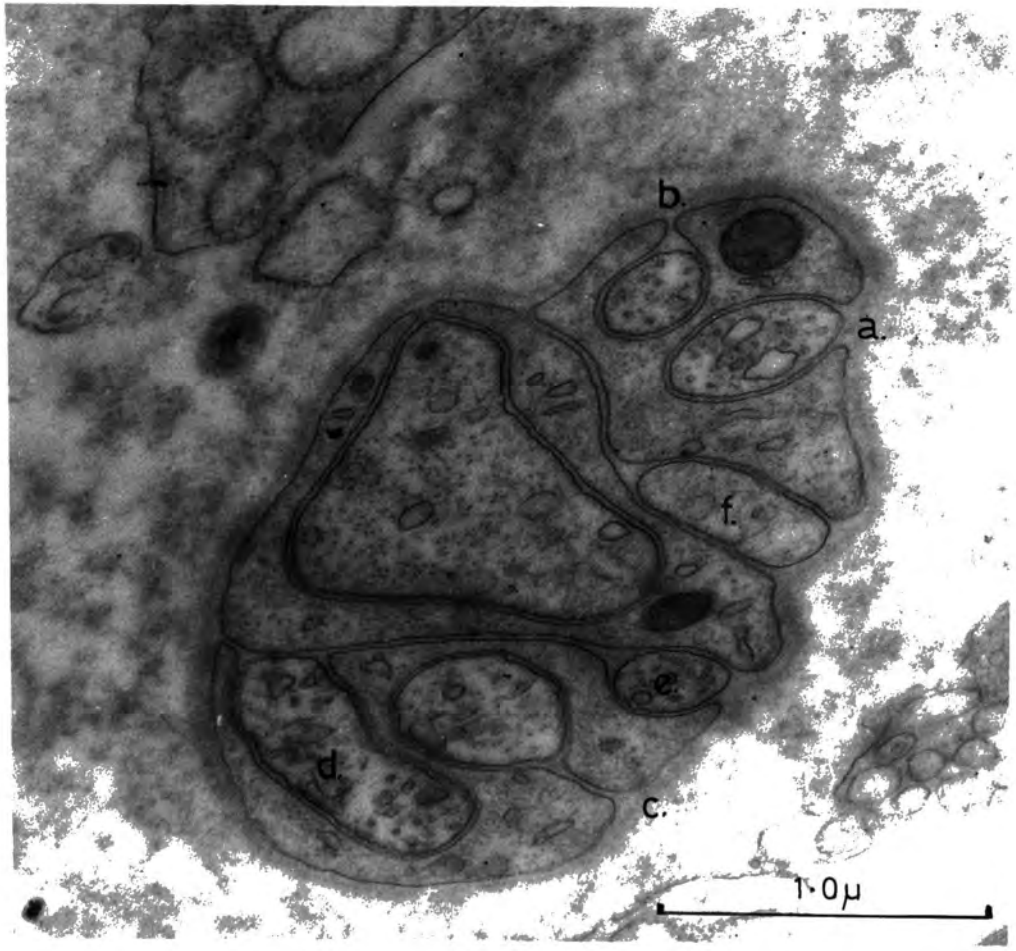
b.
a.
f.
e.
d.
c.
1·0μ

Figure 18

Non-myelinated sensory axons in Schwann-cell cytoplasm

cf - collagen fibres

'Ex.b.m. - 'external' basement membrane

'In.b.m. - 'internal' basement membrane

N - Schwann-cell nucleus

(C234, de-efferentated and sympathectomized tibialis posterior nerve; Reynolds (1963) lead-citrate method)

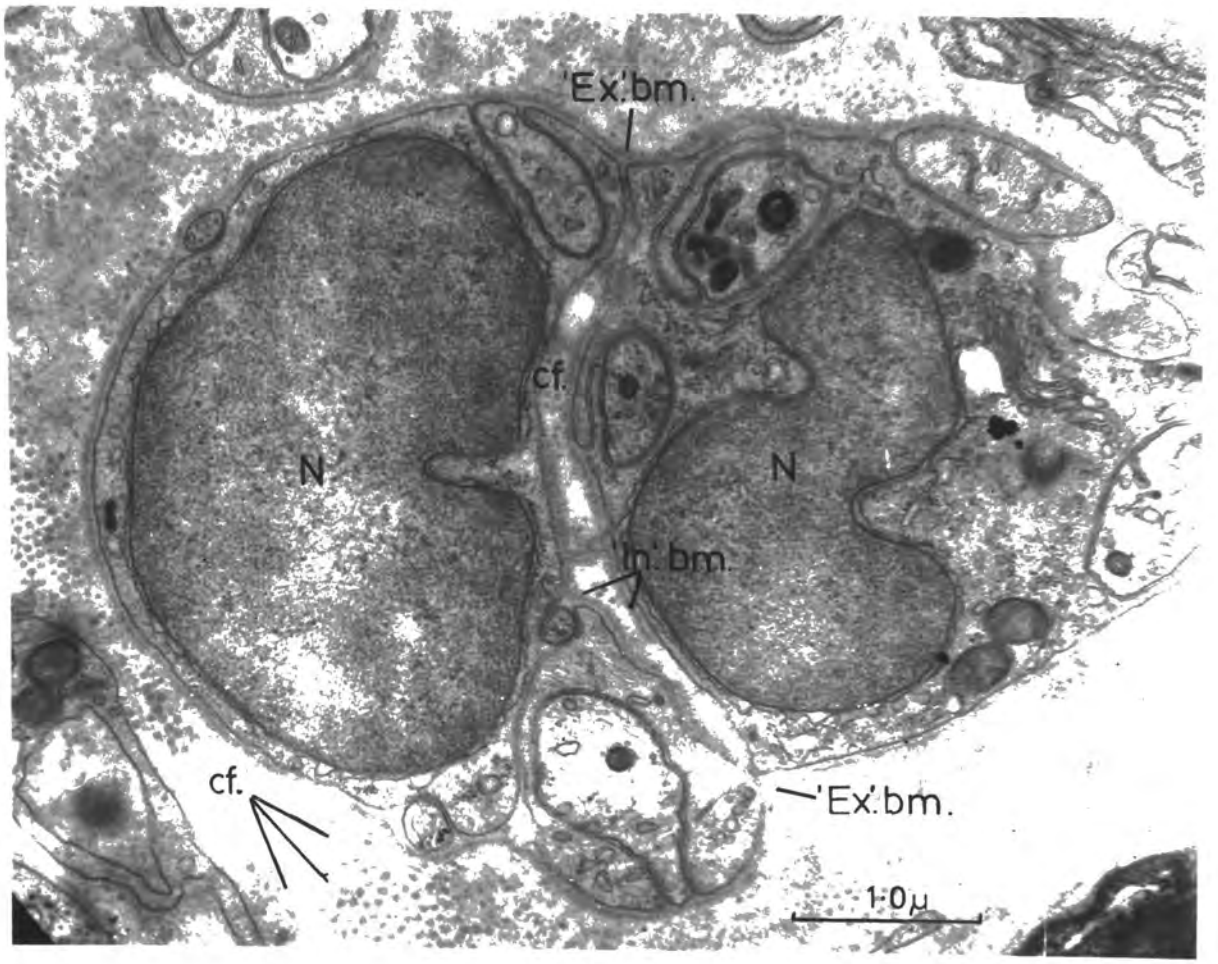
'Ex' bm.
cf.
N'
N
'In' bm.
cf.
'Ex' bm.
1·0μ

Figure 19

An illustration of the histological methods employed to obtain quantitative data of the sensory component of muscle nerves

The data in the illustration are from the tibialis posterior nerve of C235 (130 myelinated; 261 non-myelinated) and the peroneus III nerve of C234 (67 myelinated; the non-myelinated data in the remainder of the illustration)

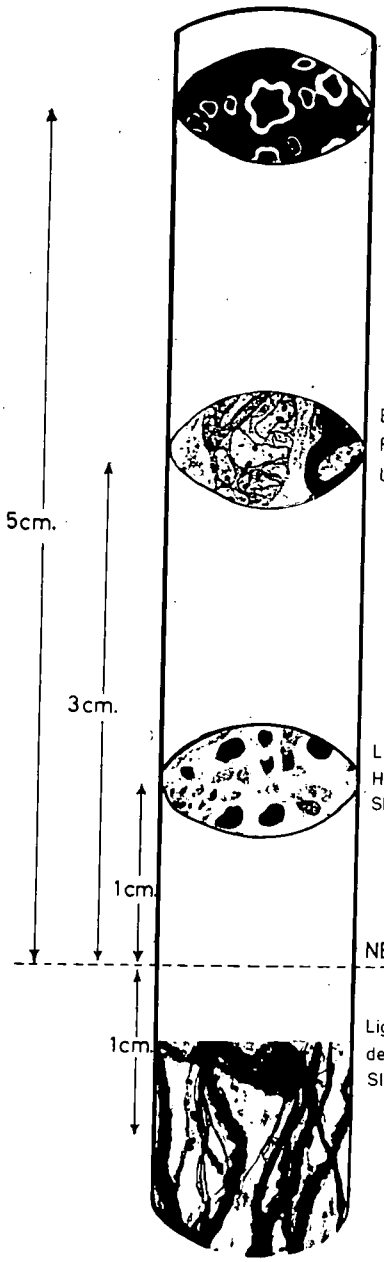

	myelinated fibres	non-myelinated axons	proportion myelinated : non-myelinated
Light microscopy Weigert-Pal method OSMIC ACID	67 & 130	— —	— —
Electron microscopy Reynolds method LEAD CITRATE	130	261	1 : 2·0
Light microscopy Holmes method SILVER	67	30	2·2 : 1
Light microscopy de Castro method SILVER	67	111	1 : 1·6

Figure 20

A comparison between sensory non-myelinated axon diameter spectra of a muscle nerve and dorsal roots

A. Diameter spectrum of 357 non-myelinated sensory axons from the tibialis posterior nerves of C234 and C235; 90% of the axons lie within the 0.15 μ to 0.60 μ diameter range and have a peak at 0.35 μ

B. Diameter spectrum of 1,941 non-myelinated sensory axons from the L_7 and S_1 dorsal roots of the cat (histogram construction of Gasser's data J.gen. physiol. vol.38. 1954-55. p.721) 96% of the axons lie within the 0.15 μ to 0.65 μ diameter range and have a peak between 0.20 μ and 0.35 μ

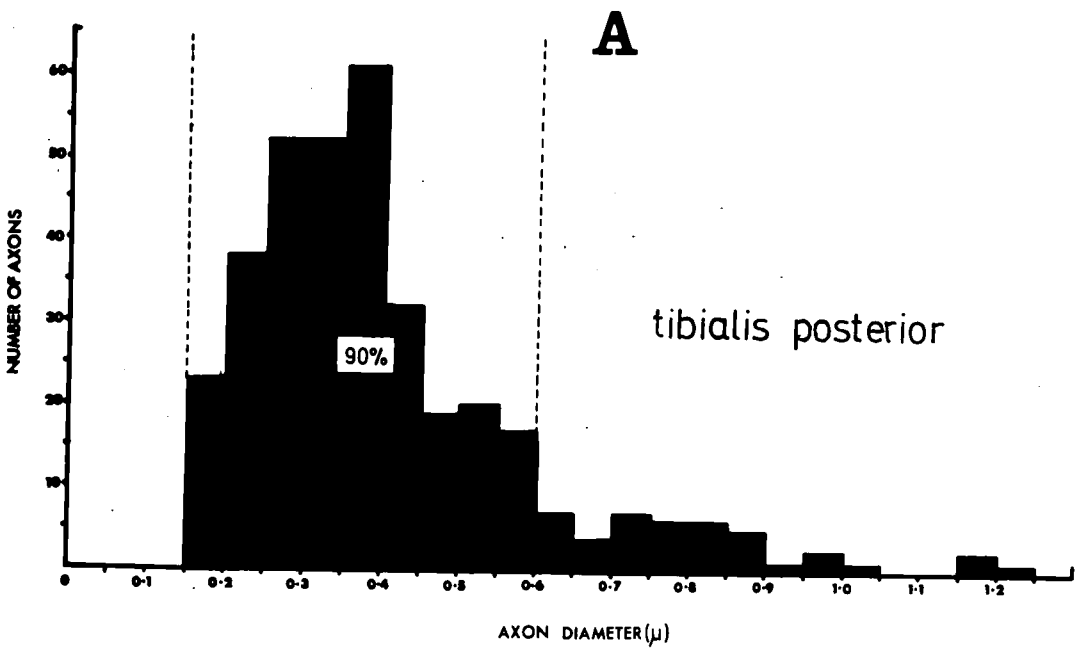
A
NUMBER OF AXONS
90%
tibialis posterior
0·1
0·2
0·3
0·4
0·5
0·6
0·7
0·8
0·9
1·0
1·1
1·2
AXON DIAMETER (μ)

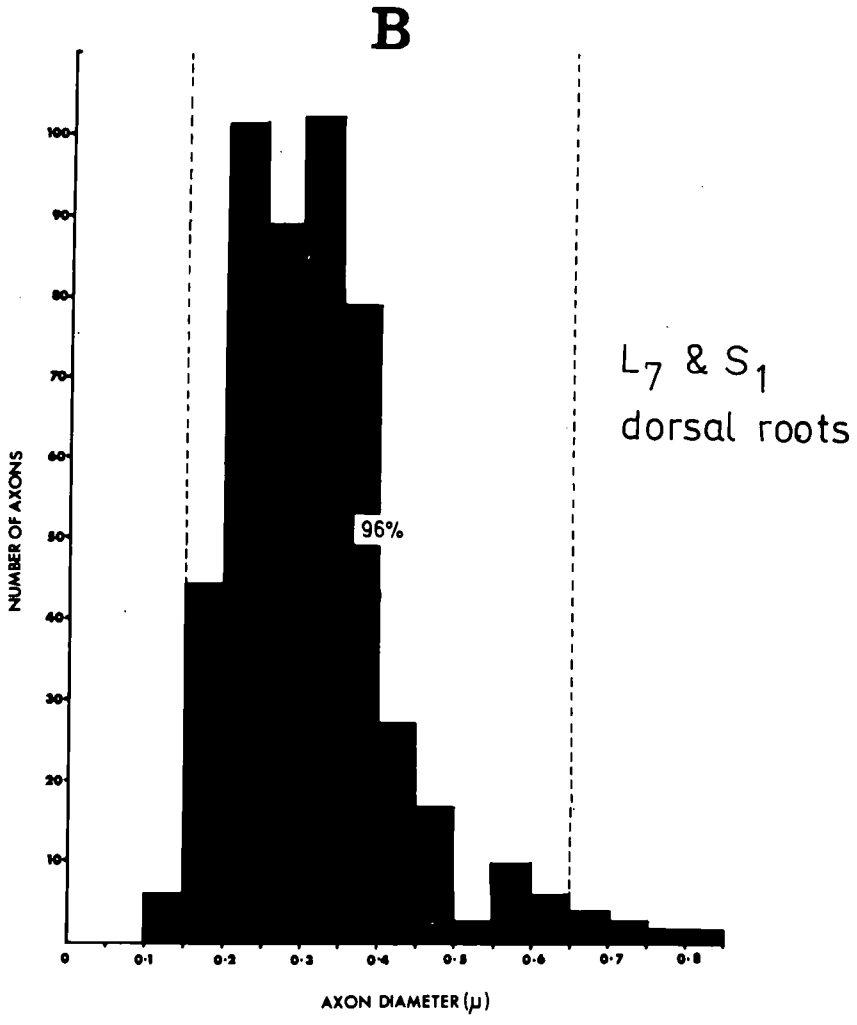
B
NUMBER OF AXONS
96%
L7 & S1
dorsal roots
0·1
0·2
0·3
0·4
0·5
0·6
0·7
0·8
AXON DIAMETER (μ)

Figure 21

The fibre-diameter spectrum of the total sensory nerve-fibre component from skeletal muscle based on light and electron microscope observations of the tibialis posterior nerve of the cat

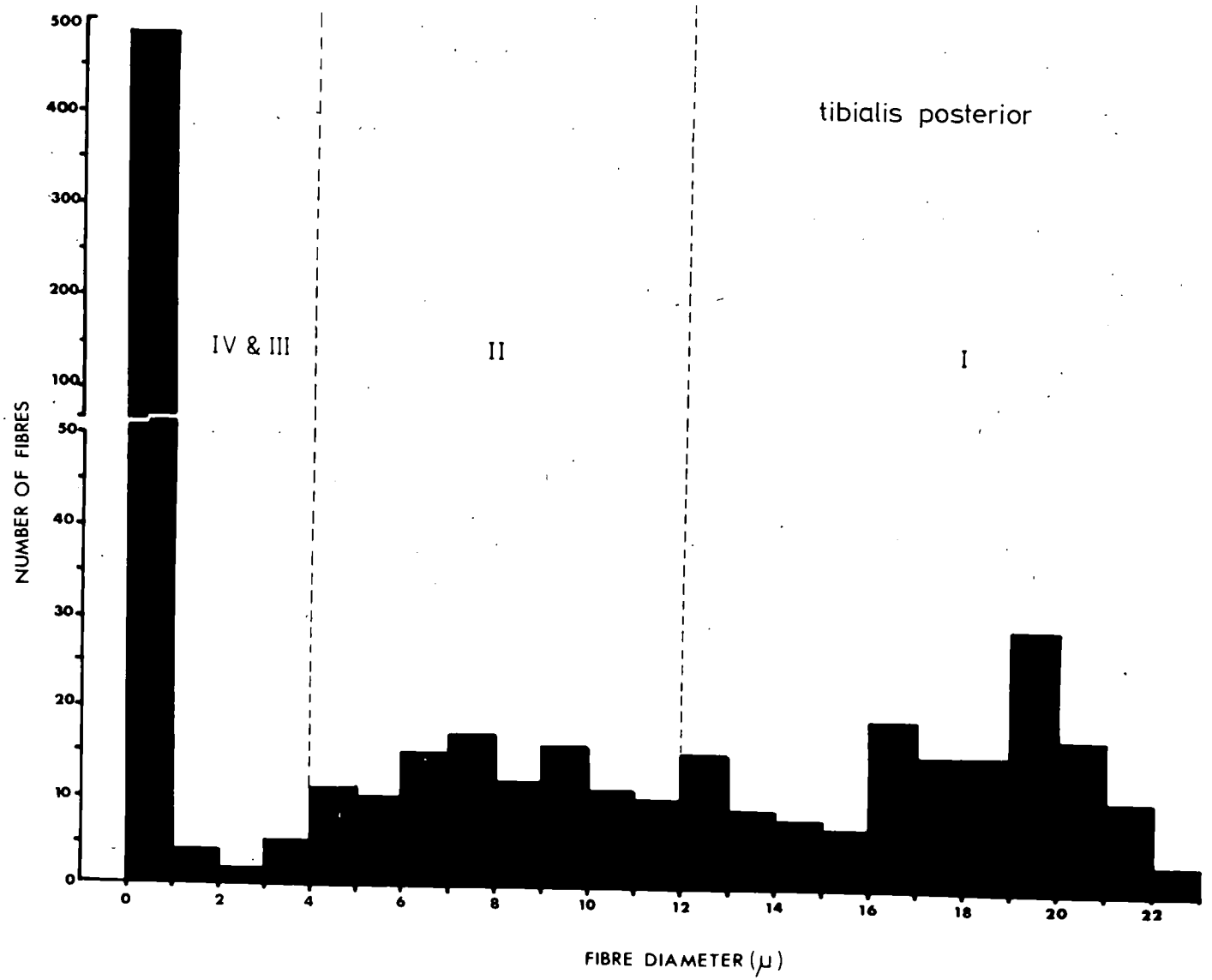
tibialis posterior
IV & III
II
I
NUMBER OF FIBRES
500
400
300
200
100
50
40
30
20
10
0
0
2
4
6
8
10
12
14
16
18
20
22
FIBRE DIAMETER (μ)

Figure 22

The deposition of fat cells along nerve trunks and in association with the blood system

(de Castro silver impregnation)


fat cells
capillary
network
intramuscular nerve trunk

Fig. 23

Part of intramuscular nerve 'tree' (de Castro impregnation, de-efferentated & sympathectomized cat peroneus muscle)

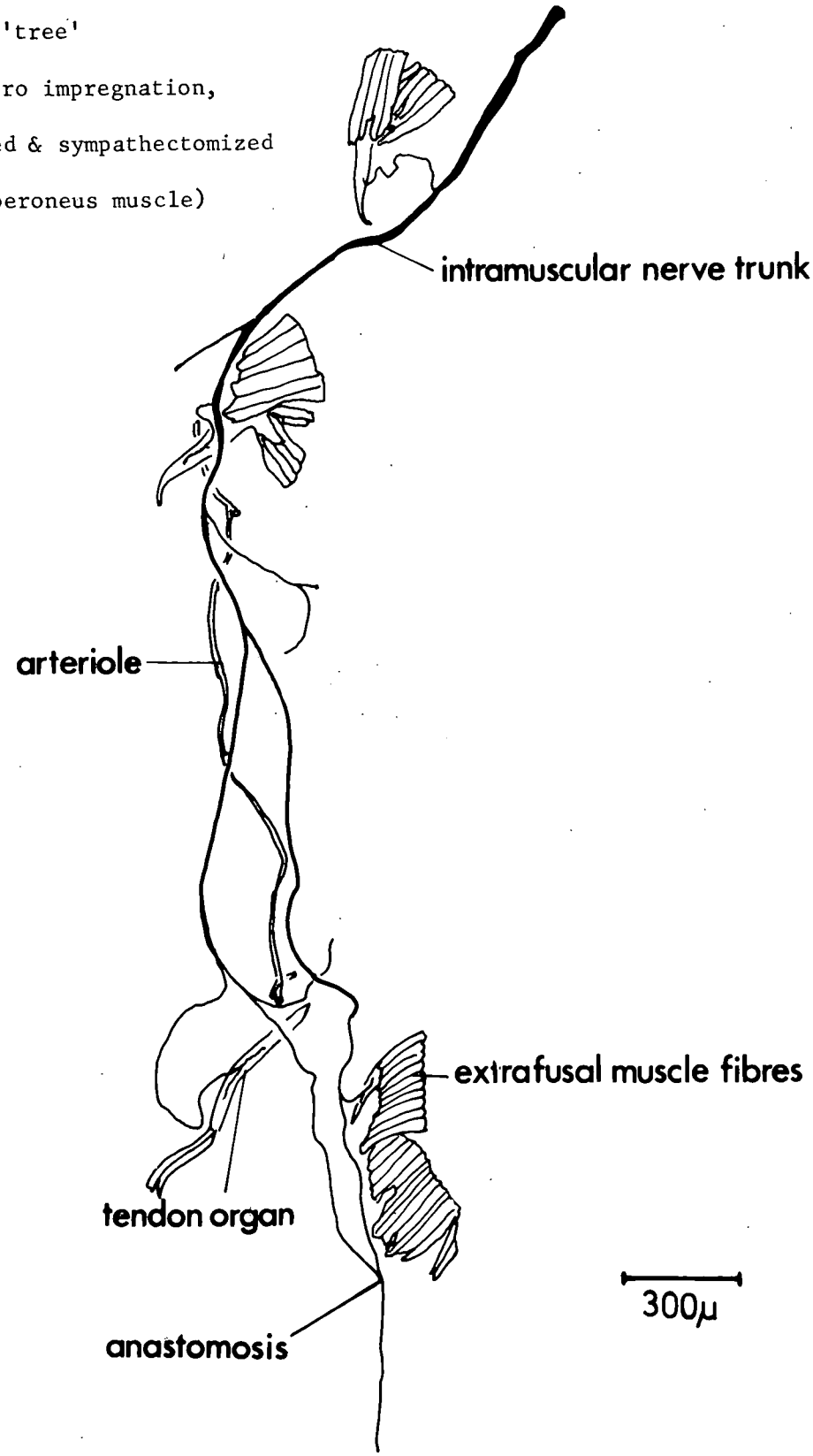

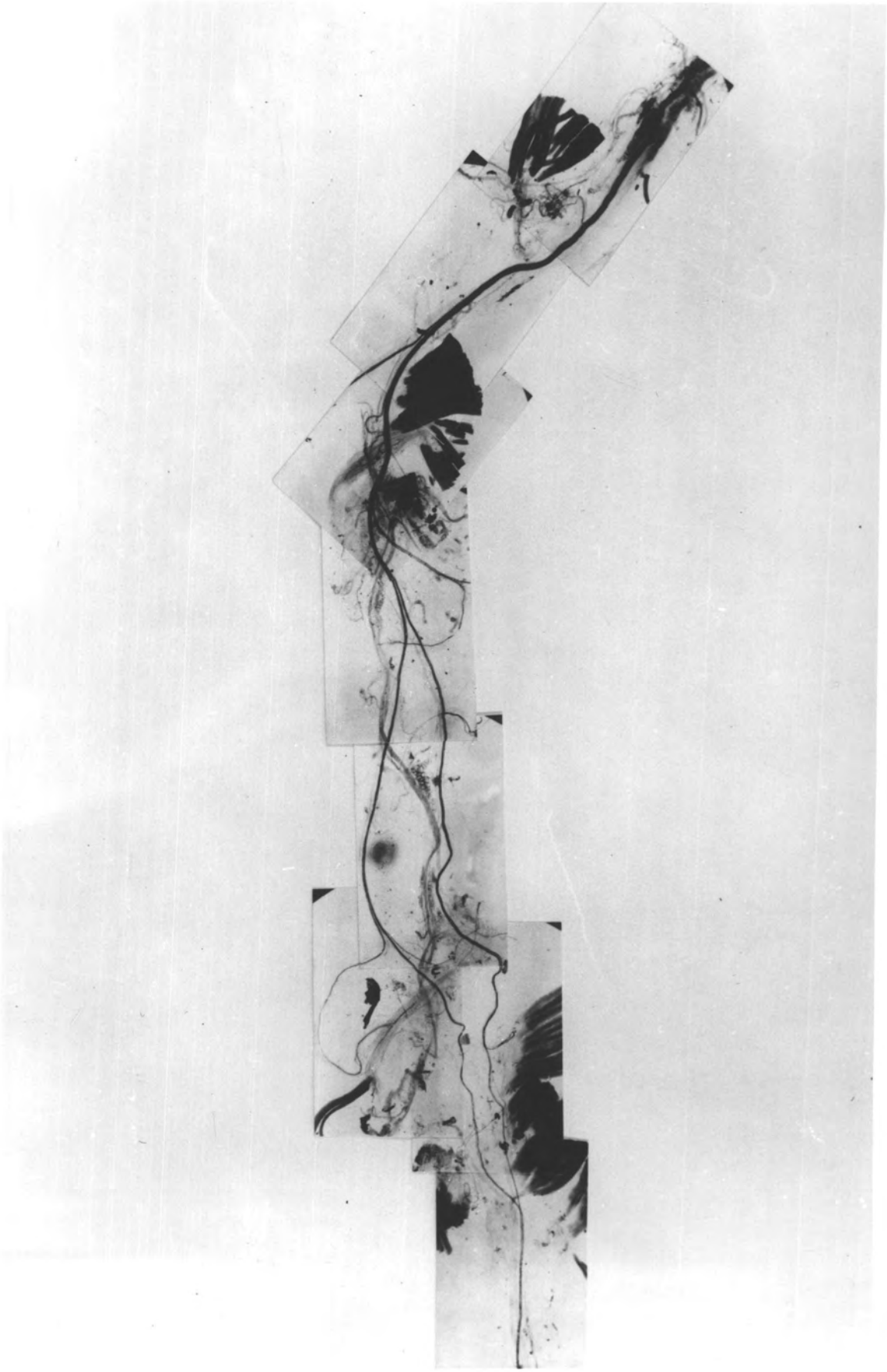

Fig. 24

Part of vascular nerve network

(de Castro impregnation, de-efferentated & sympathectomized cat peroneus muscle)

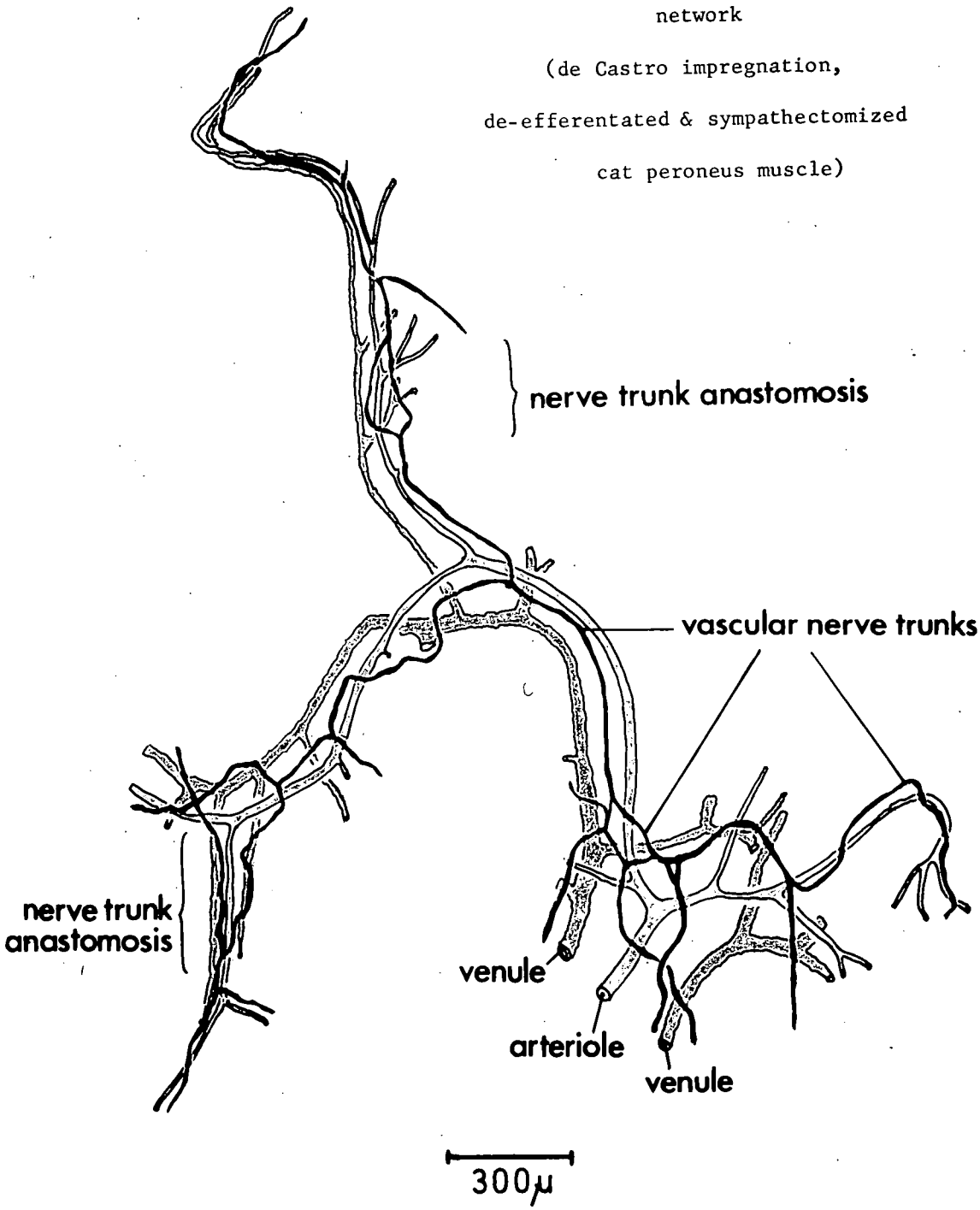

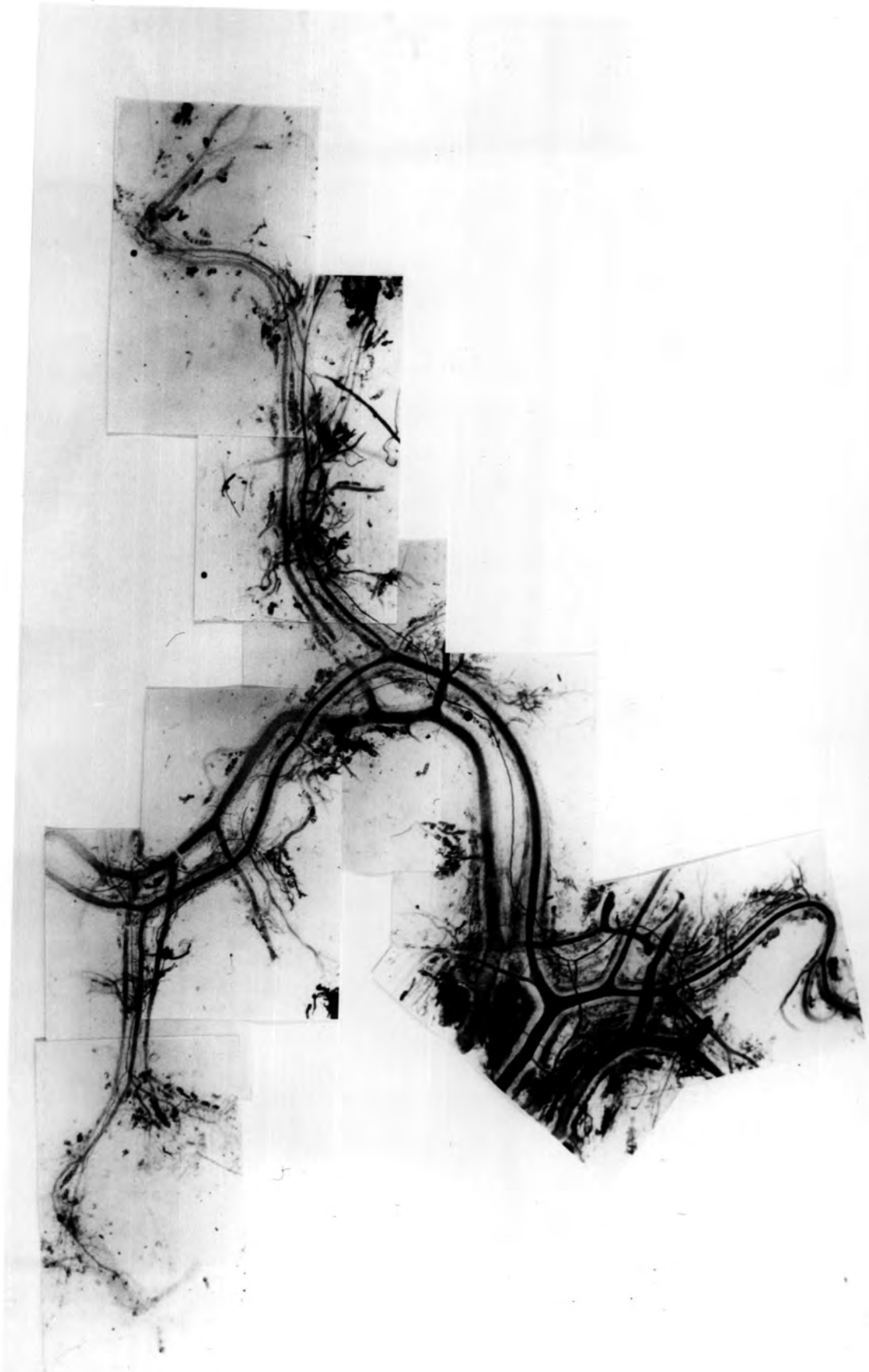

Figure 25

A diagrammatic representation of the disposition in muscles of the nerve trunks (both intramuscular and vascular) and blood vessels

A.	-	artery
a.	-	arteriole
a.v.b.	-	arterio-venular bridge
c.n.	-	capillary network
e.p.	-	epimysium
ex.m.f.	-	extrafusal muscle fibres
f.	-	fat cells
fas.	-	fascia
I.n.t.	-	intramuscular nerve trunk
M.n.	-	muscle nerve
p.	-	perimysium
t.	-	tendon
V.	-	vein
v.	-	venule
V.n.t.	-	vascular nerve trunk
V.p.	-	vascular plexus

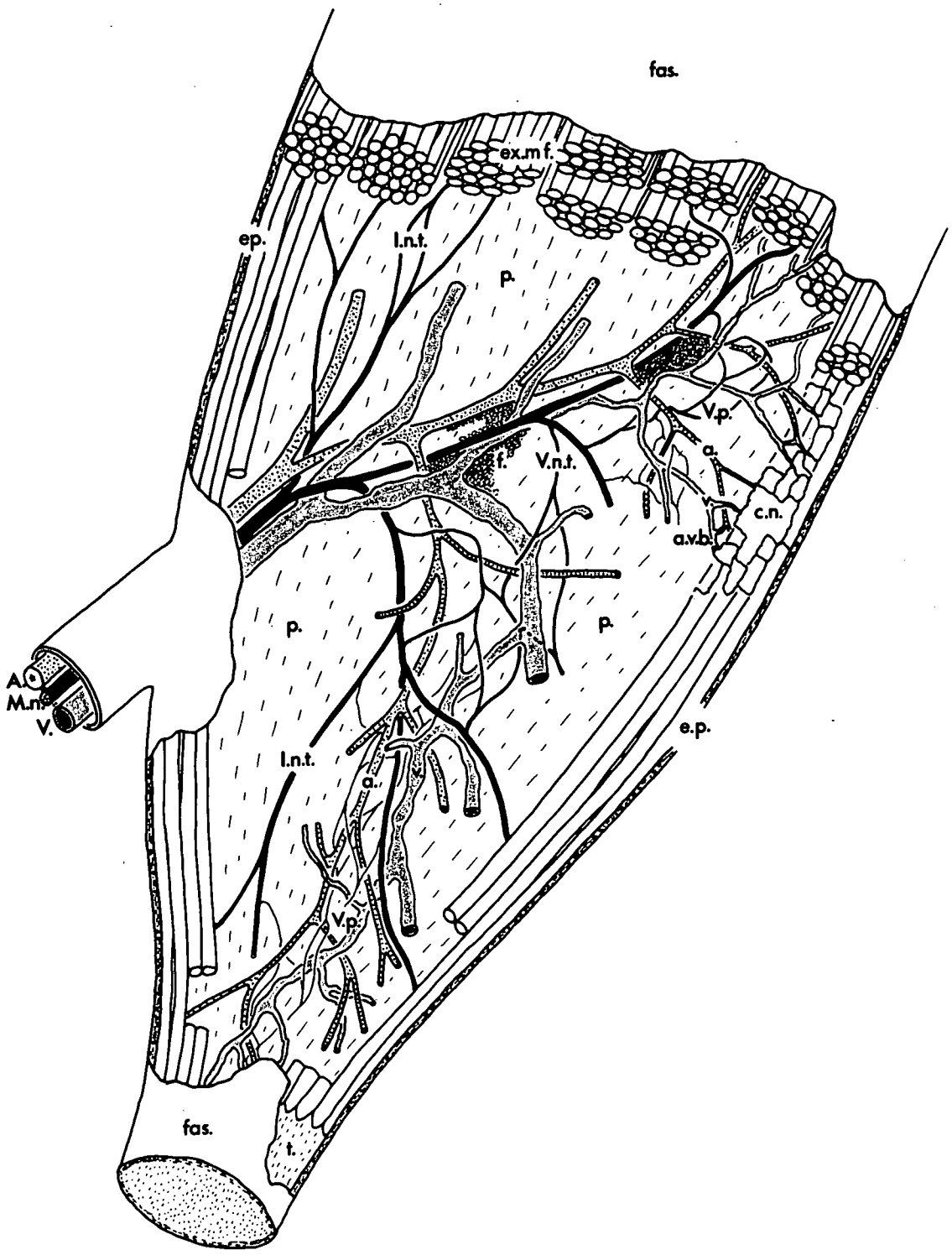
fas.
ex.m f.
ep.
l.n.t.
p.
V.p.
a.
f.
V.n.t.
c.n.
a.v.b.
p.
p.
A.
M.n.
V.
l.n.t.
a.
e.p.
V.p.
fas.
t.

Figure 26

Muscle-spindle primary and secondary endings

a. Tight coils of the primary ending around the intrafusal muscle fibres

b. S1 secondary ending with tight coils mainly around the nuclear-chain fibres

c. Tightly coiled S1 secondary and more loosely coiled S2 secondary

d. Loosely coiled S2 and S3 secondary endings

e. Loosely coiled S3 and S4 secondary endings

f. A loosely coiled S5 secondary ending with a 3.5 μ (2.5 μ) parent fibre

(All spindles from teased de Castro impregnated muscles of cat hindlimb)

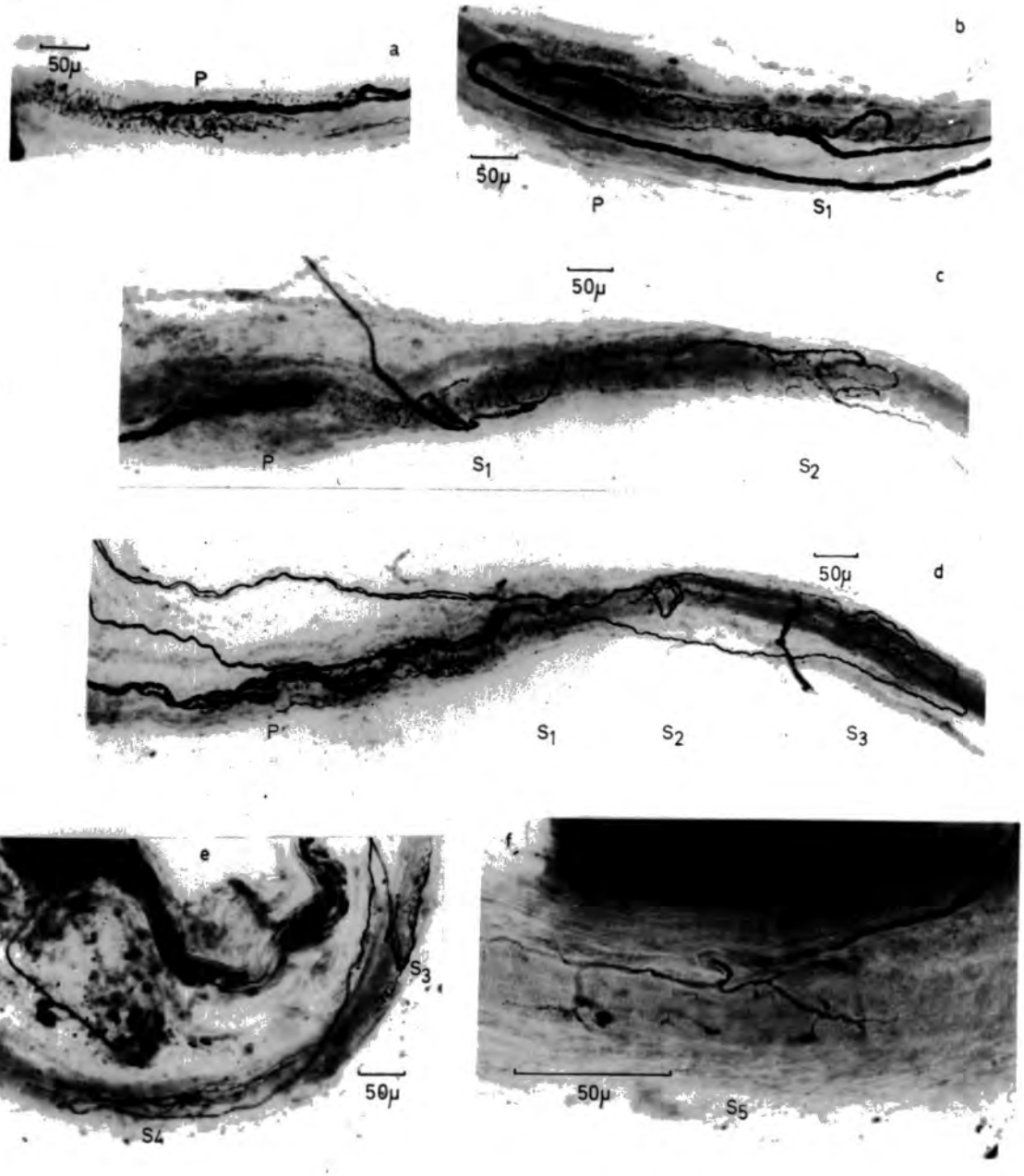
a
50μ
P
b
50μ
P
S1
c
50μ
P
S1
S2
d
50μ
P
S1
S2
S3
e
S3
50μ
S4
f
50μ
S5

Figure 27

Ramifying free terminals in a muscle spindle and surrounding connective tissue

The enclosed area is illustrated in the following figure in the form of tracings

f.t. - free terminals

P. & S1 - position of primary and S1 secondary endings

(C189, de-efferentated and sympathectomized extensor digitorum brevis muscle, de Castro silver impregnation)

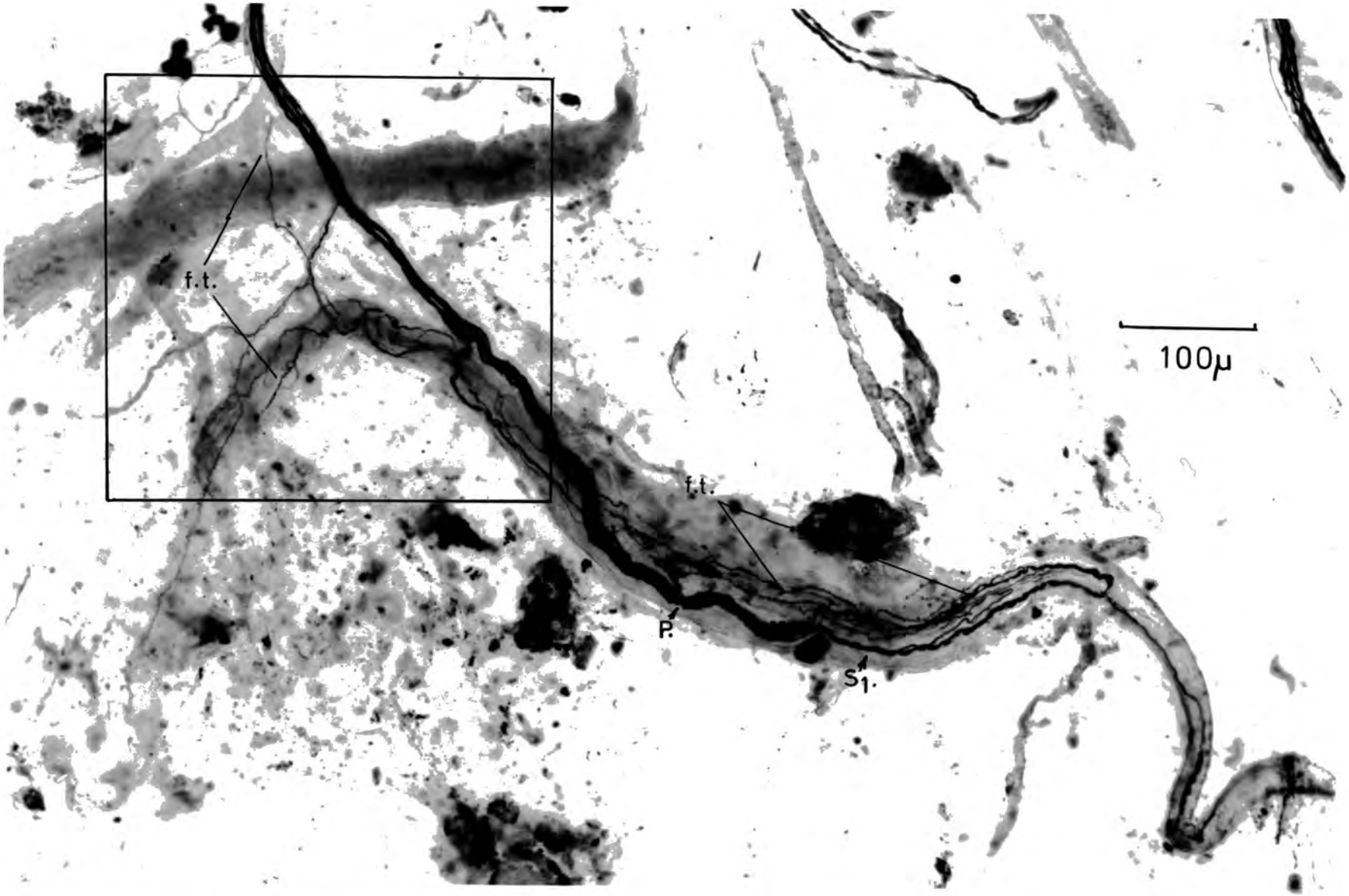
f.t.
f.t.
100μ
P.
S1.

Figure 28

Tracings of the free terminal ramifications of the two free-ending parent fibres that innervate the muscle spindle of Fig. 27

Both fibres, illustrated separately in a and b also send terminals across the equitorial region to the opposite pole of the spindle

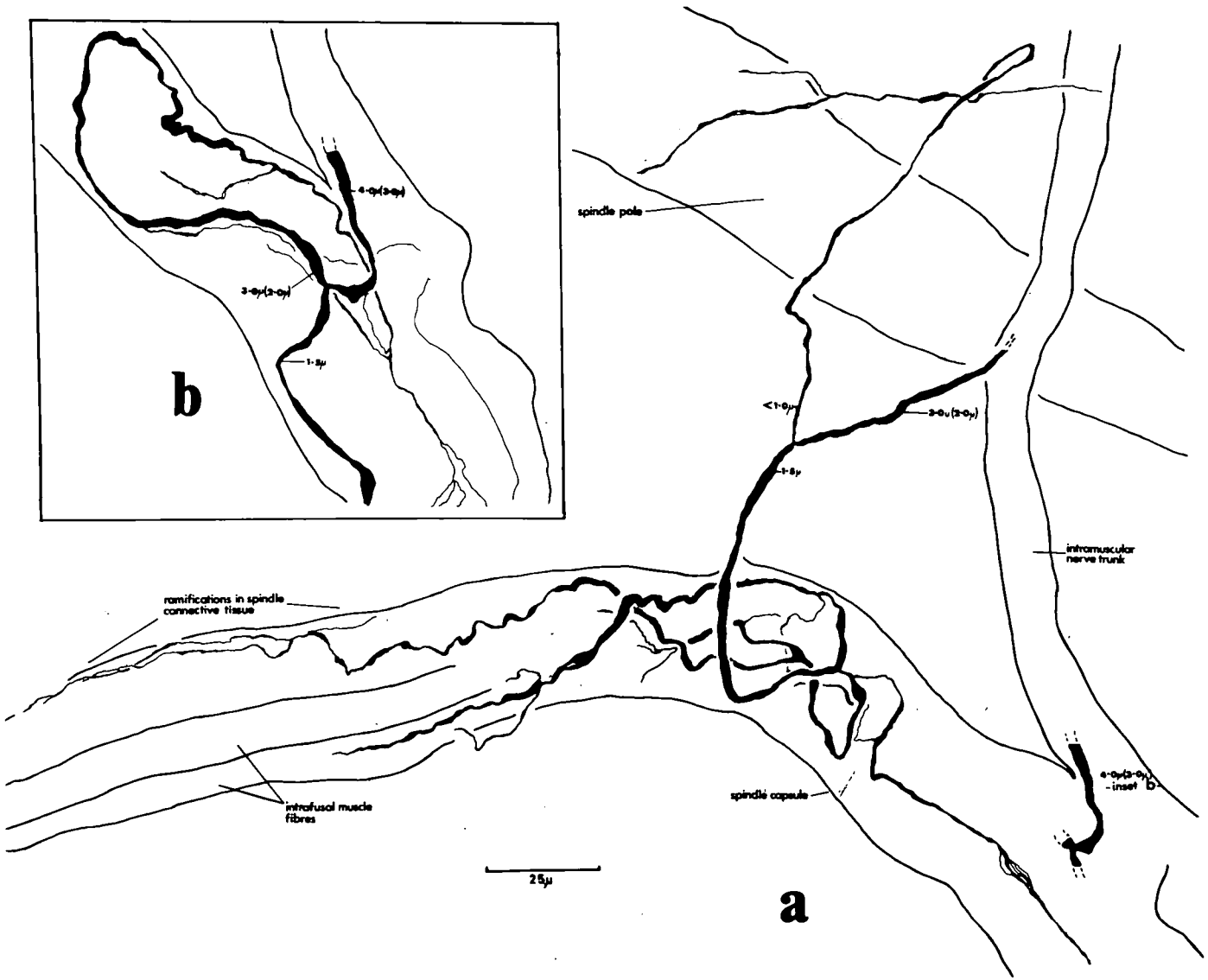
b
spindle pole
intramuscular nerve trunk
ramifications in spindle connective tissue
intrafusal muscle fibres
spindle capsule
inset b
25μ
a

Figure 29

Tracings of free terminal ramifications in the polar regions of two muscle spindles

a. Extensive free ramifications among the intrafusal muscle fibres are formed from a single parent fibre 1.5 μ in diameter. One of the terminals leaves the spindle and re-enters the intramuscular nerve trunk

b. A single free terminal ramification in the connective tissue between two intrafusal muscle fibres is derived, as far as can be seen in the intramuscular nerve trunk, from a 0.5 μ - 1.0 μ parent fibre

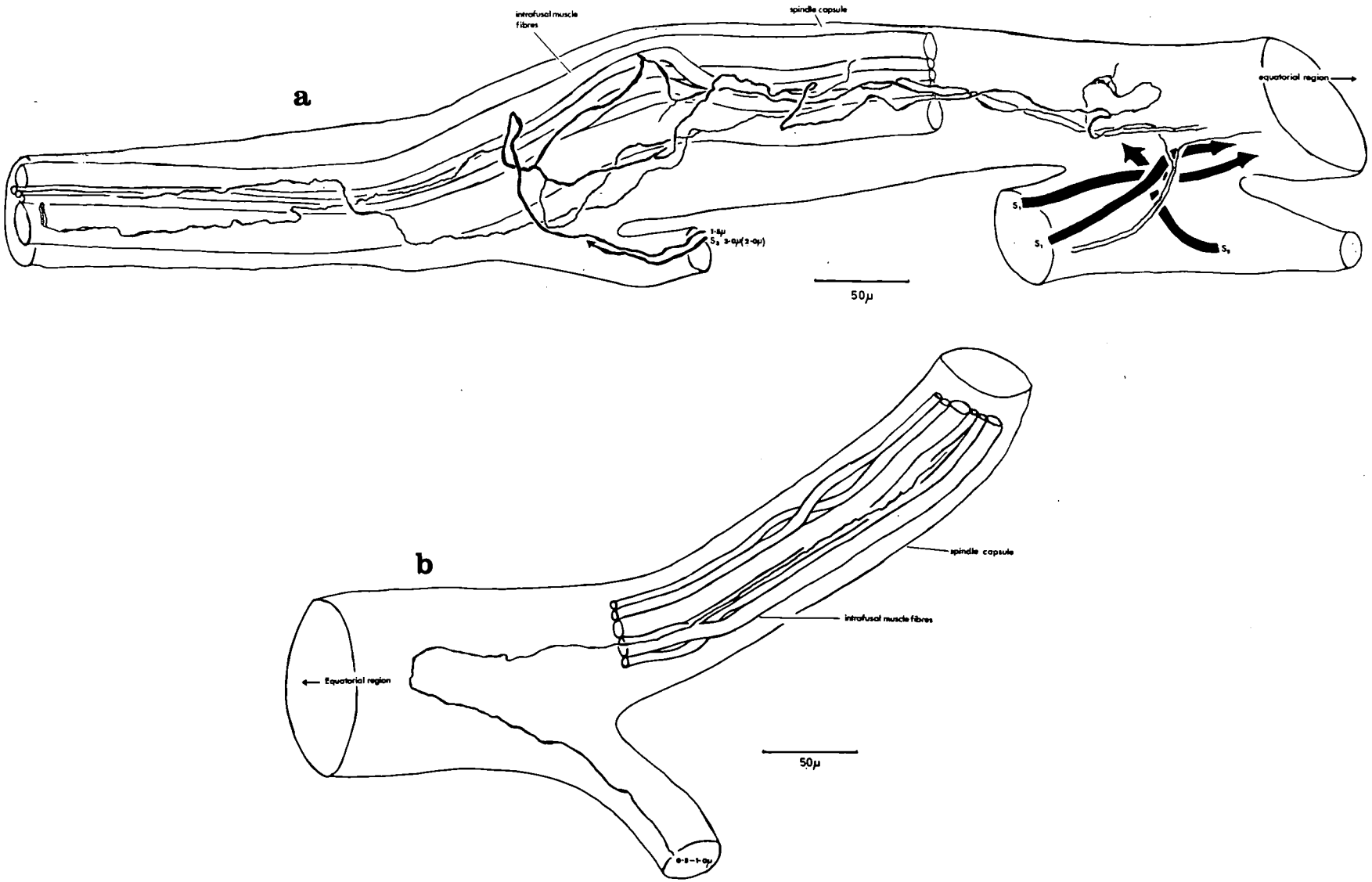
a
intrafusal muscle fibres
spindle capsule
equatorial region
1-8μ
S2 3-0μ(2-0μ)
S1
S1
S2
50μ
b
spindle capsule
intrafusal muscle fibres
Equatorial region
0·8–1·0μ
50μ

Figure 30

Ramifying free terminals in a tendon organ and surrounding tendon tissue

a - arteriole

Ib - tendon organ innervation

f_1 - free-ending parent fibres referred to in the text

f_2

f.c. - fat cells

t. - tendon tissue

t.n. - terminal node

t.o. - tendon organ

(C189, de-efferentated and sympathectomized peroneus III muscle, de Castro silver impregnation)

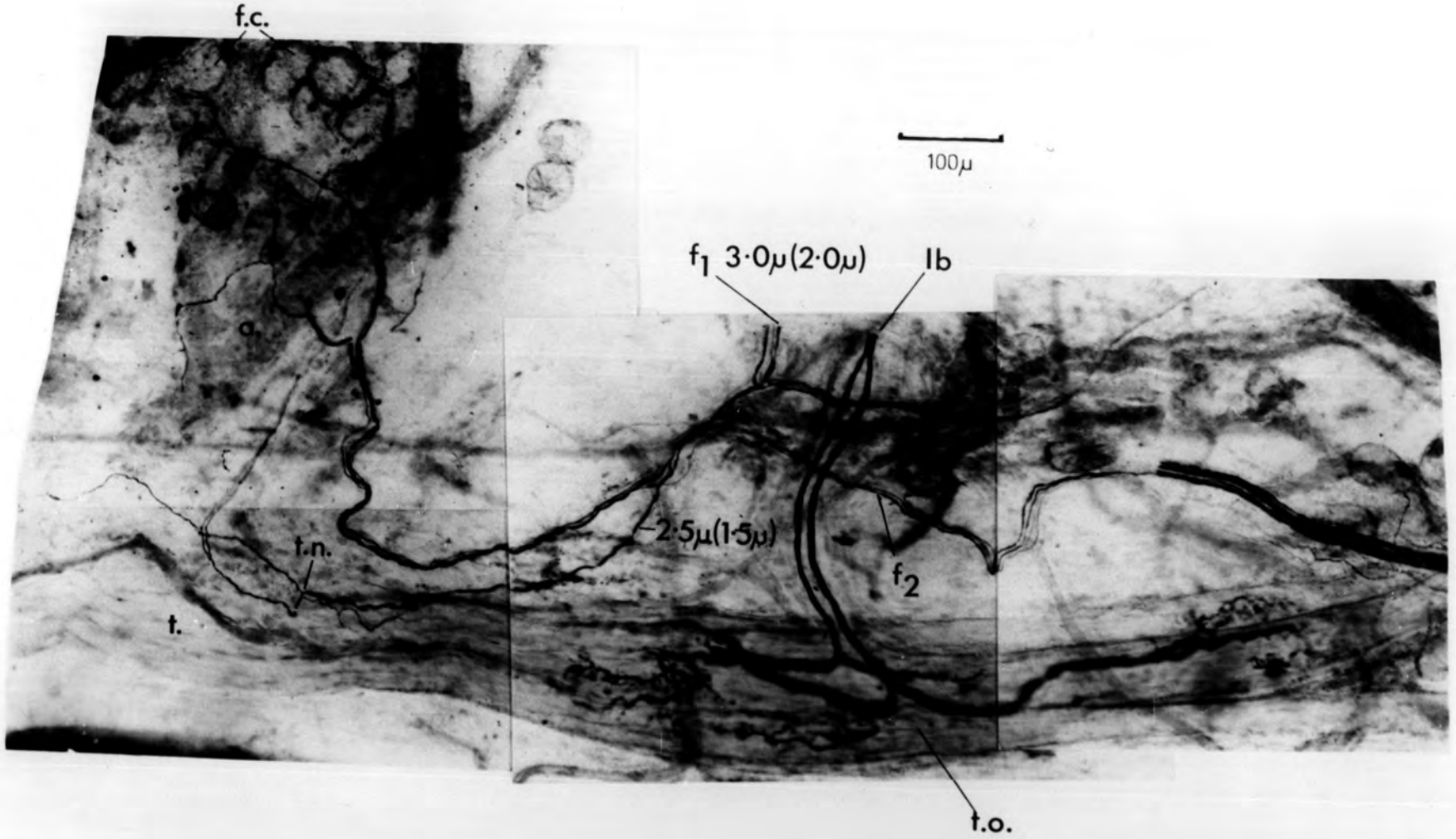
f.c.
100μ
f1 3·0μ(2·0μ)
Ib
a.
2·5μ(1·5μ)
t.n.
f2
t.
t.o.

Figure 31

a. Free ramifying terminals in the capsule of a tendon organ

(C213, de-efferentated and sympathectomized tibialis anterior muscle; de Castro silver impregnation)

b. Free ramifying terminals in tendon tissue close to a tendon organ

The 1.5 μ fibre runs with the Ib fibre across the tendon organ and then divides repeatedly to produce free terminals in the tendon tissue (C160, normal flexor digitorum brevis muscle, de Castro impregnation)

c. Free ramifying terminals in tendon organ capsule

(Rb. 41; normal peroneus I muscle; de Castro silver impregnation)

Ib - tendon organ innervation

ex.m.f. - extrafusal muscle fibres

f.t. - free terminals

int.n.t. - intramuscular nerve trunk

T - tendon

t.o. - tendon organ

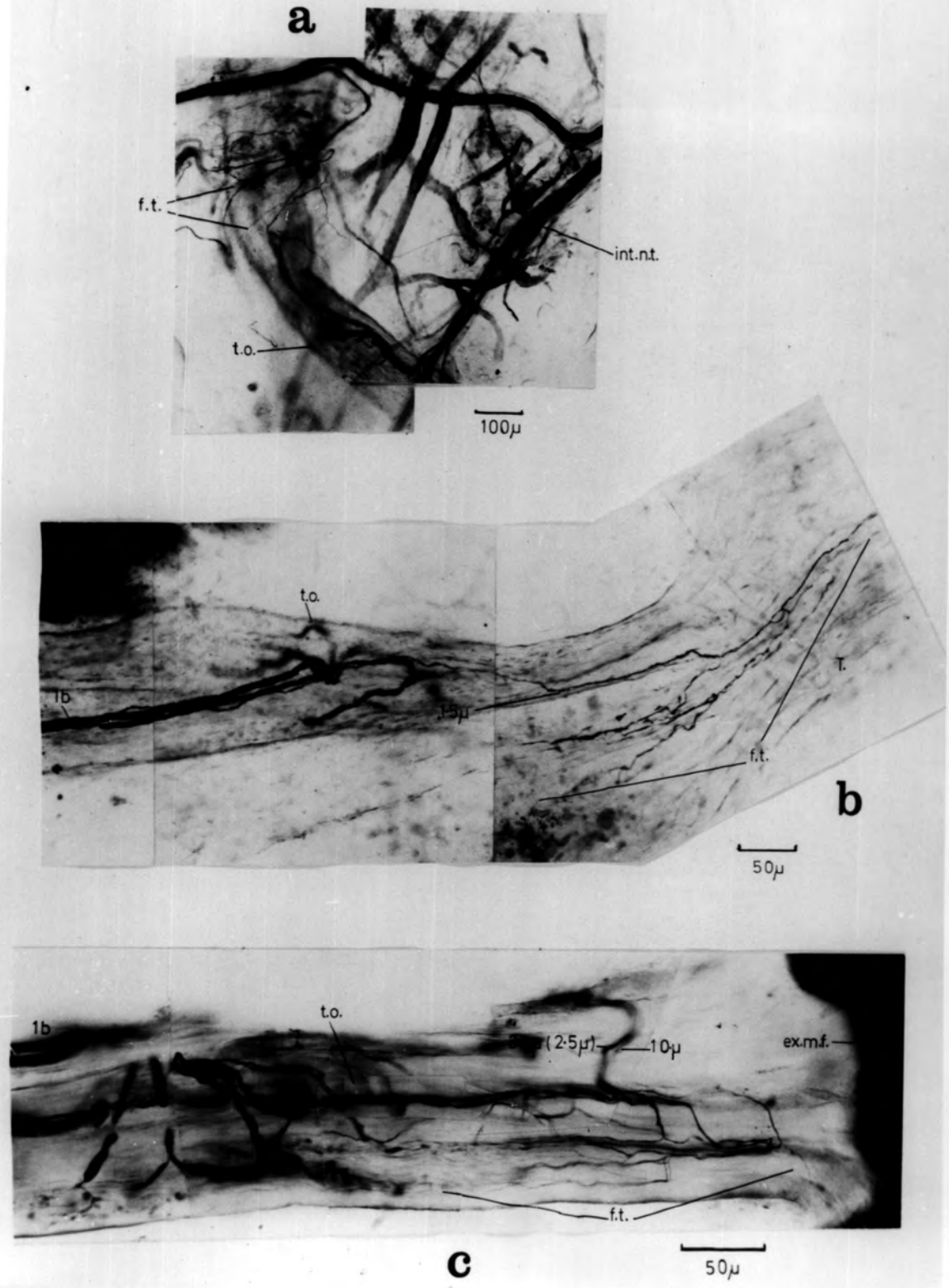
a
f.t.
int.n.t.
t.o.
100μ
t.o.
1b
1·5μ
T.
f.t.
b
50μ
1b
t.o.
(2·5μ)
10μ
ex.m.f.
f.t.
c
50μ

Figure 32

Paciniform corpuscles

a. A single corpuscle on the capsule of a tendon organ

b. Three corpuscles inside the capsule of a tendon organ

c. A single corpuscle in tendon tissue at a musculo-tendinous junction

d. A single corpuscle in the permysium between a blood vessel and a small vascular nerve trunk

(de-efferentated and sympathectomized hindlimb muscle of the cat; de Castro silver impregnation)

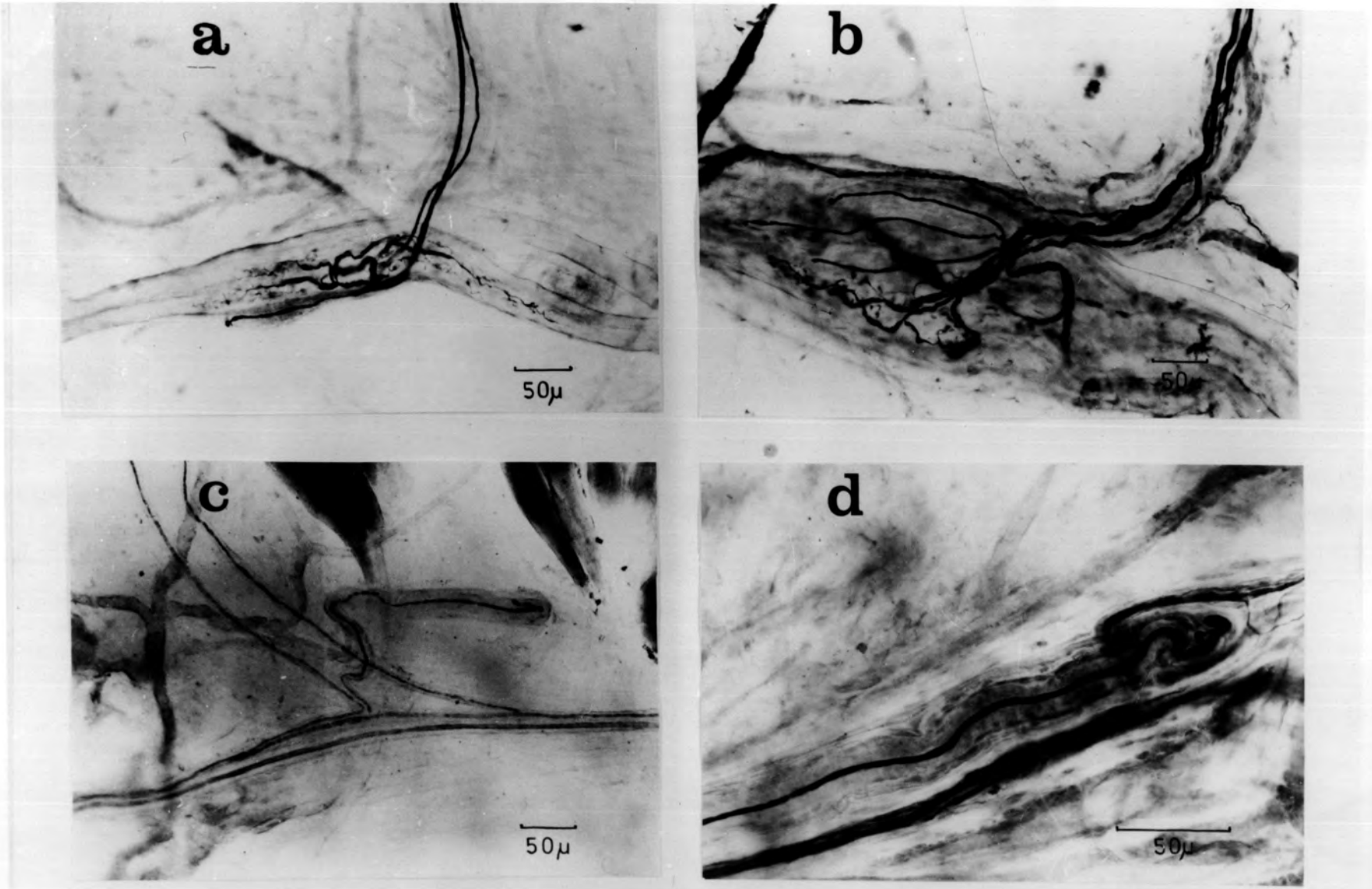
a
50μ
b
50μ
c
50μ
d
50μ

Figure 33

Paciniform corpuscle innervation derived from Group II parent fibres

a. Two corpuscles, one inside and one outside of a tendon organ innervated by a 7.0 μ (5.0 μ) parent fibre
(C178; de-efferentated peroneus III muscle; de Castro silver impregnation)

b. Five corpuscles on the outside of a tendon organ innervated by an 11.5 μ (7.5 μ) parent fibre
(C160; de-efferentated extensor digitorum longus muscle; de Castro silver impregnation)

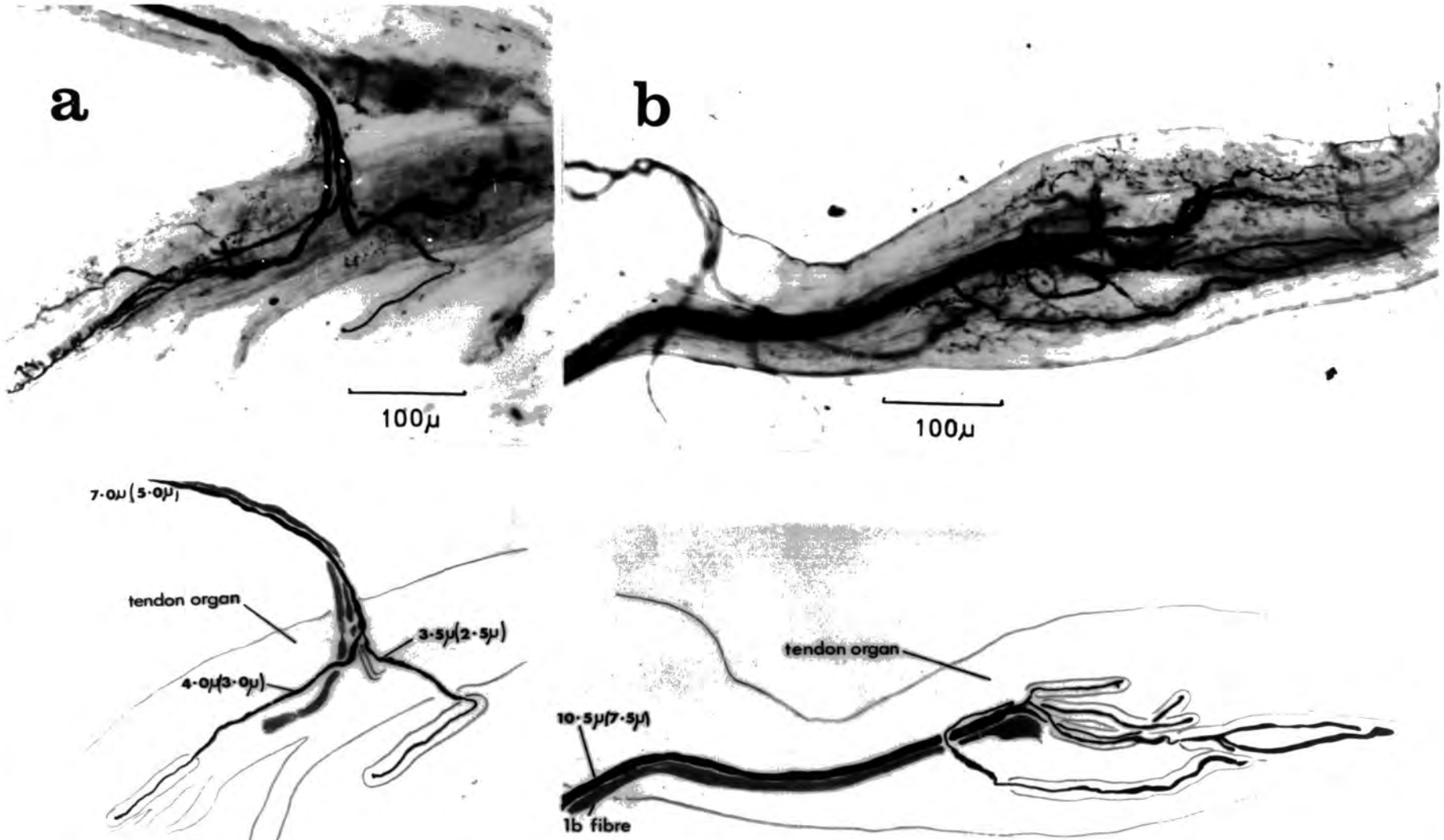
a
100μ
b
100μ
7·0μ (5·0μ)
tendon organ
3·5μ(2·5μ)
4·0μ(3·0μ)
tendon organ
10·5μ(7·5μ)
1b fibre

Fig. 34

Innervation of 8 paciniform corpuscles by a 12.0 u parent fibre (de Castro impregnation: de-afferentated & sympathectomized cat extensor digitorum longus muscle)
Diameter of nerve fibres in large diagram not to scale

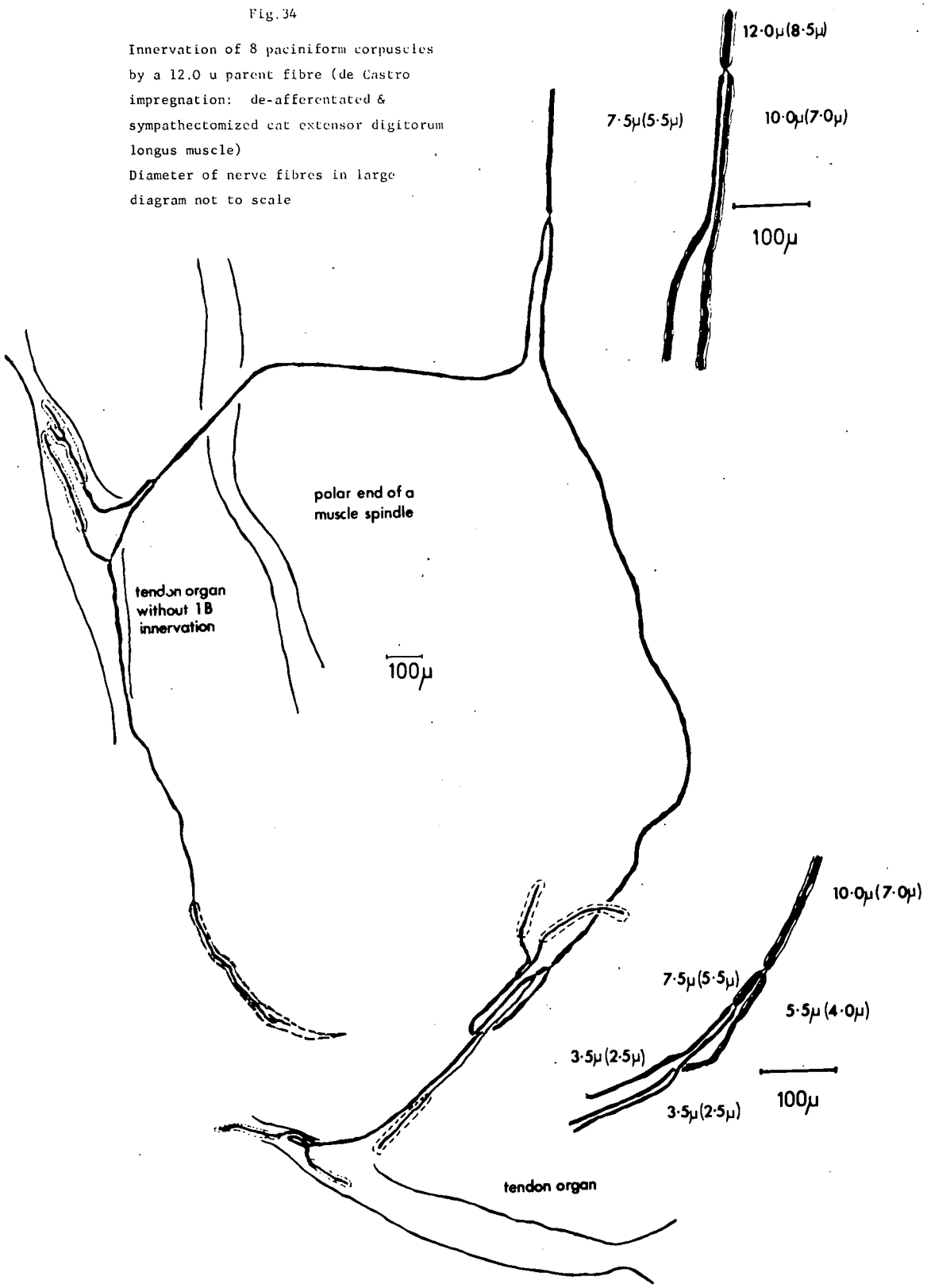

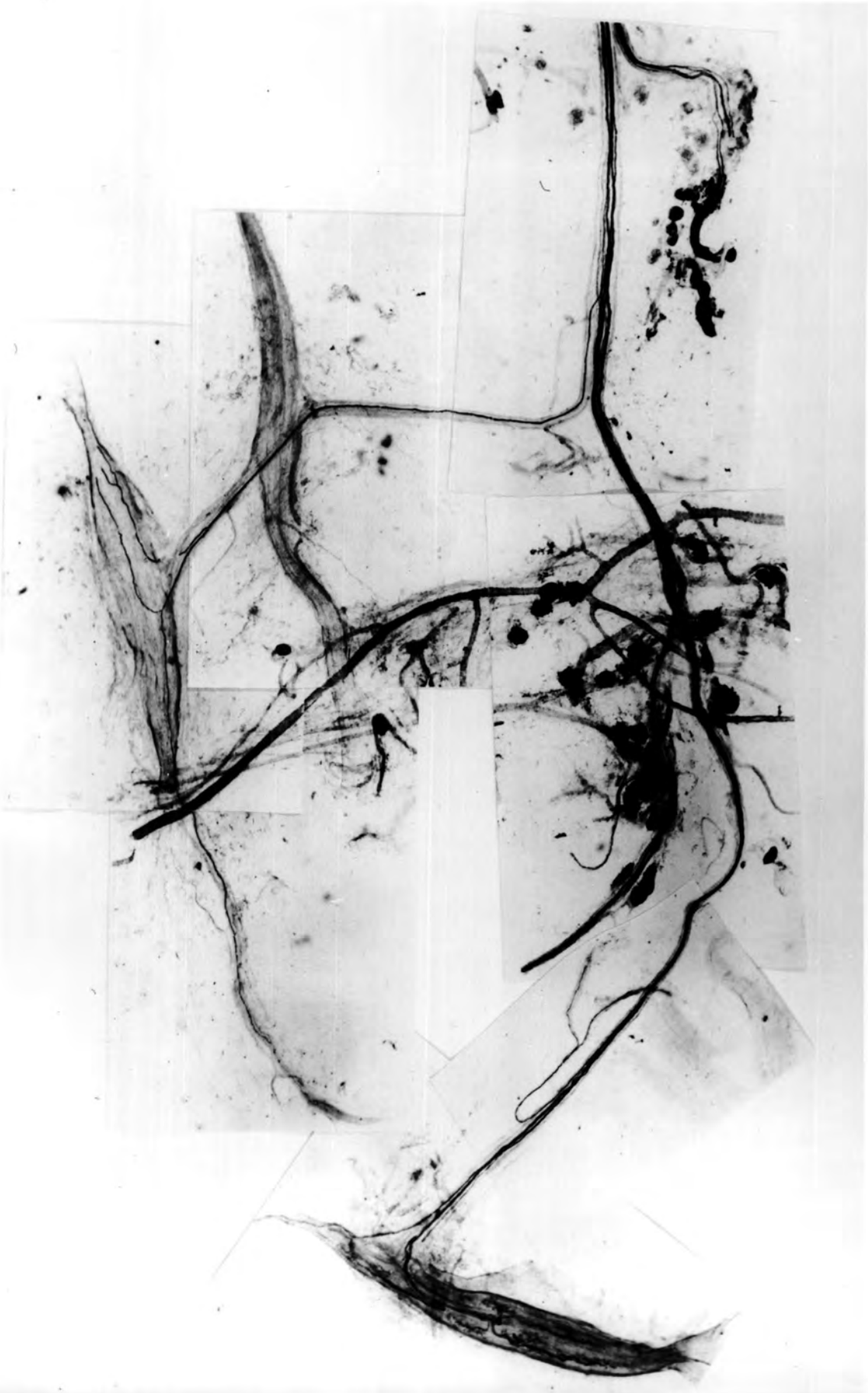

Figure 35

Axon ramifications of free sensory endings

a. n-f.ex. - neurofibrillary expansion

t.ex. - terminal expansion

Sch.n. - Schwann-cell nucleus

b. t. - axon terminal ramifications

(de-efferentated and sympathectomized cat hindlimb muscle; de Castro silver impregnation)

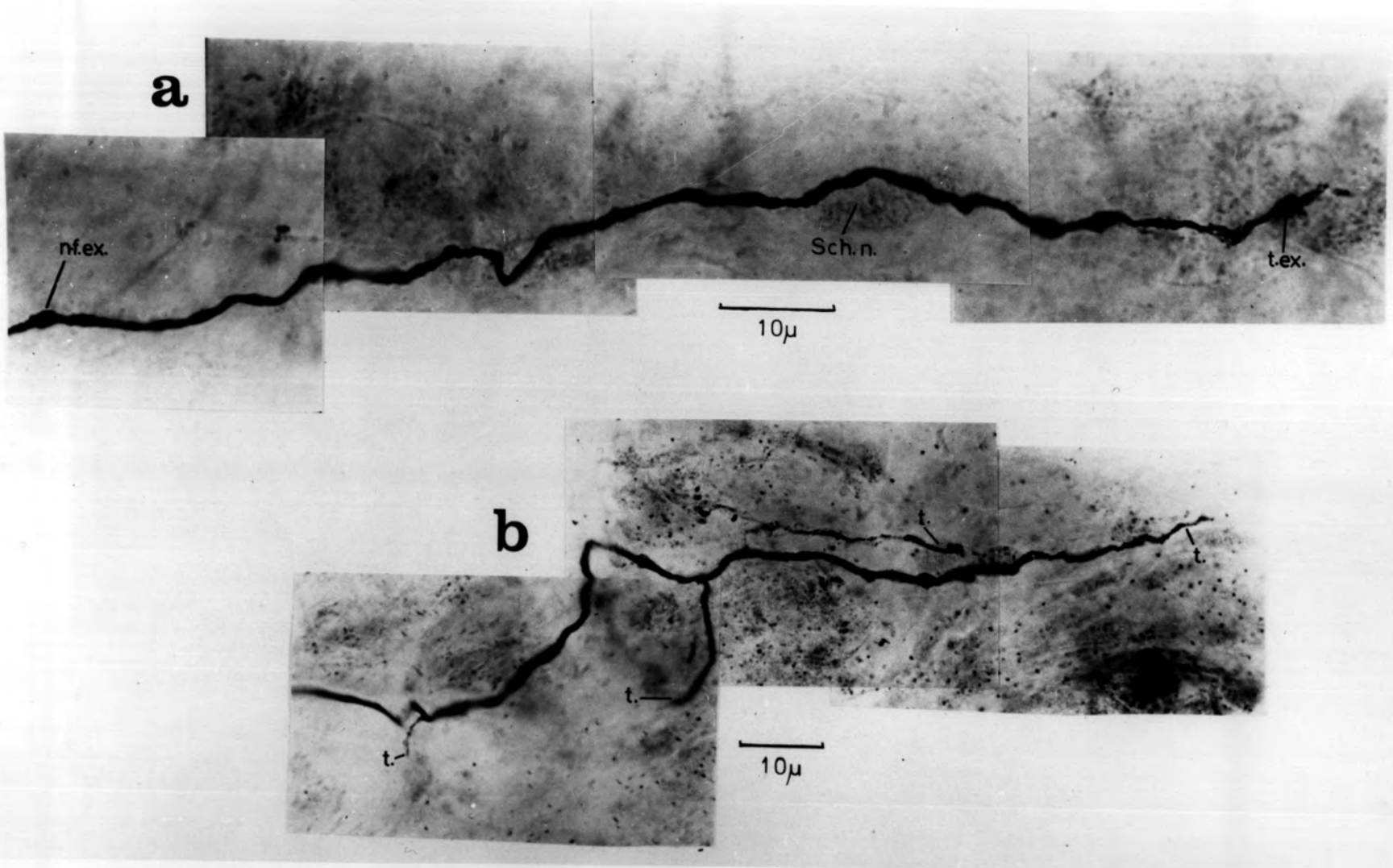
a
nf.ex.
Sch.n.
t.ex.
10μ
b
t.
t.
t.
t.
10μ

Figure 36

The form of the free ending

a. Simple ending with two terminal ramifications

b. Intermediate ending with three terminal ramifications

c. The same as b. illustrating the terminal node (t.n.) with subsequent naked axons that are the terminal ramifications (see Fig.37)

my. - myelin sheath

end. - endoneural tube

d. Complex ending with six terminal ramifications (a detailed tracing of this ending is illustrated in Fig.41)

(de-efferentated and sympathectomized cat hindlimb muscle; de Castro silver impregnation)

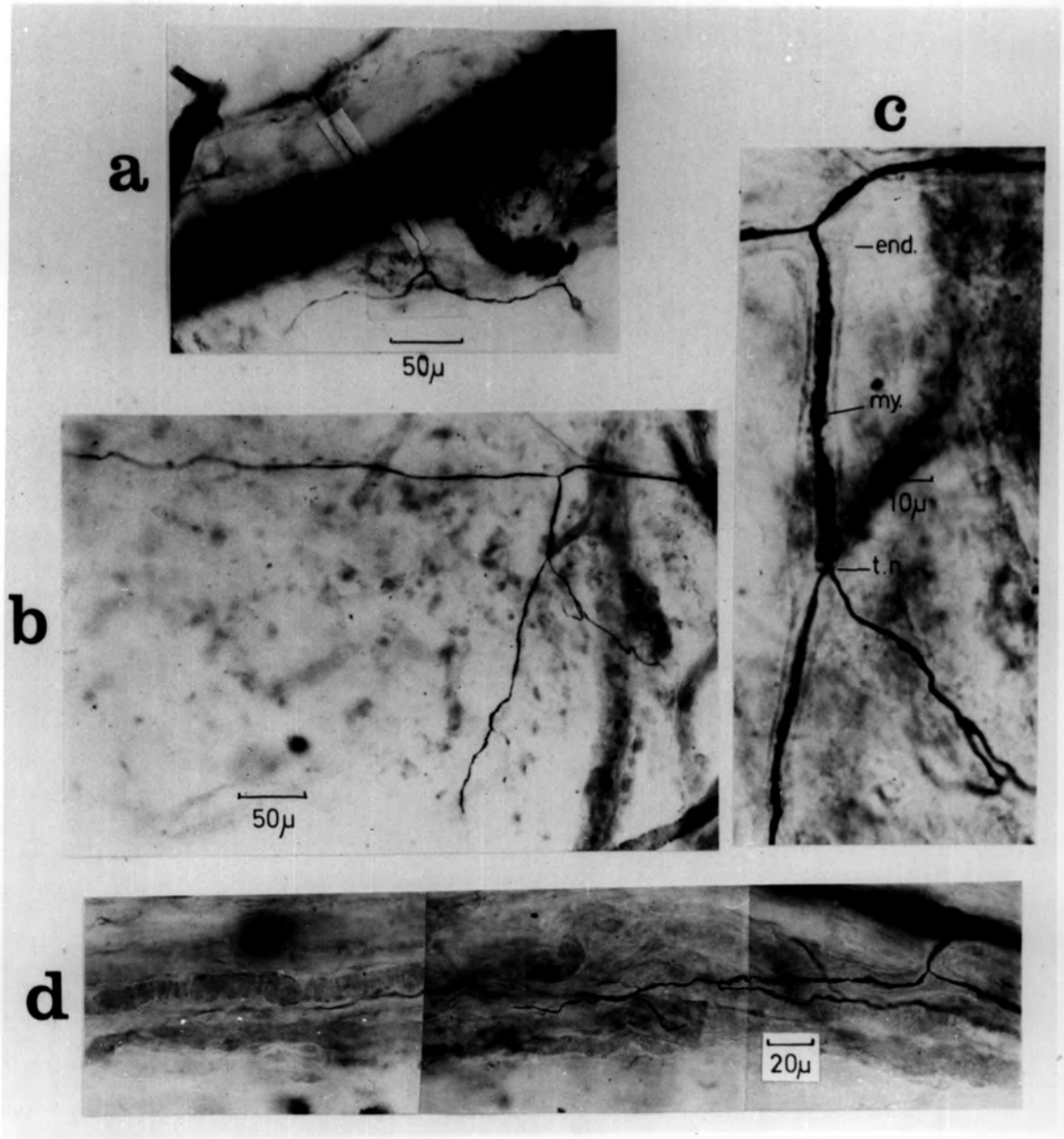
a
50μ
c
—end.
my.
10μ
t.n
b
50μ
d
20μ

Figure 37

The classification of free endings

a. The myelinated-fibre free endings are classified as nodal and terminal

b. The non-myelinated-axon free endings are equivalent to the terminal type of myelinated-fibre free ending

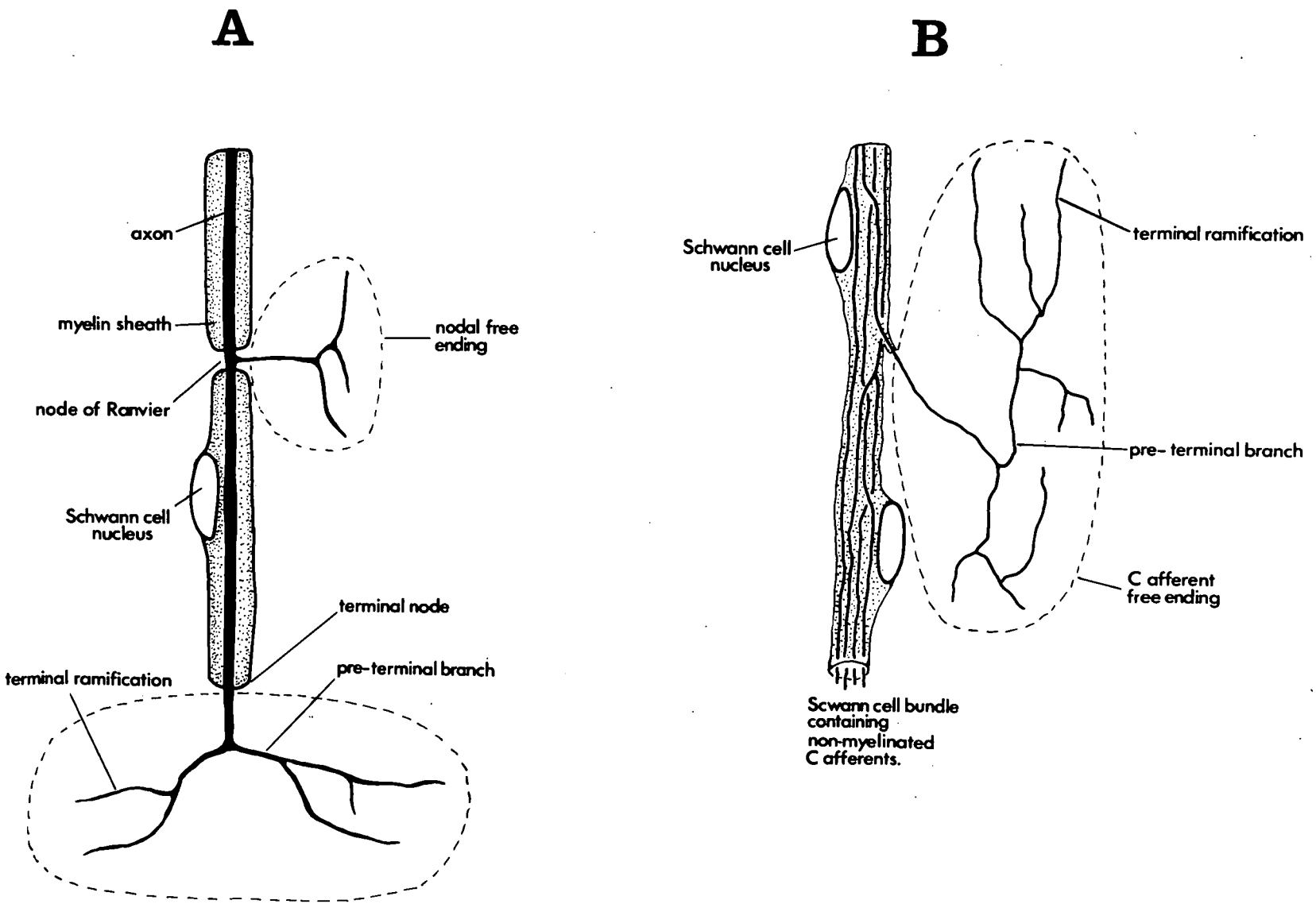
A
axon
myelin sheath
node of Ranvier
Schwann cell nucleus
nodal free ending
terminal node
pre-terminal branch
terminal ramification
B
Schwann cell nucleus
terminal ramification
pre- terminal branch
C afferent free ending
Schwann cell bundle containing non-myelinated C afferents.

Figure 38

Nodal free endings

a. Simple type, with terminals in connective tissue (c.t.)

b. Simple type, with terminals associated with blood-vessel adventitia (b.v.)

c. Intermediate type: one of the three terminals remains in the small vascular nerve trunk along which it travels in the opposite direction to the myelinated parent fibre

c.t. - connective tissue

b.v.a. - blood-vessel adventitia

d. Complex type: five terminals are produced from the 3.0 μ parent fibre and are associated with blood-vessel adventitia (b.v.), fat cells (f.c.) connective tissue, and nerve trunk perineurium

(de-efferentated and sympathectomized cat hindlimb muscle; de Castro silver impregnation)

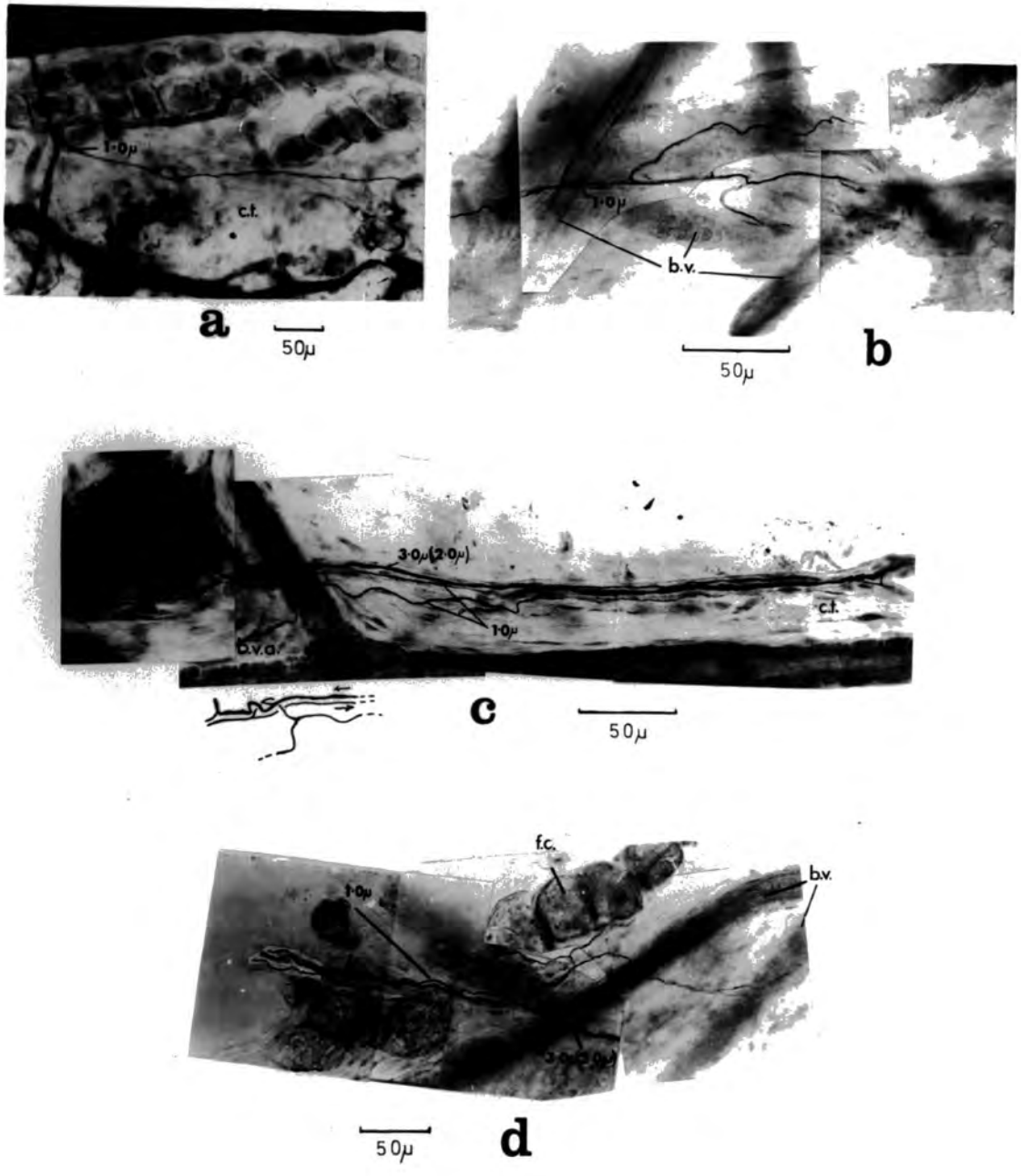
1·0μ
c.f.
a
50μ
1·0μ
b.v.
50μ
b
3·0μ(2·0μ)
1·0μ
b.v.a.
c.f.
c
50μ
f.c.
b.v.
1·0μ
50μ
d

Figure 39

Terminal free endings

a. Complex type

b. Intermediate type

(de-efferentated and sympathectomized cat hindlimb muscle; de Castro silver impregnation)

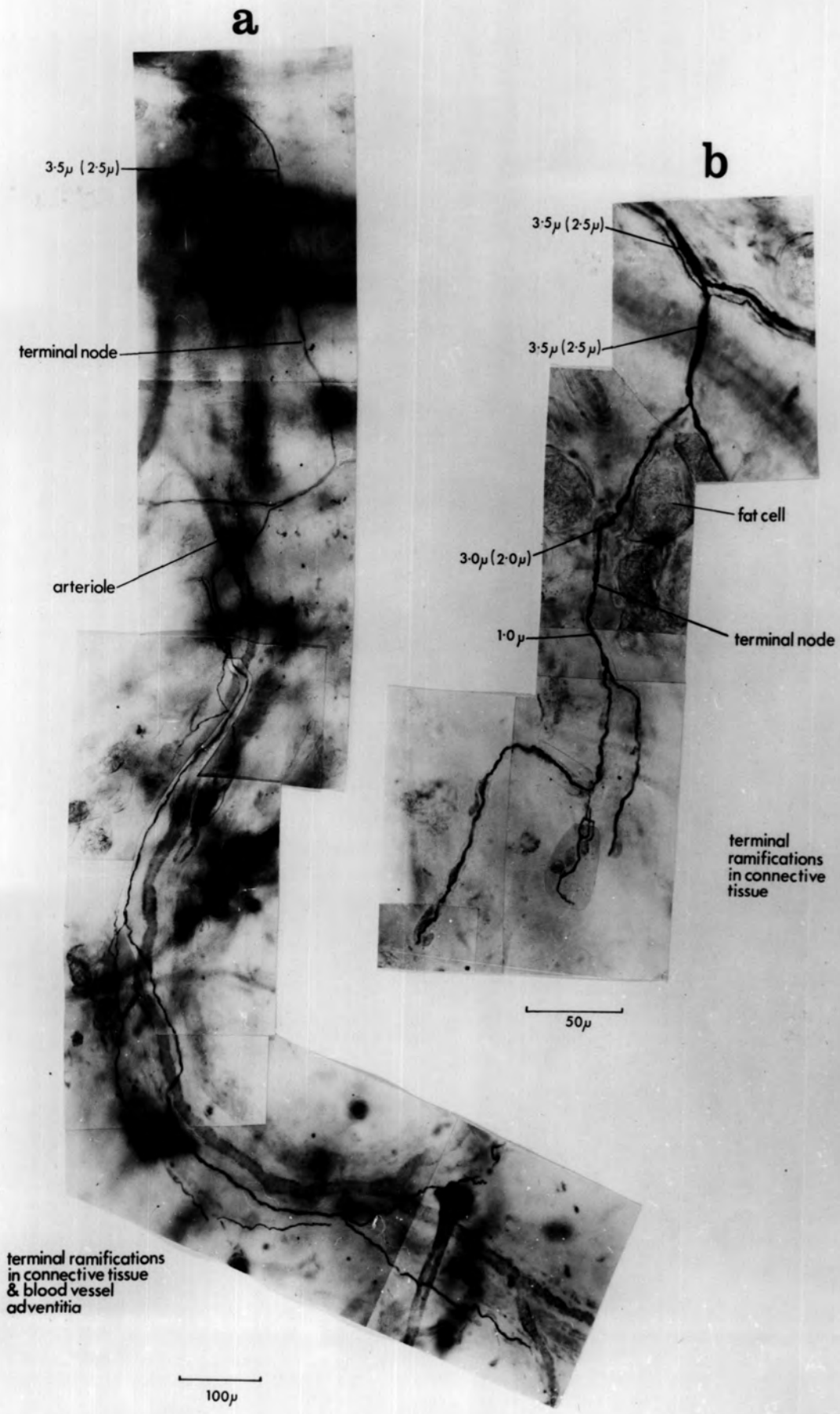
a
3·5μ (2·5μ)
terminal node
arteriole
terminal ramifications in connective tissue & blood vessel adventitia
100μ
b
3·5μ (2·5μ)
3·5μ (2·5μ)
fat cell
3·0μ (2·0μ)
1·0μ
terminal node
terminal ramifications in connective tissue
50μ

Figure 39 (Cont.)

Terminal free endings

c. Complex type

d. Complex type

e. Simple type

(de-efferentated and sympathectomized cat hindlimb muscle; de Castro impregnation)

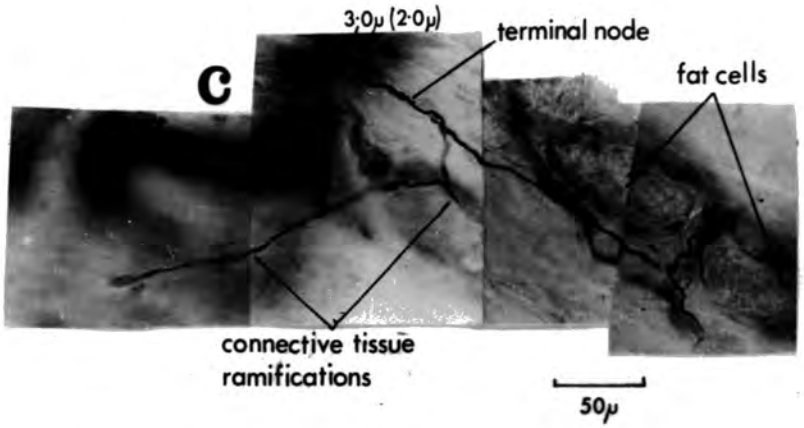
c
3·0μ (2·0μ)
terminal node
fat cells
connective tissue
ramifications
50μ

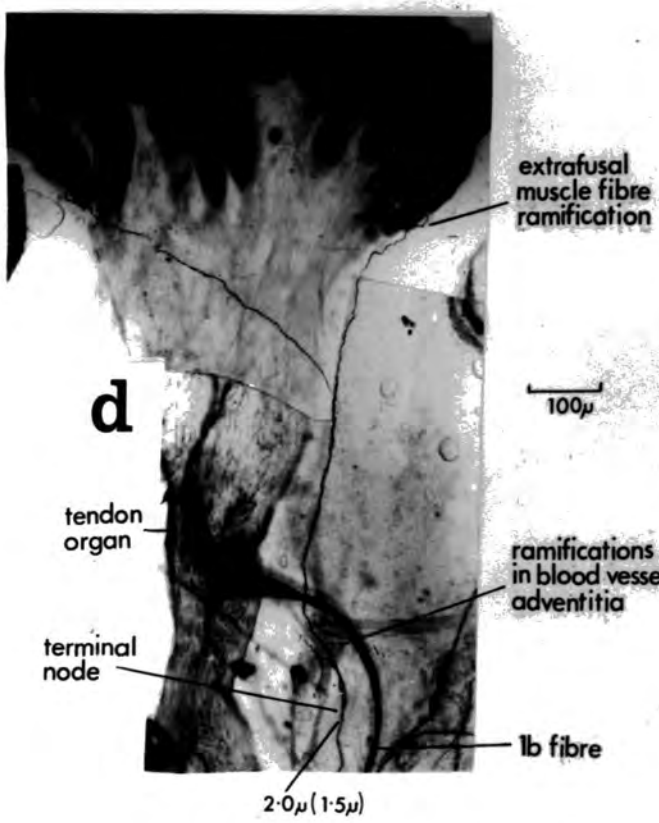
d
extrafusal
muscle fibre
ramification
100μ
tendon
organ
ramifications
in blood vessel
adventitia
terminal
node
Ib fibre
2·0μ (1·5μ)

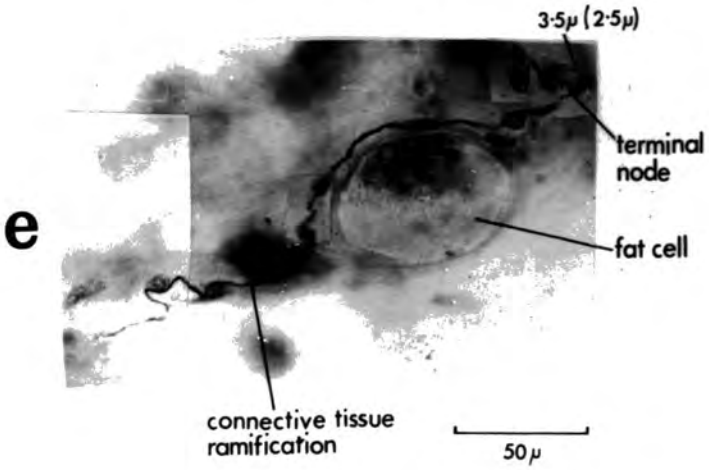
e
3·5μ (2·5μ)
terminal
node
fat cell
connective tissue
ramification
50μ

Figure 40

The relationship between nodal endings of the same myelinated parent fibre

The lower ending is illustrated in Fig.38d

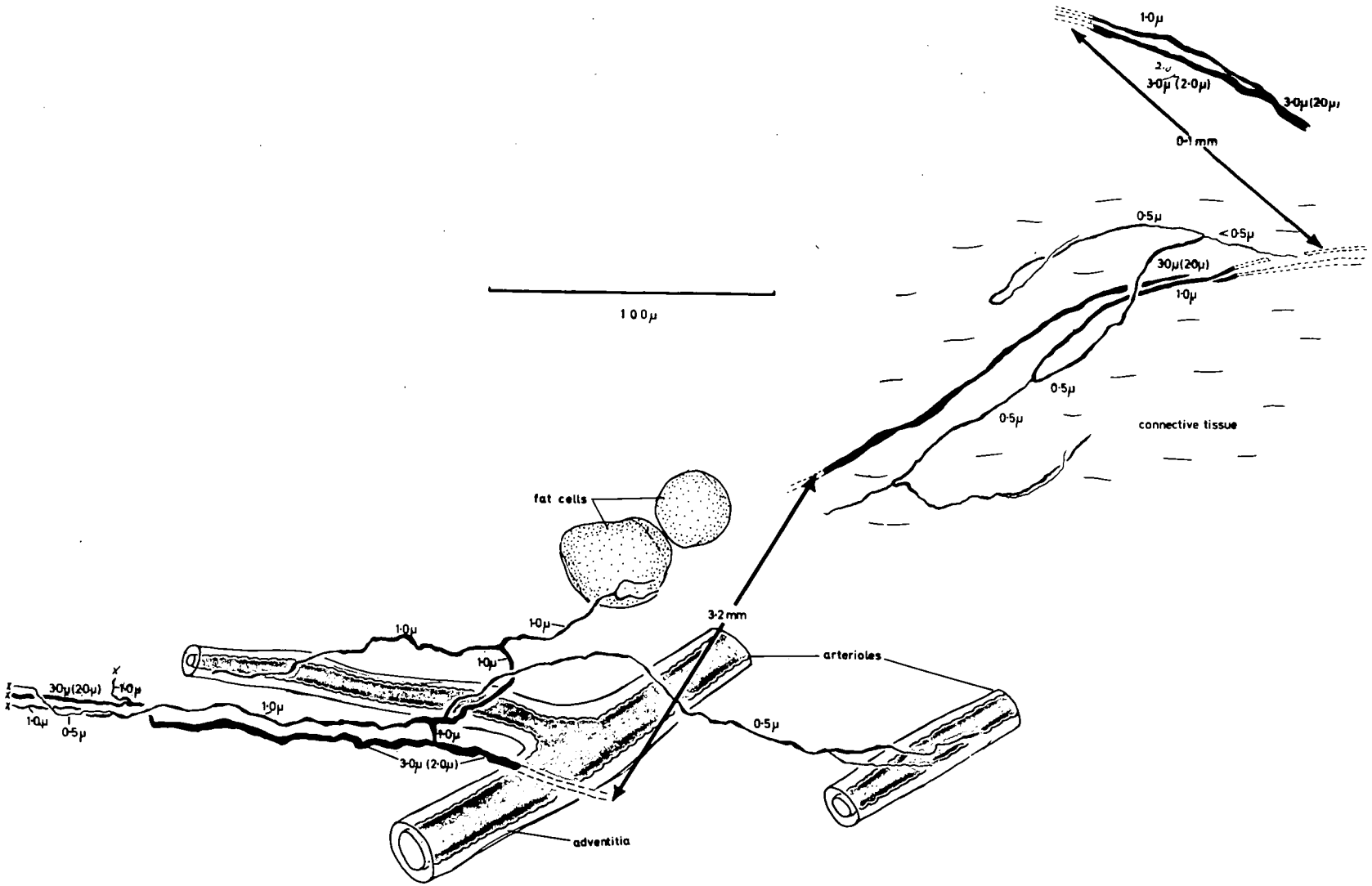
1·0μ
3·0μ (2·0μ)
3·0μ(20μ)
0·1 mm
0·5μ
<0·5μ
3·0μ(20μ)
1·0μ
100μ
0·5μ
0·5μ
connective tissue
fat cells
1·0μ
1·0μ
1·0μ
3·2 mm
arterioles
3·0μ(20μ)
1·0μ
1·0μ
0·5μ
1·0μ
0·5μ
3·0μ (2·0μ)
adventitia

Figure 41

The relationship between a nodal and a terminal ending of the same myelinated parent fibre

The upper ending is illustrated in Fig.36d

The lower ending is illustrated in Fig.39c

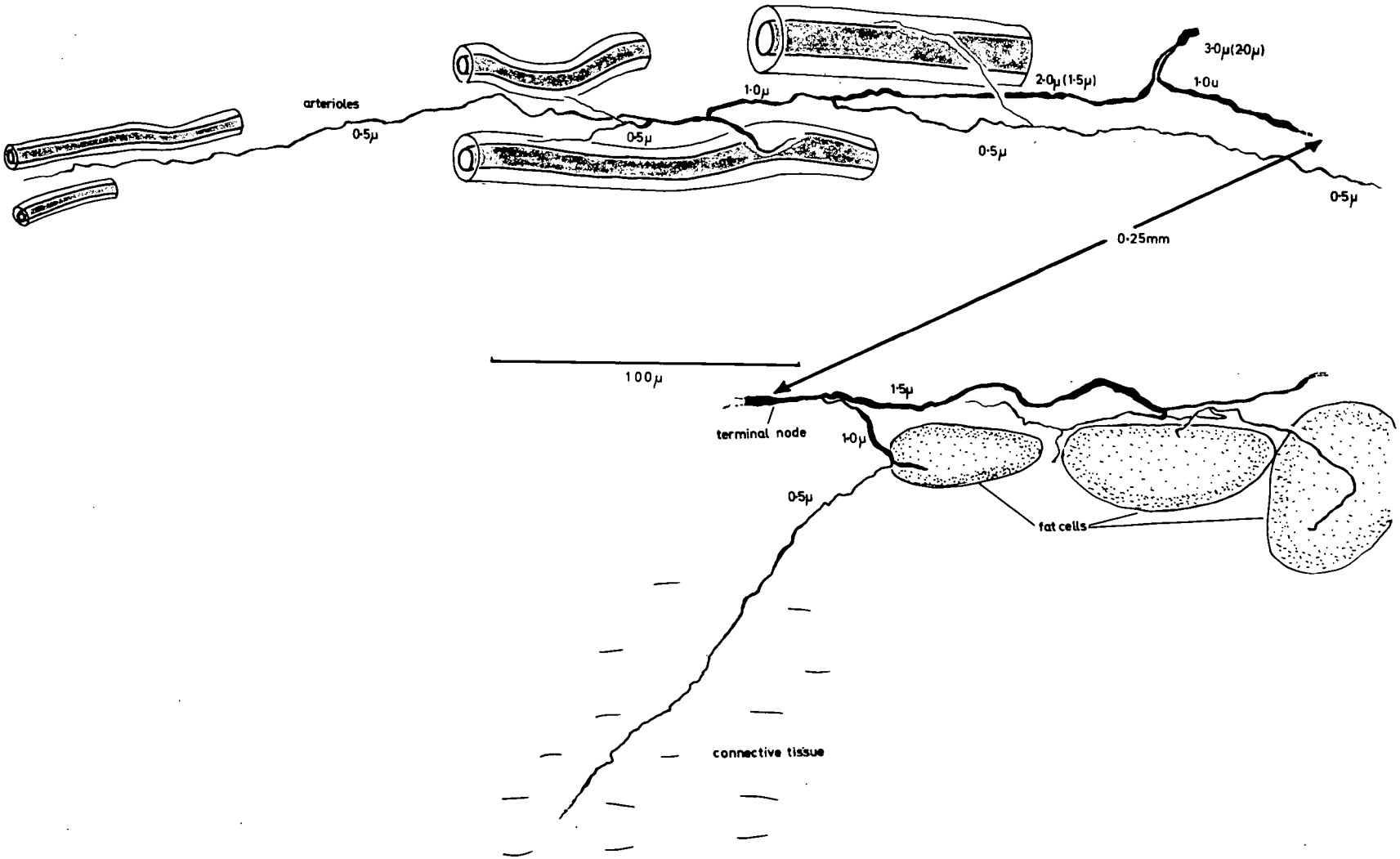
arterioles
0·5μ
0·5μ
1·0μ
2·0μ(1·5μ)
3·0μ(20μ)
1·0u
0·5μ
0·5μ
0·25mm
100μ
1·5μ
terminal node
1·0μ
0·5μ
fat cells
connective tissue

Figure 42

Ramifications of terminal endings from the same myelinated parent fibre

b. A ramification in blood-vessel adventitia

a. Ramifications in connective tissue and around fat cells

(de-efferentated and sympathectomized cat hindlimb muscle; de Castro silver impregnation)

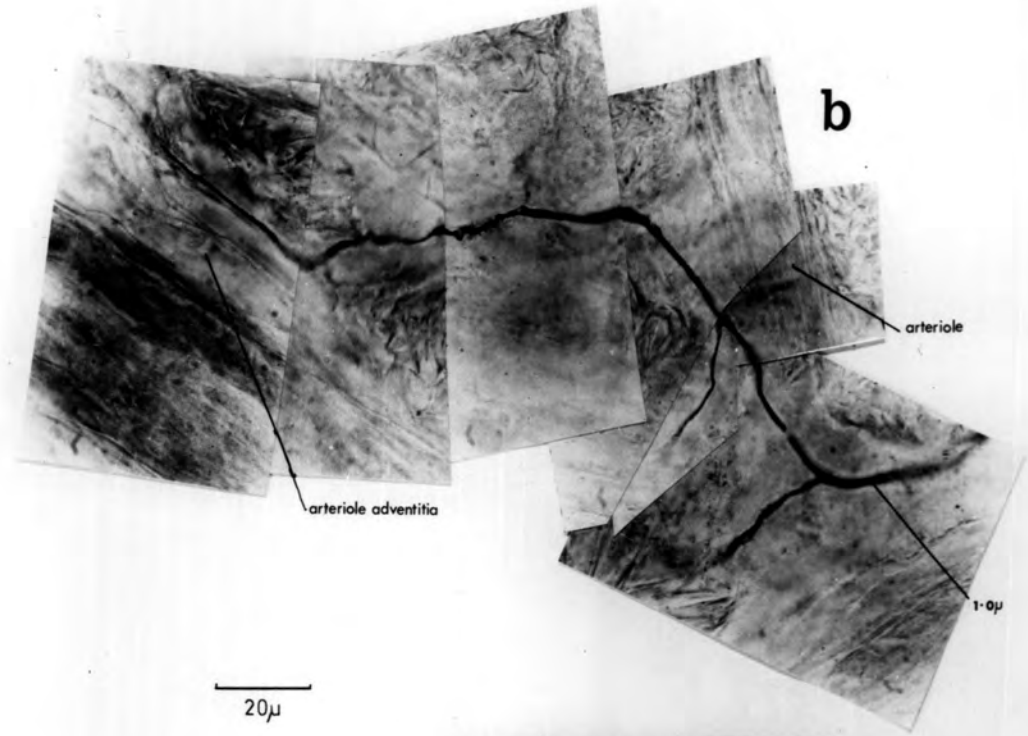
b
arteriole
arteriole adventitia
1·0μ
20μ

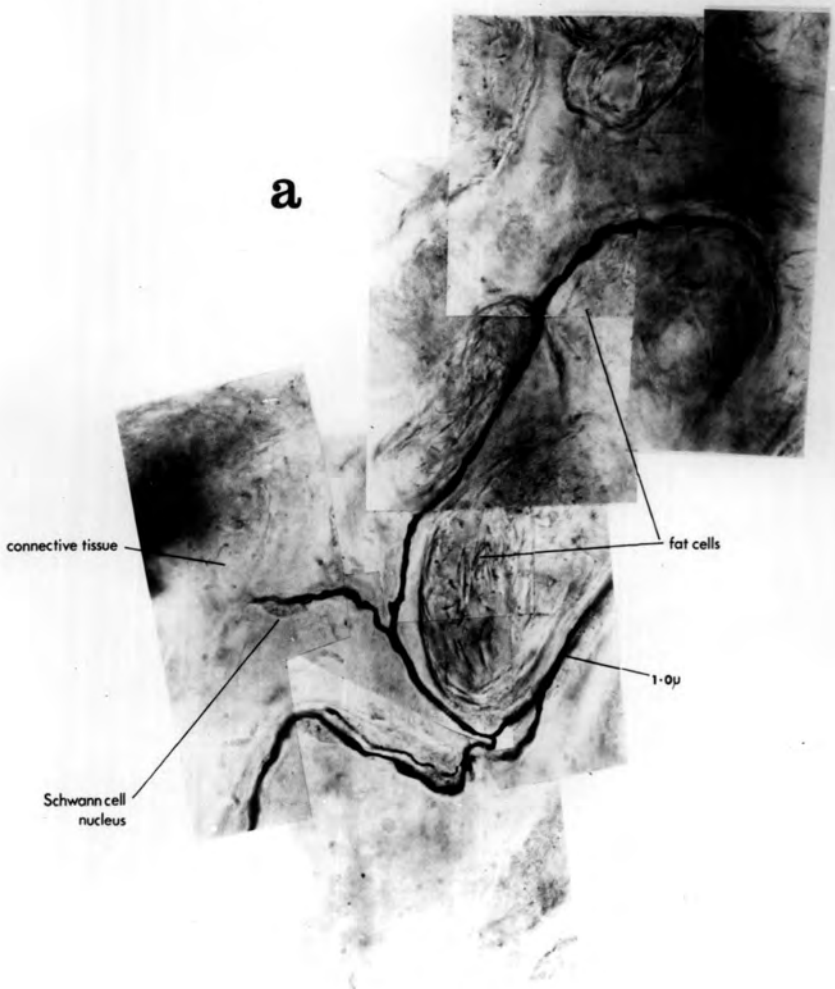
a
connective tissue
fat cells
1·0μ
Schwann cell
nucleus

Figure 43

The relationship between the ramifications illustrated in Figure 42a and b

Both endings with ramifications at a. and b. are derived from the same 5.5 μ (4.0 μ) parent fibre in the small vascular nerve trunk. The position of the terminal nodes is indicated (t.n.). The distance between a. and b. is approximately 0.8mm. The distance between a. and the ramification in blood-vessel adventitia (top right of figure) and also derived from the same parent fibre, is approximately 1.5mm.

(de-efferentated and sympathectomized cat hindlimb muscle; de Castro silver impregnation)

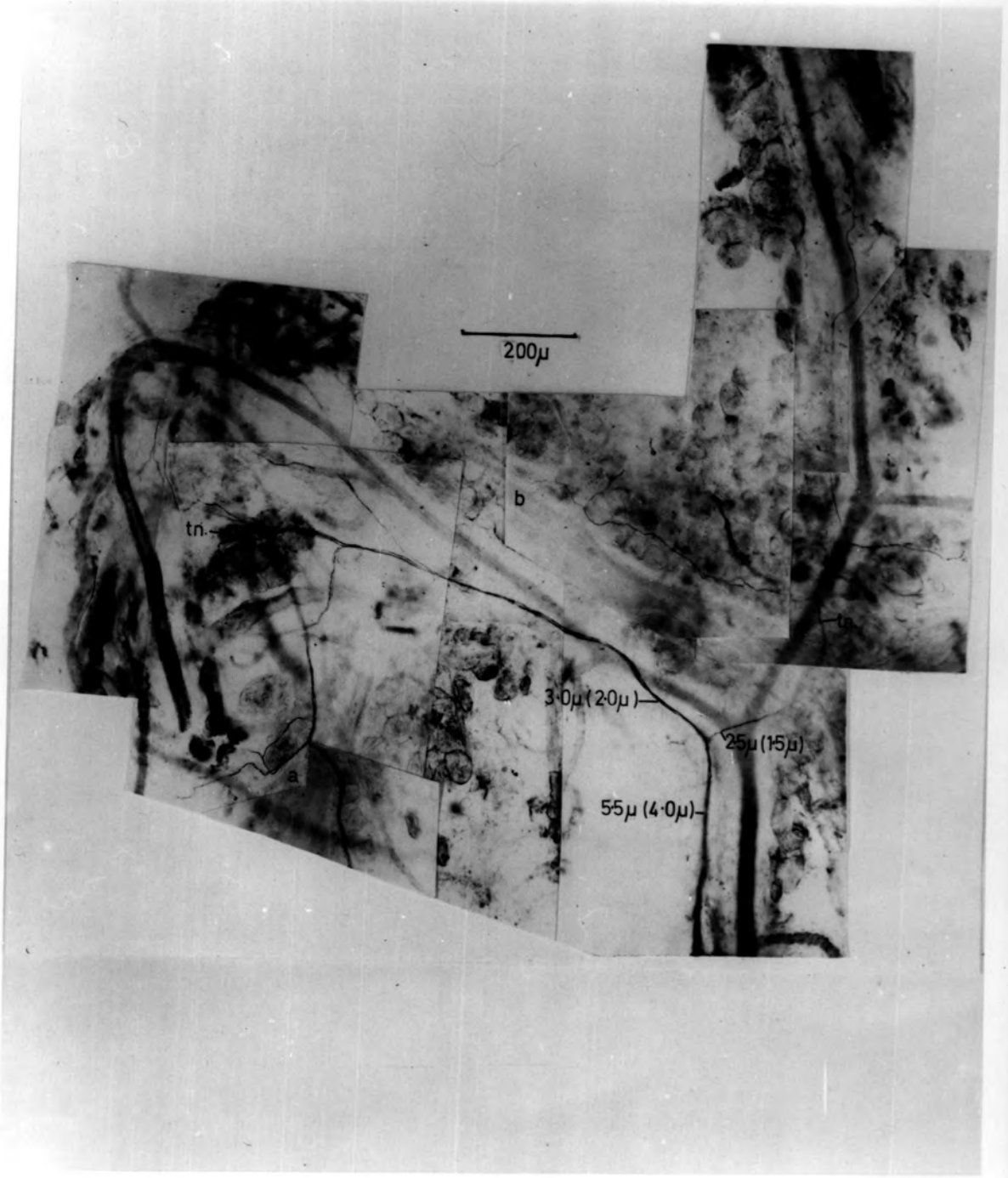
200μ
tn.
b
tn.
3·0μ (2·0μ)
2·5μ (1·5μ)
5·5μ (4·0μ)
a

Figure 44

Free endings of Group IV sensory axons

a. Ramifications in connective tissue close to a small intramuscular nerve trunk (I.n.t.)

b. Ramifications in arteriole adventitia (a.a.)

a. - arteriole

Sc.b.- Schwann bundle

(de-efferentated and sympathectomized cat hindlimb muscle; de Castro silver impregnation)

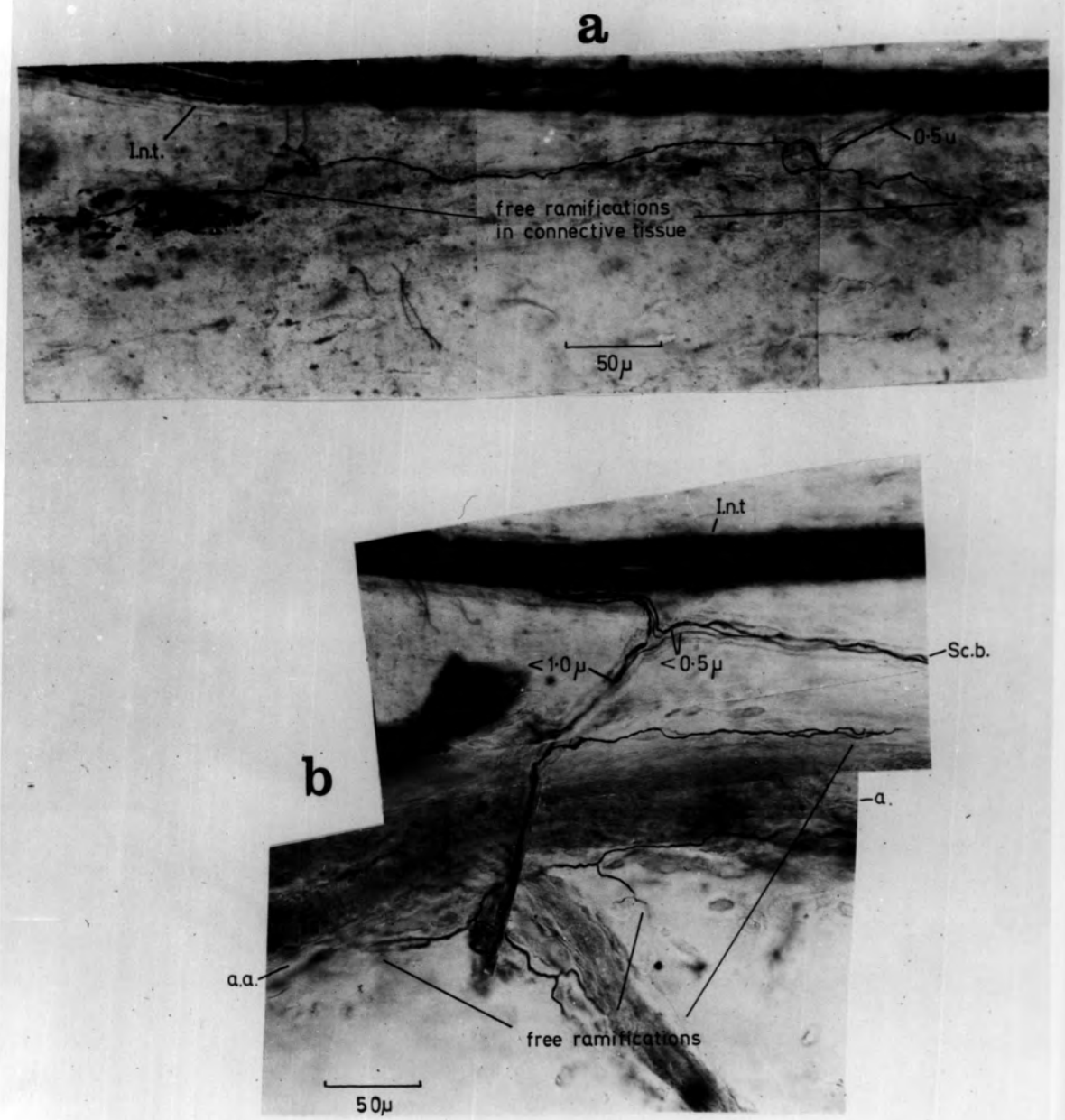
a
l.n.t.
0·5 µ
free ramifications
in connective tissue
50µ
b
l.n.t
<1·0µ
<0·5µ
Sc.b.
a.
a.a.
free ramifications
50µ

Figure 45

The free ending of a non-myelinated, sensory Group IV axon

The tracing shows the extensive distribution of the terminals that occur in many different planes of focus

The photographs illustrate at high magnification the form of the terminal ramifications in blood-vessel adventitia and the course of the Schwann-cell bundle from which the parent fibre of the ending emerges

(de-efferentated and sympathectomized cat hindlimb muscle;
de Castro silver impregnation)

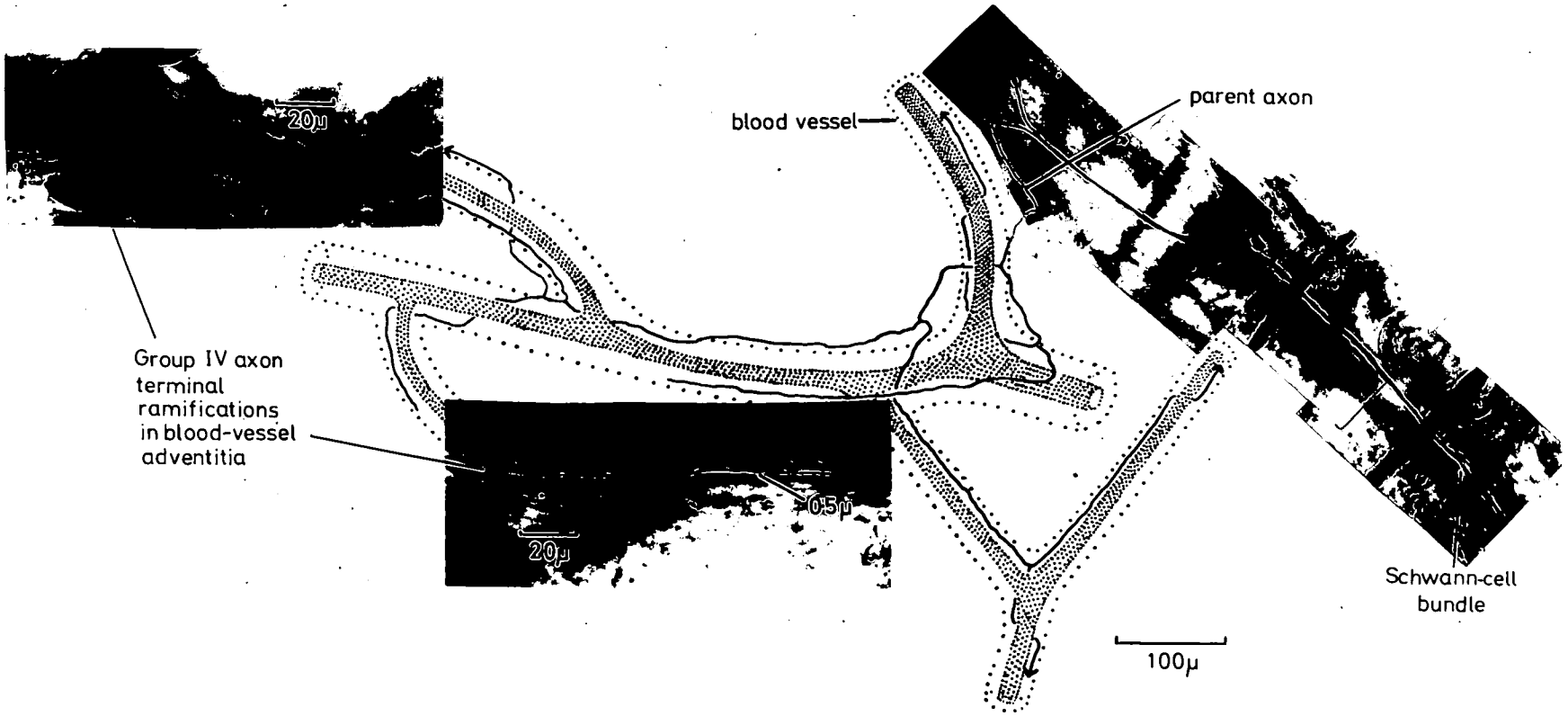
20μ
blood vessel
parent axon
Group IV axon
terminal
ramifications
in blood-vessel
adventitia
0·5μ
20μ
Schwann-cell
bundle
100μ

Figure 46

The intramuscular course of a Group II sensory fibre and its free ending terminal ramifications in the muscle

The terminal ramifications occur in connective tissue (ct.t.) and among fat cells (f.t.)
The terminals among the fat cells are illustrated in greater detail in Figure 35b

(de-efferentated and sympathectomized cat hindlimb muscle; de Castro silver impregnation)

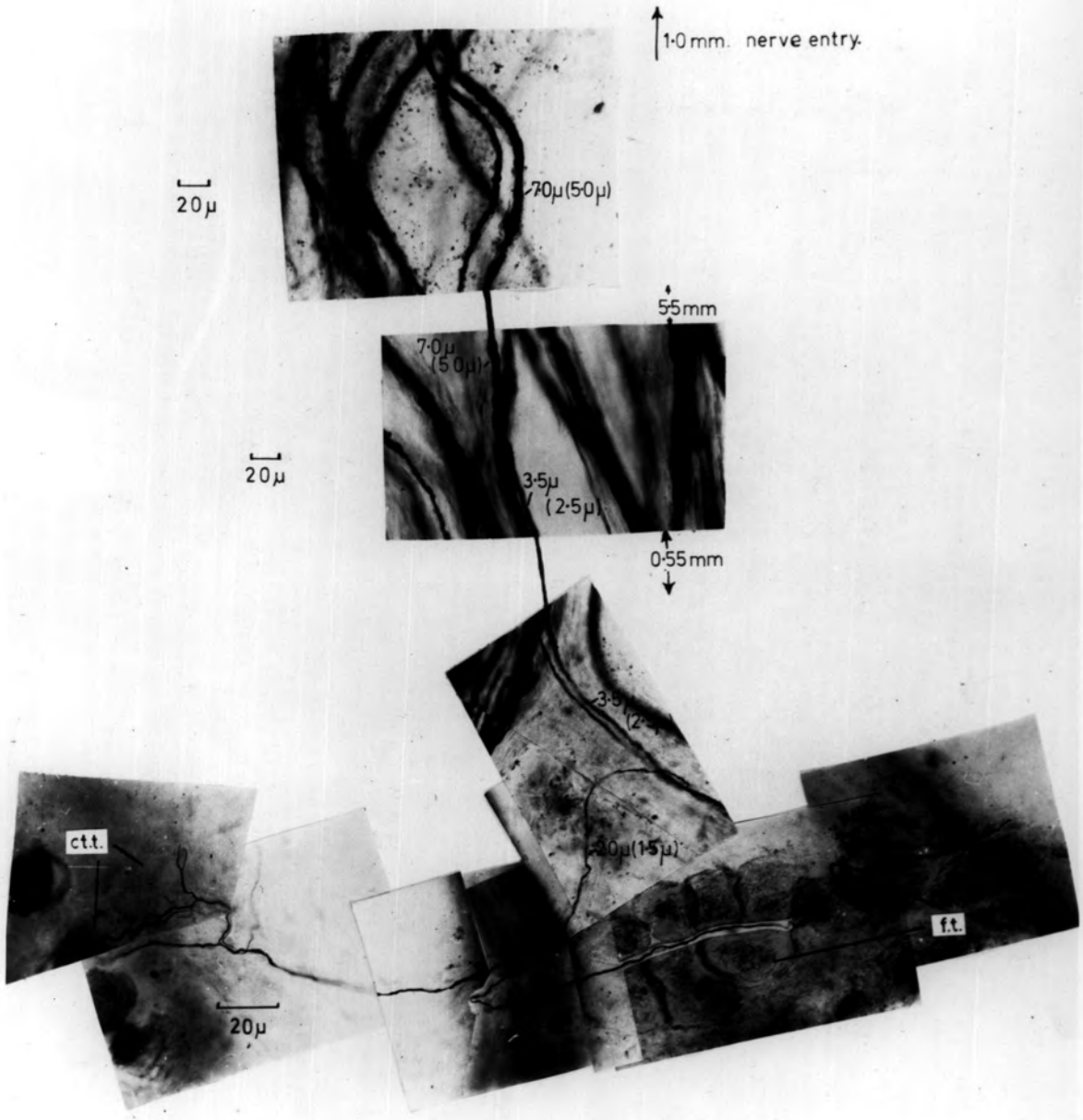
1·0 mm. nerve entry.
20 μ
7·0 μ (5·0 μ)
5·5 mm
7·0 μ
(5·0 μ)
20 μ
3·5 μ
(2·5 μ)
0·55 mm
2·0 μ (1·5 μ)
ct.t.
f.t.
20 μ

Figure 47

The intramuscular course of a Group III sensory fibre and its free ending terminal ramifications in the muscle

The terminal ramifications occur in connective tissue (ct.t.)

(de-efferentated and sympathectomized cat hindlimb muscle; de Castro silver impregnation)

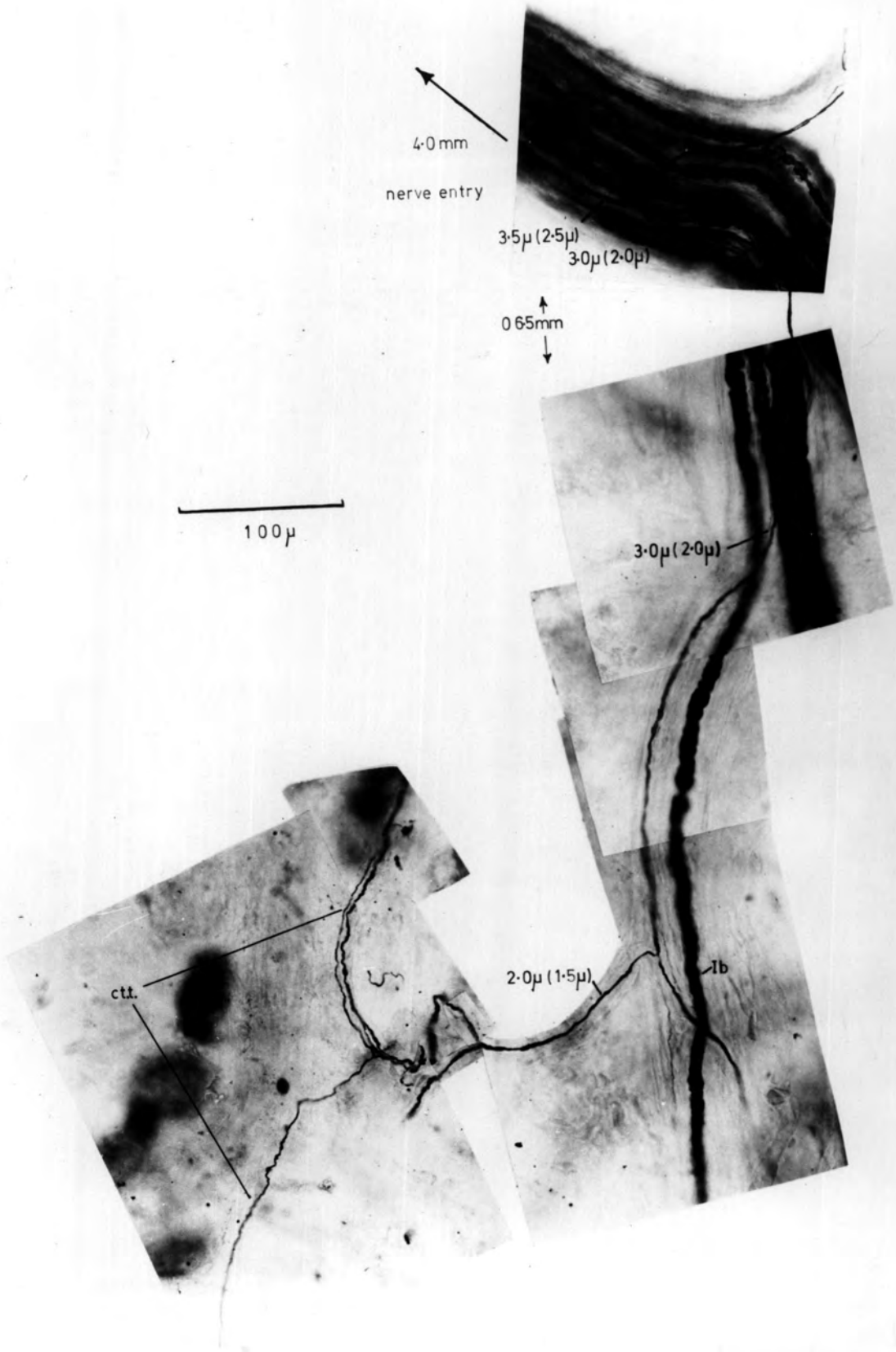
4·0 mm
nerve entry
3·5μ (2·5μ)
3·0μ (2·0μ)
0·65mm
100μ
3·0μ (2·0μ)
ctt.
2·0μ (1·5μ)
Ib

Figure 48

The intramuscular course of a Group IV sensory fibre and pre-terminal branches of the free ending

The terminal ramifications of this ending occur in blood-vessel adventitia and are illustrated in detail in Fig.45

Scw.b. - Schwann-cell bundle in which the free-ending axon courses to nerve entry

(de-efferentated and sympathectomized cat hindlimb muscle; de Castro silver impregnation)

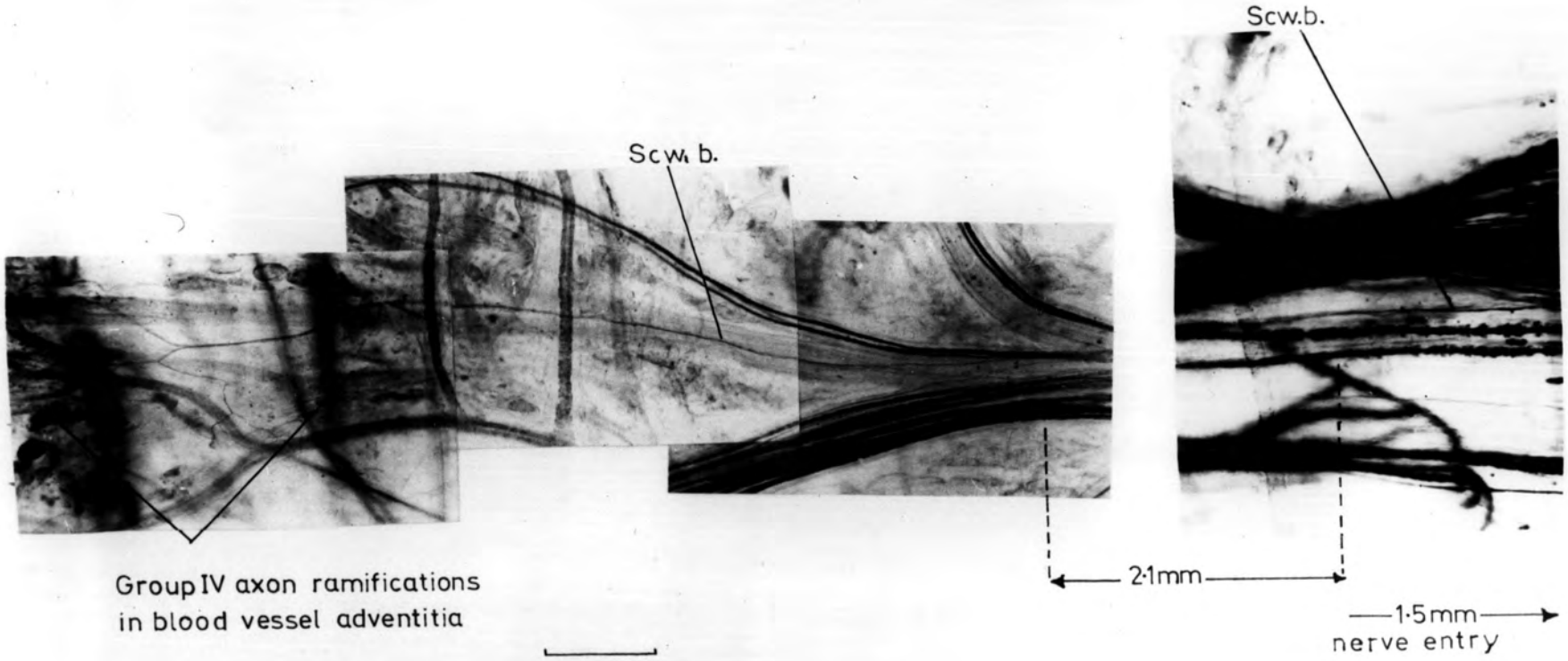
Scw.b.
Scw. b.
Group IV axon ramifications
in blood vessel adventitia
200μ
2·1mm
1·5mm
nerve entry

Figure 49

The mode of branching in an intramuscular nerve trunk of Group I and III free ending nerve fibres

The 100 μ scale line applies only to the individual photographs. The distance between various points on each photograph is indicated in millimetres (mm)

(C213; de-efferentated and sympathectomized tibialis anterior muscle; de Castro silver impregnation)

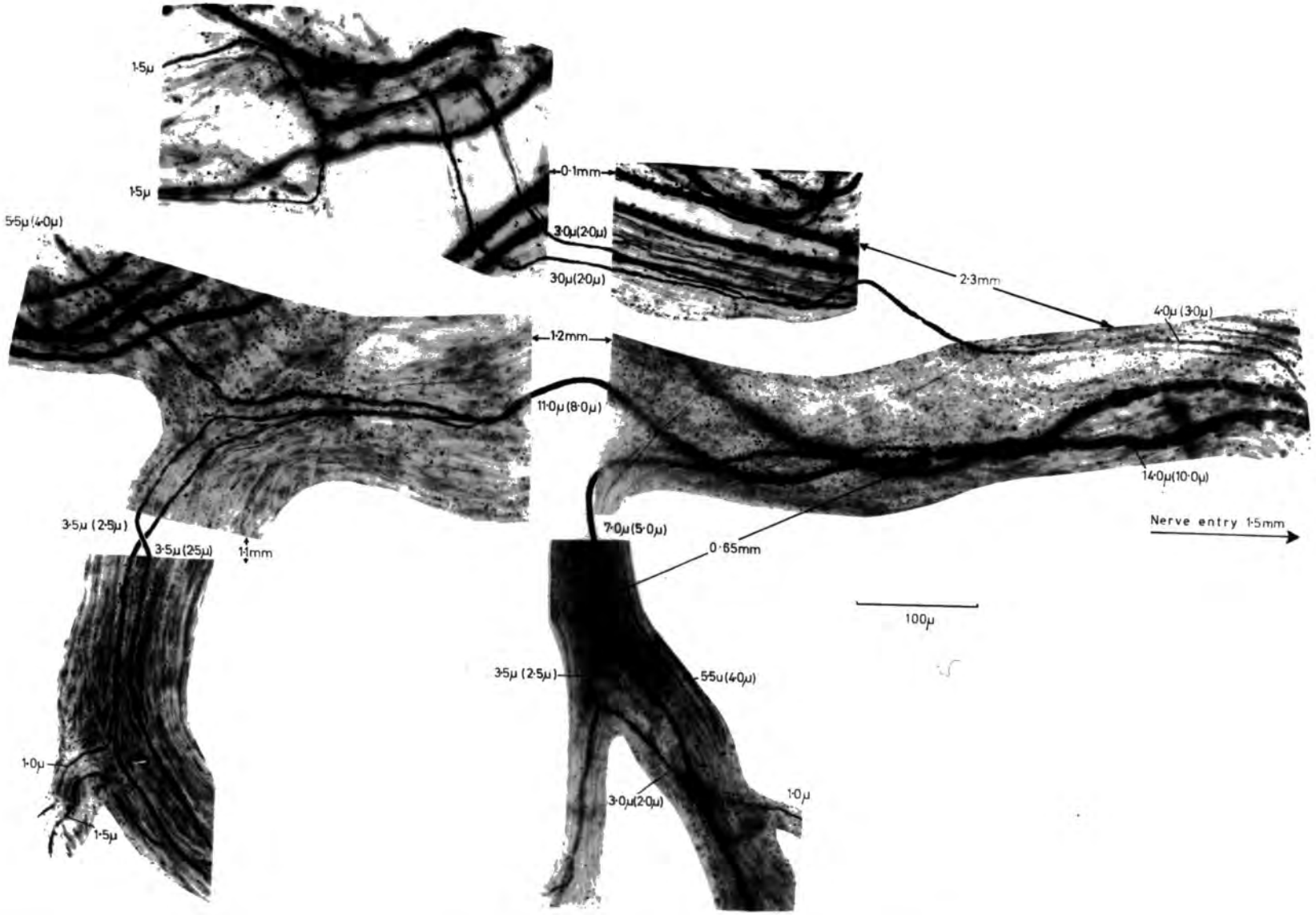
1·5μ
1·5μ
0·1mm
3·0μ(2·0μ)
3·0μ(2·0μ)
2·3mm
5·5μ(4·0μ)
1·2mm
4·0μ(3·0μ)
11·0μ(8·0μ)
14·0μ(10·0μ)
3·5μ(2·5μ)
3·5μ(2·5μ)
1·1mm
7·0μ(5·0μ)
0·65mm
Nerve entry 1·5mm
100μ
3·5μ(2·5μ)
5·5μ(4·0μ)
1·0μ
1·5μ
3·0μ(2·0μ)
1·0μ

Figure 50

The mode of branching in an intramuscular nerve trunk of a Group II free-ending nerve fibre

(C213; de-efferentated and sympathectomized tibialis anterior muscle; de Castro silver impregnation)

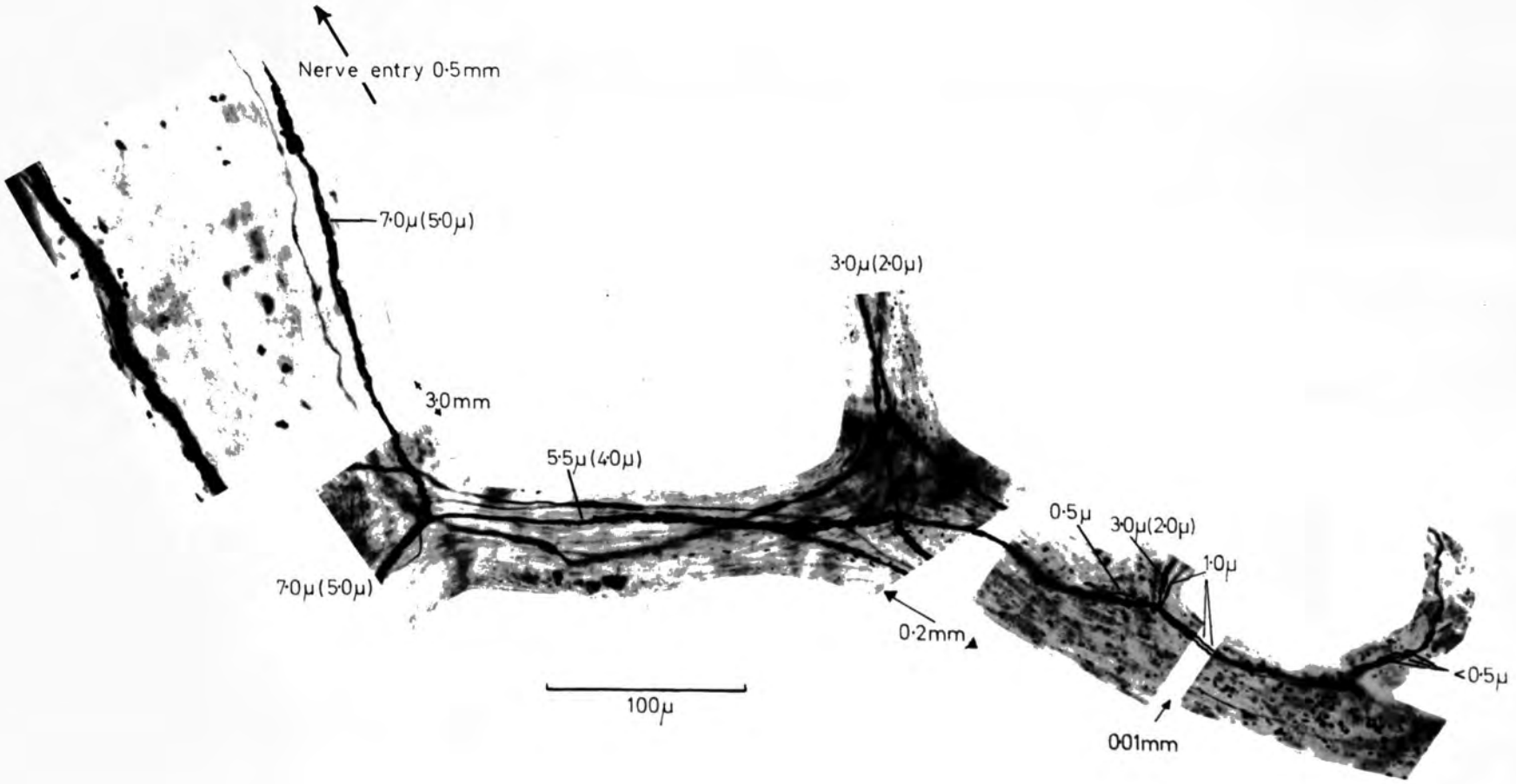
Nerve entry 0·5mm
7·0μ(5·0μ)
3·0μ(2·0μ)
3·0mm
5·5μ(4·0μ)
0·5μ
3·0μ(2·0μ)
1·0μ
7·0μ(5·0μ)
0·2mm
100μ
<0·5μ
001mm

Figure 51

The derivation of small-myelinated fibres and non-myelinated axons of the vascular nerve trunks

a. A vascular nerve trunk containing small-myelinated fibres (my.) and non-myelinated axons (n.my.)

b. A small myelinated nerve fibre enters a vascular nerve trunk as a result of larger myelinated parent fibre branching

c. Direct entry of Group III fibres (my.) from a small intramuscular nerve trunk into a vascular nerve trunk

d. Derivation of a non-myelinated axon (1.0 μ) in the vascular nerve trunk (v.n.t.) from a myelinated parent fibre (3.0 μ (2.0 μ)) in the intramuscular nerve trunk (i.n.t.)

e. Non-myelinated (1.0 μ) axon division in an intramuscular nerve trunk (i.n.t.), which produces axons (0.5 μ), that enter a small vascular nerve trunk (v.n.t.)

(de-efferentated and sympathectomized cat hindlimb muscles;
de Castro silver impregnation)

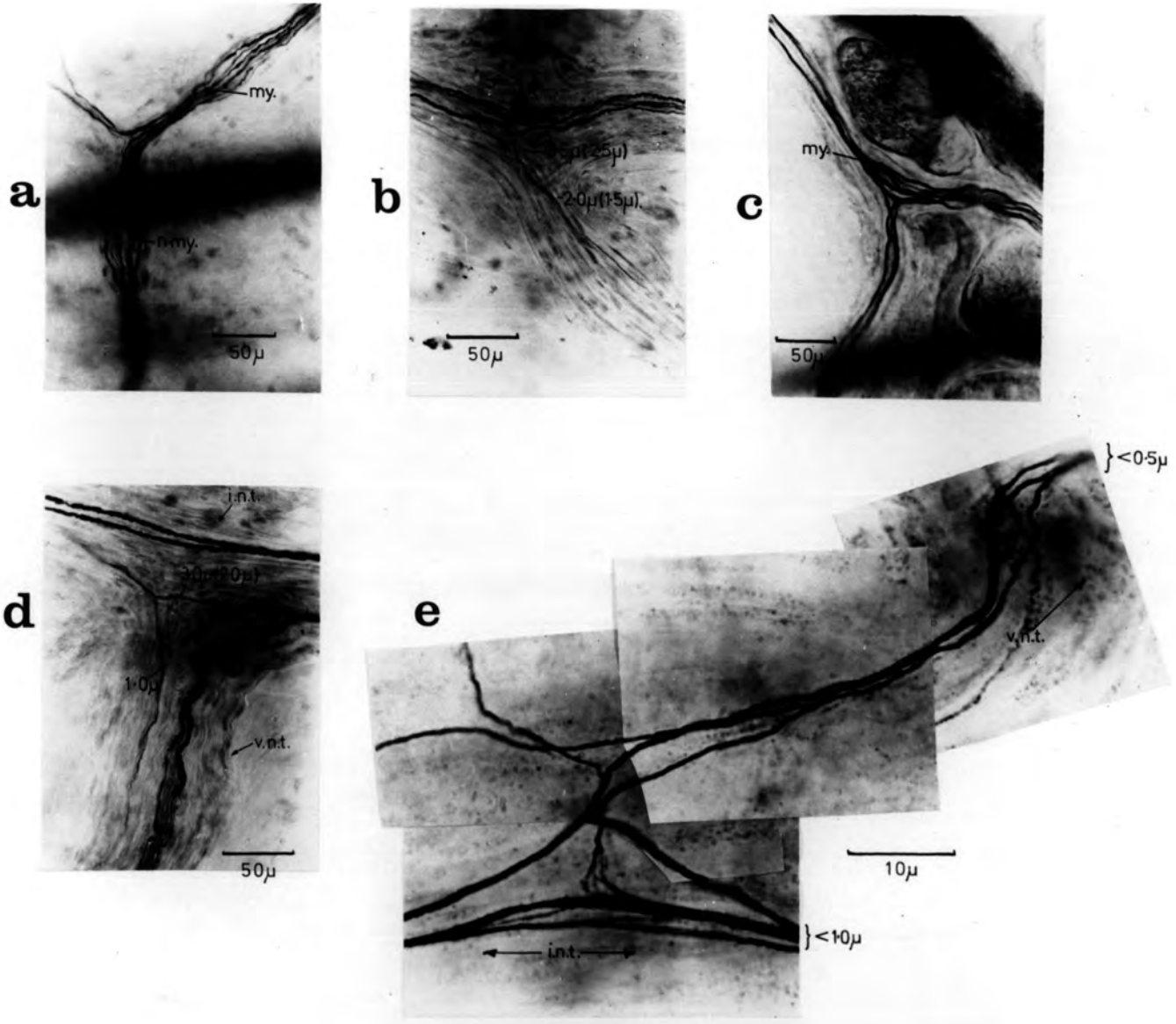
a
my.
n.my.
50μ
b
2·0μ(1·5μ)
50μ
c
my.
50μ
d
i.n.t.
1·0μ
v.n.t.
50μ
e
}<0·5μ
v.n.t.
10μ
}<1·0μ
i.n.t.

Figure 52

The behaviour of small-myelinated fibres and non-myelinated axons in intramuscular and vascular nerve trunks

a. A myelinated fibre (3.0 μ (2.0 μ)) produces a non-myelinated axon (1.0 μ) that enters the Schwann-cell bundle of Group IV axons

b. The myelinated fibre (3.0 μ (2.0 μ)), which is travelling from left to right, produces a non-myelinated axon (1.0 μ) that takes a recurrent path (right to left) in the nerve trunk

c. The Group IV axon divides twice in this small-vascular nerve trunk and no matter in what direction it is travelling, one of the resultant branches is recurrent in nature

(de-efferentated and sympathectomized cat hindlimb muscle;
de Castro silver impregnation)

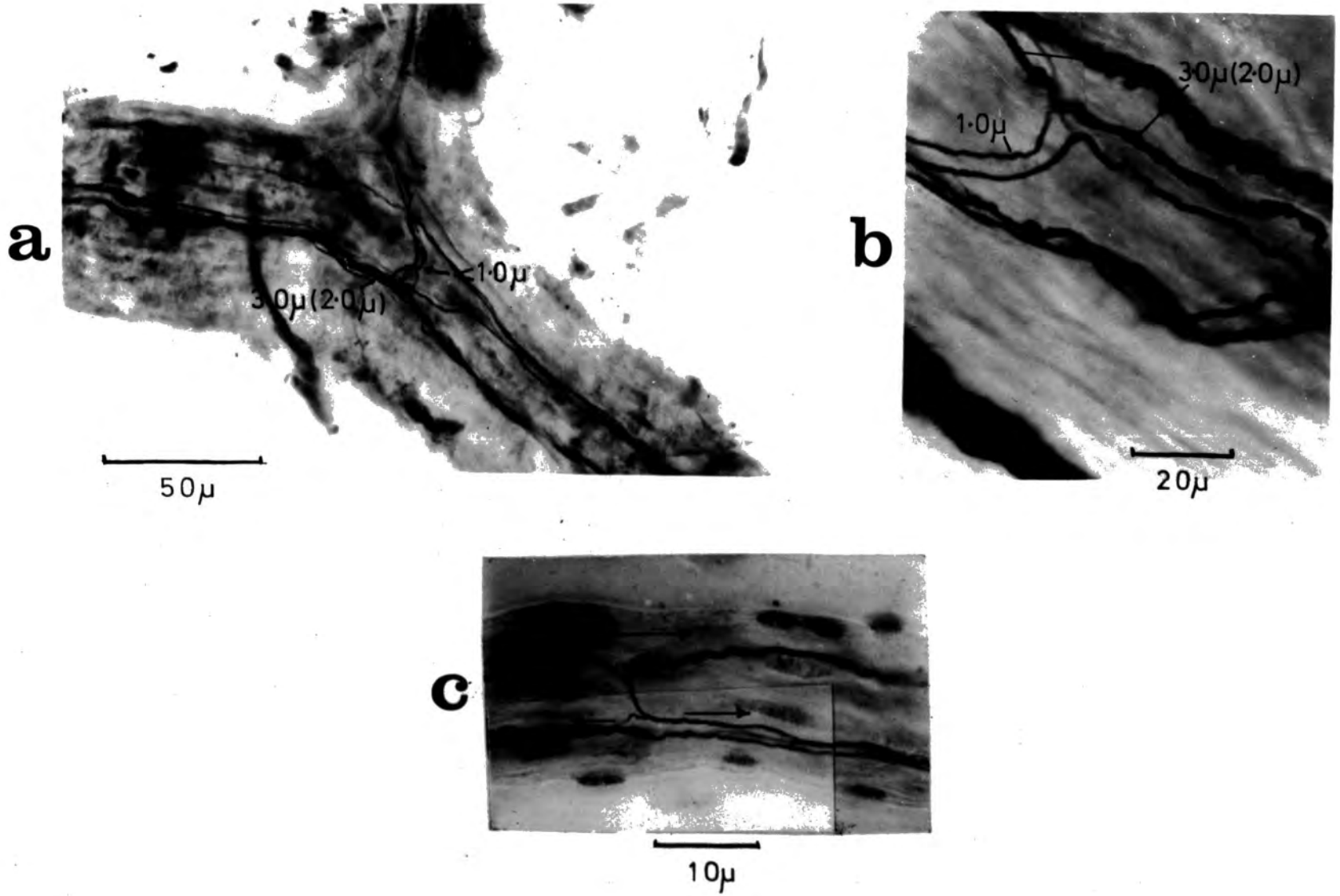
a
1·0μ
3·0μ(2·0μ)
50μ
b
3·0μ(2·0μ)
1·0μ
20μ
c
10μ

Figure 53

A schematic representation of the sensory innervation of cat skeletal muscle

Ia
Ib
II - sensory-fibre Group at nerve entry
III
IV

a. - arteriole
ad. - blood-vessel adventitia
c.t. - connective tissue (perimysium)
ep. - epimysium
Ex.m.f. - extrafusal muscle fibres
f. - fat deposits
f.e. - free-ending ramifications
P. - primary ending
p.f.c. - paciniform corpuscle
S_1 - secondary endings
S_5
Sp. - muscle spindle
t.o. - tendon organ
v. - venule

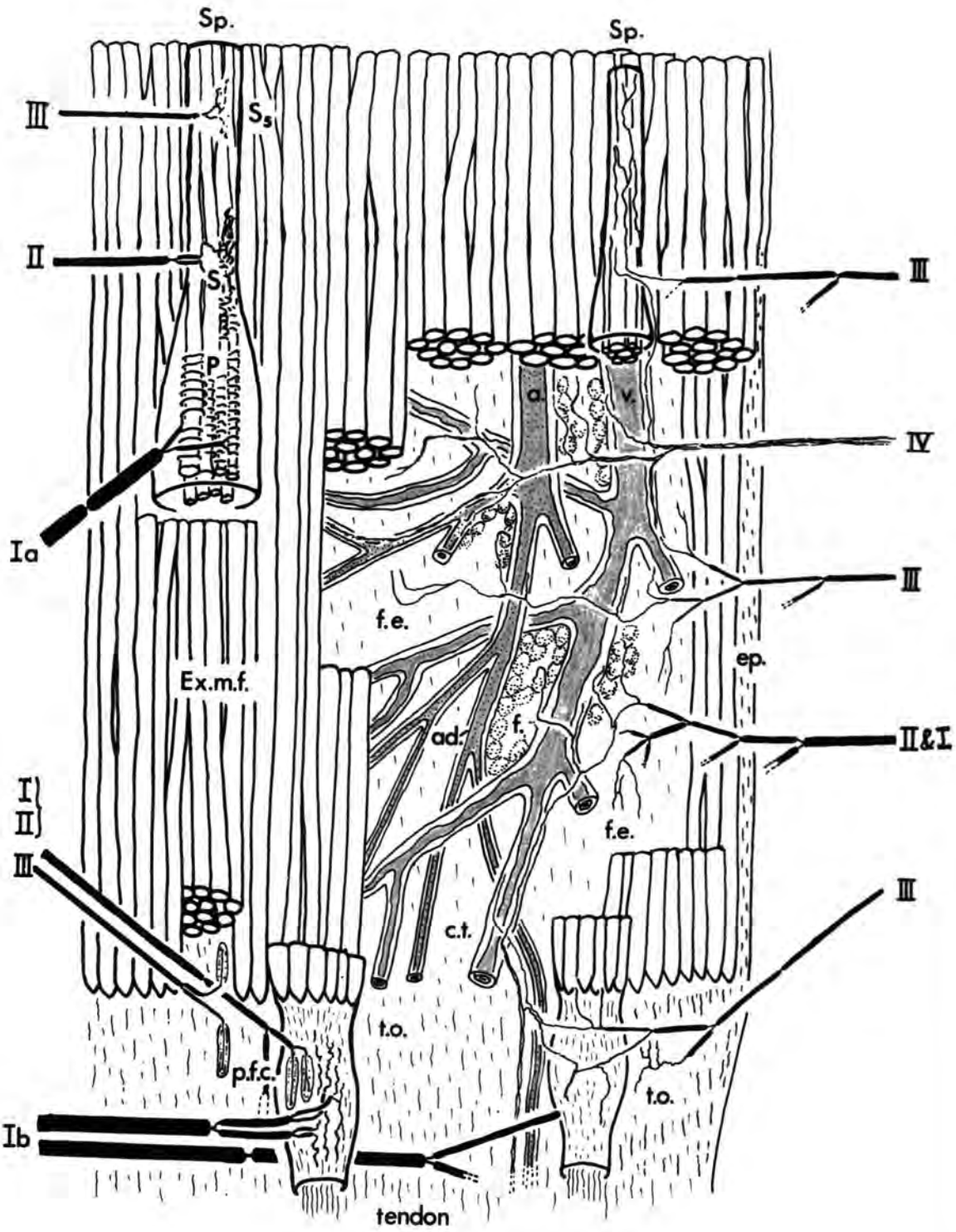
Sp.
Sp.
III
S_s
II
S_i
P
a.
v.
III
IV
Ia
III
f.e.
ep.
Ex.m.f.
ad.
f.
II&I
I
II
III
f.e.
III
c.t.
t.o.
p.f.c.
t.o.
Ib
tendon

Figure 54

Diagram of the gate control theory of pain mechanisms

A slightly modified version of Melzack & Wall's (1965) original figure.

T - first central transmission cells

sg - substantia gelatinosa

\+ - excitation

\- - inhibition

PAIN GATE CONTROL SYSTEM
(modified from Melzack & Wall)
1965

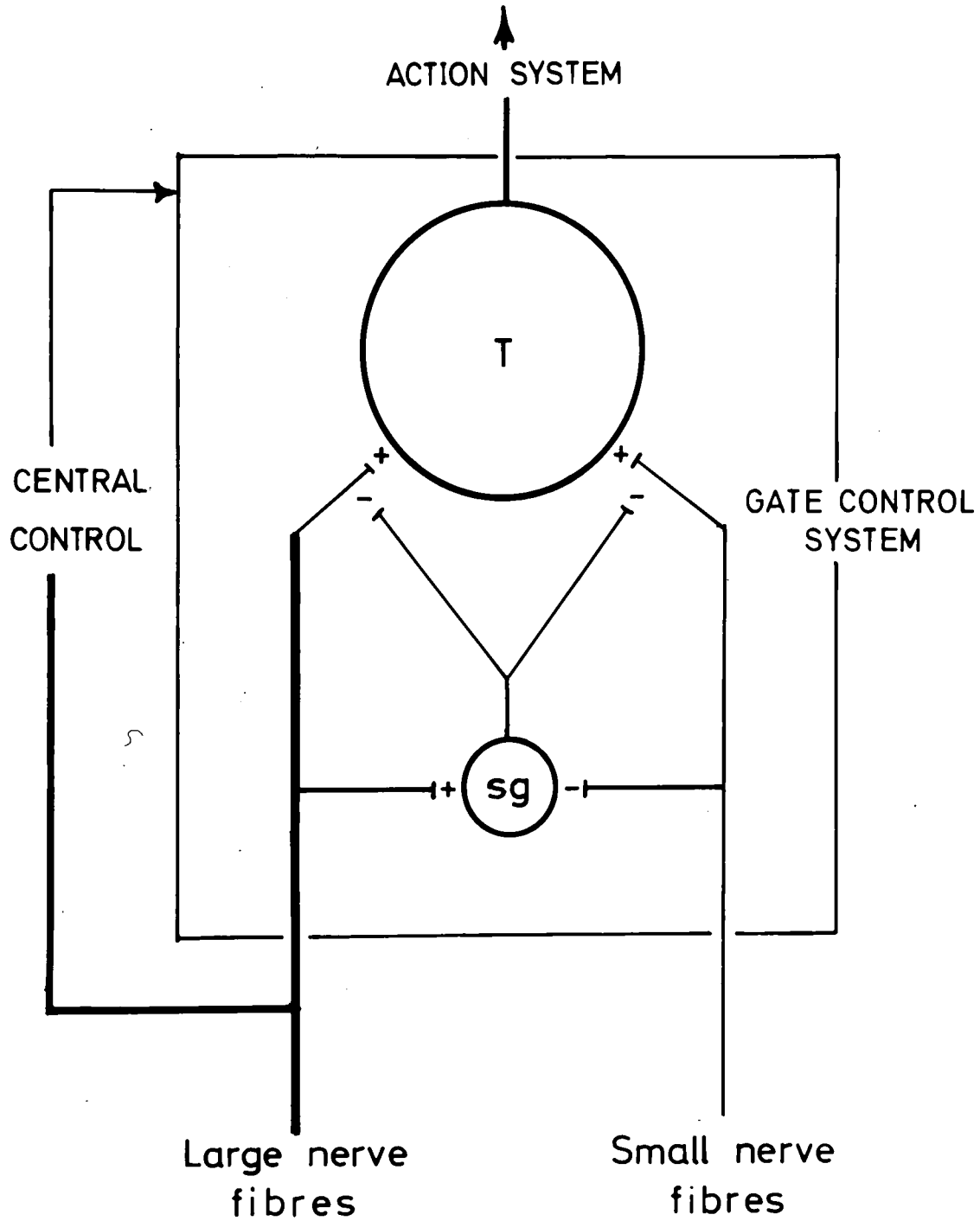

Figure 55

Cutaneous and muscle sensory input to the pain gate control system

A modified version of Melzack & Wall's (1965) original figure.

T - first central transmission cells

sg - substantia gelatinosa

\+ - excitation

\- - inhibition

PAIN GATE CONTROL SYSTEM
(modified from Melzack & Wall)
1965

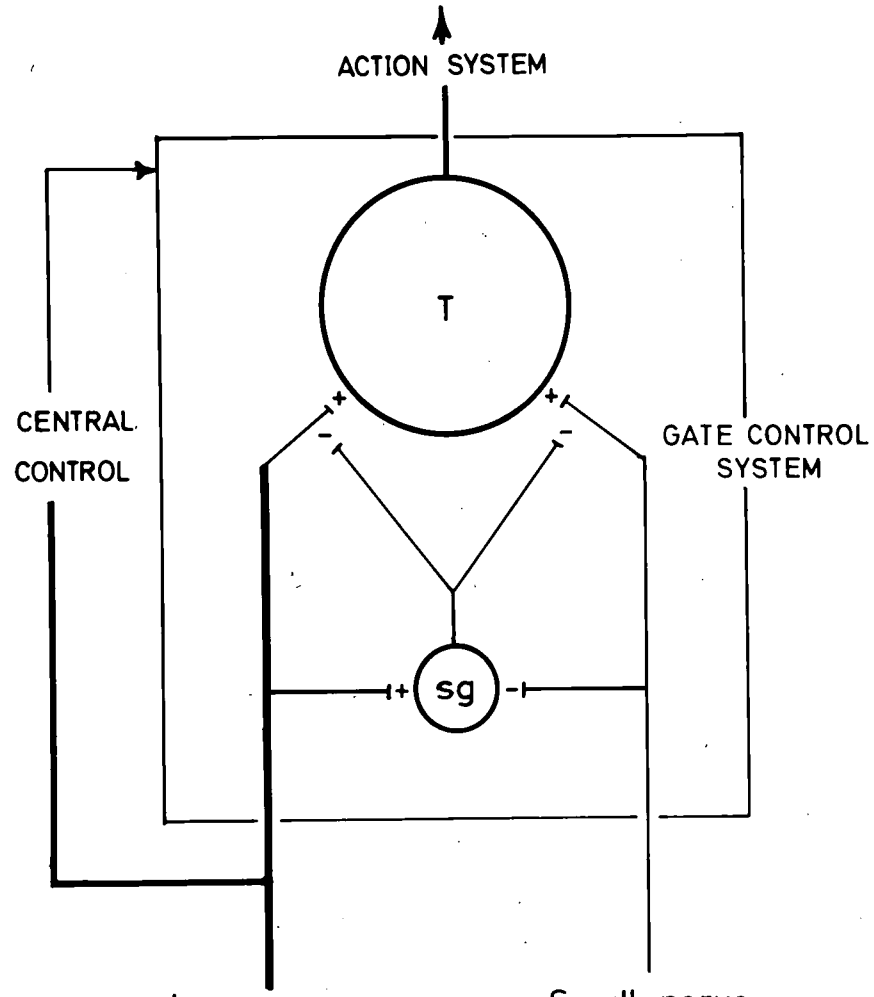

CUTANEOUS SENSORY INPUT

A fibres (mostly α & β) — Aδ & C fibres

MUSCLE SENSORY INPUT

GROUP I & II — GROUP III & IV

free ending and paciniform corpuscle fibres